Dissertations (2009 -)　　　　　　　　Dissertations, Theses, and Professional Projects

Mechanism Of Gaba$_b$ Receptor-Activated Increases In L-Type Calcium Current In The Neonatal Mammalian Hippocampus

Andrew S. Karls
Marquette University

MECHANISM OF GABA$_B$ RECEPTOR-ACTIVATED INCREASES IN L-TYPE CALCIUM CURRENT IN THE NEONATAL MAMMALIAN HIPPOCAMPUS

By

Andrew Karls, B.S.

A Dissertation submitted to the Faculty of the
Graduate School, Marquette University,
in Partial Fulfillment of the Requirements for
the Degree of Doctor of Philosophy

Milwaukee, Wisconsin

May 2014

ABSTRACT
MECHANISM OF GABA_B RECEPTOR-ACTIVATED INCREASES
IN L-TYPE CALCIUM CURRENT IN THE NEONATAL
MAMMALIAN HIPPOCAMPUS

Andrew Karls, B.S.

Marquette University, 2014

Activation of the metabotropic GABA_B receptor has most commonly been demonstrated to produce inhibitory effects on neurons, including the attenuation of voltage-dependent calcium current. However, during the early neonatal period in mammalian development, activation of GABA_B receptors leads to an enhancement of calcium current through a specific class of calcium channels, termed L-type channels, (because they conduct Long-lasting current) . This response peaks at 7 days postnatal, and is only demonstrated in a subset of cells. In the work presented here, the signal transduction pathway of GABA_B receptor-mediated increase of L-type current is described.

GABA_B receptors couple to G proteins, traditionally believed to be $G\alpha_{i/o}$. However, previous data from the laboratory suggested that the enhancing effect observed was not due to $G\alpha_{i/o}$, but a different G protein not previously described in GABA_B receptor signaling. Indeed, when the $G\alpha_q$ G protein was knocked down in cell culture, the enhancement of L-type channels was no longer observed. These data suggest that GABA_B receptors couple to $G\alpha_q$ G proteins to mediate calcium current enhancement.

Protein kinase C (PKC) had previously been demonstrated as a requisite member of this pathway. Furthermore, there was precedence for PKC to work through calcium/calmodulin-dependent kinase II (CaMKII) to enhance L-type current. However, the isozyme of PKC was not known, nor was the involvement of CaMKII on L-type current enhancement. Confocal imaging analysis suggests PKCα is the isozyme that is activated by GABA_B receptor activation, and pharmacological studies indicate CaMKII is not a participant in this pathway.

In seeking to inhibit CaMKII signaling, highly specific pharmacological inhibitors are often required. However, several inhibitors that were thought to be specific initially demonstrate nonspecific effects. A newly synthesized molecule, CK59, has been described to potently inhibit CaMKII activity ($IC_{50} < 10$ μm). However, data presented here describe off-target effects of CK59, specifically its ability to inhibit voltage-gated calcium channels. Treatment of cells with CK59 significantly reduced calcium influx in depolarized neurons, whereas other CaMKII inhibitors did not change calcium influx. Thus, CK59 is not a useful tool when studying the interplay between voltage-caged calcium channels and CaMKII signaling.

ACKNOWLEDGEMENTS

Andrew Karls, B.S.

I would like to express my most sincere gratitude to my advisor, Dr. Michelle Mynlieff, for her guidance and teaching over the past several years. I consider myself fortunate to have worked under her the last several years, and believe that any of my current or future accomplishments can be directly traced back to her.

I would also like to thank my committee members, Dr. James Buchanan, Dr. Stephen Downs, Dr. Thomas Eddinger, and Dr. Robert Peoples. My committee has always been available to help guide me and offer constructive criticism. I am certain I am a better scientist because of their input.

Thank you to the multitude of undergraduates with whom I worked throughout my time in the laboratory. I have enjoyed working alongside them, and it gave me a chance to explain my science to those eager to learn. I believe a strength of this program lies in the talents of the undergraduates who perform research here, and it was a privilege to work with several of them.

Special thanks to the entire faculty and staff of the department. I have interacted with almost all of you during my time here, and have overwhelmingly positive things to say. I believe this department fosters an environment of achievement, and it would not be possible without each and every faculty and staff member.

Lastly, I would like to thank my family, friends, and loved ones for their never-ending patience, support, encouragement, and love over these past years. There are no

words that can ever confer my gratitude and love. All I can humbly say is "Thank you for everything. I could not be any more fortunate than to have you in my life."

TABLE OF CONTENTS

LIST OF TABLES

LIST OF FIGURES

ABBREVIATIONS

AIP – Autocamtide 2-related inhibitory peptide

AMPA – α-Amino-3-hydroxy-5-methyl-4-isoxazolepropionic acid

Ant-AIP-II – Autocamtide 2-related inhibitory peptide, fused to *Antennapedia* transport

peptide sequence

BDNF – Brain-derived neurotrophic factor

CaM – Calmodulin

CaMKII – Calcium/calmodulin-dependent protein kinase II

cAMP – Cyclic adenosine monophosphate

CaRE – Calcium response element

CaRF – Calcium response factor

CCAT – Calcium channel associated transcription factor

CCK – Cholecystokinin

CIR – Calcium imaging Ringer's solution

CREB – cAMP response element-binding protein

CTX – Cone snail toxin

DAG – Diacylglycerol

DAPI – 4',6-diamidino-2-phenylindole

DG – Dentate gyrus

DMSO – Dimethyl sulfoxide

Egr4 – Early growth factor 4

EGTA – Ethylene glycol tetraacetic acid

ERK1/2 – Extracellular-signal related kinase 1/2

Fura-2 AM — Fura-2-acetoxymethyl ester

GABA — γ-aminobutyric acid

GAP — GTPase activating protein

GIRK — G protein-coupled inwardly-rectifying potassium channel

GLUT4 — Glucose transporter type 4

HRP – Horseradish peroxidase

HVA – High voltage-activated

IOD – Integrated optical density

IP3 — Inositol 1,4,5-trisphosphate

IV — Current-voltage

KCC2 — Potassium-chloride cotransporter 2

KCTD — K(+) channel tetramerization domain

LTP — Long term potentiation

LTCC – L-type calcium channel

L-type – Long-lasting type

LVA — Low voltage-activated

MAPK — Mitogen-activated protein (MAP) kinase

MeCP2 — Methyl CpG binding protein 2

MO — Morpholino

NMDA —N-methyl-D-aspartate

OCT — Optimal Cutting Temperature compound

PBS — Phosphate-buffered saline

PCC — Pearson's correlation coefficiant

PIP2 — Phosphatidylinositol 4,5-bisphosphate

PIPES — piperazine-N,N'-bis(ethanesulfonic acid)

PKA — Protein kinase A

PKC — Protein kinase C

PLC — Phospholipase C

PMA — Phorbol 12-myristate 13-acetate

PMT — Pasteurella multocida toxin

PTX — Pertussis toxin

PV — Parvalbumin

RACK — Receptor for activated C kinase

RGS — Regulator of G protein signaling

VGCC – Voltage-gated calcium channel

CHAPTER 1

INTRODUCTION

A cell's ability to receive and integrate external stimuli is critical to maintain

processes required for its function. For example, stimulation of cells lining the gut cause

secretion of enzymes required to break down food and obtain nutrients. In a similar way,

the response to extracellular signals in neurons is critical to sensory perception, synaptic

plasticity, gene expression, and cellular communication via neurotransmission. One of

the most common ways neurons respond to extracellular stimuli is modulation of

intracellular calcium. Calcium serves as an effective signal, because it is kept very low

(low nM) within the neuron, but is much higher outside the cell (mM range). When

calcium is allowed to enter the cell through various channels or transporters, it stimulates

an intracellular change crucial to neuronal function or survival. Thus, the ability to

modulate calcium entry helps to influence myriad intracellular signals.

One of the most common ways to affect calcium entry is to change the behavior

of ion channels. This can be done directly, where a change in voltage or binding of a

ligand directly opens a channel. Also common are intracellular signaling pathways,

which cause calcium channels to be modified by various signaling molecules, such as

protein kinases. These pathways involve a signaling cascade, where binding of a

neurotransmitter to its receptor sets in motion a cascade of events. One example of this

cascade affecting calcium entry is the binding of the neurotransmitter γ-aminobutyric

acid (GABA) to the metabotropic $GABA_B$ receptor.

A central focus of the Mynlieff laboratory is to understand how binding of GABA to its receptor leads to an increase in the amount of calcium entering the cell. Several studies have detailed the opposite effect: that GABA$_B$ receptor activation attenuates calcium entry (Takahashi et al., 1998; Carter and Mynlieff 2004; Perez-Garci et al., 2013). However, the Mynlieff lab showed that in hippocampal cell cultures derived from rats early in development, GABA$_B$ receptor activation increases long lasting (L-type) calcium current in a subset of cells (Carter and Mynlieff 2004; Bray and Mynlieff 2009; Bray and Mynlieff, 2011). Furthermore, this response peaks between postnatal day 6 (P6) and P8 (Bray and Mynlieff, 2009). The phenomenon of GABA$_B$ receptor activation leading to enhanced calcium entry had been identified only once before, in non-mammalian cells of the salamander retina (Shen and Slaughter 1999). Currently, there are still very few reports of GABA$_B$ receptor-mediated enhancement of L-type current (Park et al., 2010; Im and Rhim 2012), and no complete pathway or mechanism has yet been described. Therefore, the enhancing effect of GABA$_B$ receptor activation on enhanced L-type current continues to be an area of intense interest in the laboratory.

Tight regulation of intracellular concentrations is required for proper neuronal growth and development (for review, see Michaelsen and Lohmann 2010). L-type channels are the first calcium channels to be expressed in neurons; calcium flowing through these channels is responsible for the initiation of regulatory events that may play a role in neuronal differentiation (Pravettoni et al., 2000). Furthermore, the rats used in experiments to be detailed here range in age from P6 to P8, roughly equivalent to a 6 month old human infant (Sengupta 2013). This time span is commonly associated with seizure activity generated in the hippocampus (Korff and Nordli, Jr. 2006). How

regulation of calcium flowing through L-type channels may be involved is unclear, but there is emerging corollary evidence that L-type channels may play a role. First, inhibiting L-type channels changes the distribution in chloride transporters necessary for establishing a proper chloride ion gradient (Bray and Mynlieff 2009). Changes in expression patterns of the same specific chloride transporters examined by Bray and Mynlieff led to epilepsy-associated malformations of cortical development (Aronica et al., 2007). Thus, one hypothesis is that during the rodent neonatal period (roughly correlating to the first six months of human life), L-type channel activity is responsible for changes that establish a neuron's identity, including electrical properties. When L-type current signaling is disrupted during development, the intrinsic electrical gradients cannot be established. Thus, the circuit becomes vulnerable to epileptiform activity, where neurons fire excessively in a synchronous manner. It can be hypothesized that any pathway which functions to regulate intracellular calcium levels, such as $GABA_B$ receptor activation in these cells, is imperative to proper function.

The principal focus of my research has been to further describe the components of the signal transduction pathway, beginning with $GABA_B$ receptor activation, and resulting in L-type current enhancement. Using work done by previous members of the laboratory as a basis for my studies, I explored what signaling molecules might be participating in this pathway; my results presented here suggest a novel mechanism that corresponds with the Mynlieff laboratory's discovery of a novel signaling pathway. A recent report suggests the interplay between $GABA_B$ receptors and their regulation of intracellular calcium may play a role in Parkinson's disease, underscoring the importance of understanding these data (Hillman et al., 2012). Furthermore, a better understanding of

how cells communicate in general provides a better framework for potentially modifying

the system in certain diseases.

The Hippocampus

Studies in the Mynlieff laboratory examine dissociated neurons from the murine

hippocampus. The hippocampus is part of the medial temporal lobe of the brain, where it

plays a central role in formation and retrieval of memories. It is also a well-known site

for seizure formation.   Morphologically, the hippocampus is composed of a "c"-shaped

sheet of neurons (the dentate gyrus) folded around another "c"-shaped sheet, known as

Ammon's horn (Figure 1.2). This area can be subdivided into 3 distinct regions, CA1 –

CA3 (CA is rooted in the Latin term for Ammon's horn). The neurons of the pyramidal

cell layer are densely packed through the CA1- CA3 region; however once it folds under

the dentate gyrus, neurons are much less dense. Thus, neurons with their cell bodies

outside the two cell layers tend to be much more diffuse; in general these cells are

identified as inhibitory GABAergic interneurons. The hippocampus is also described

depthwise with different strata (Figure 1.2). The stratum oriens is the most superficial

layer of the hippocampus, and sits above the primarily excitatory glutamatergic cell

bodies of the stratum pyramidale. Below the stratum pyramidale sits the stratum

radiatum, which is enriched in dendrites. Many of the Schaffer collateral fibers are found

here, as well as a diverse group of interneurons, rich in dendrites. Below the radiatum is

the stratum lacunosum and stratum moleculare, which are often grouped together, as well

as a host of interneurons. Finally, the dentate gyrus sits most ventral. Studies described

here focus primarily on neurons dorsal to the dentate gyrus, primarily in CA1 and CA3

regions; for a more complete description of dentate gyrus structure and function, see

Scharfman, 2007.
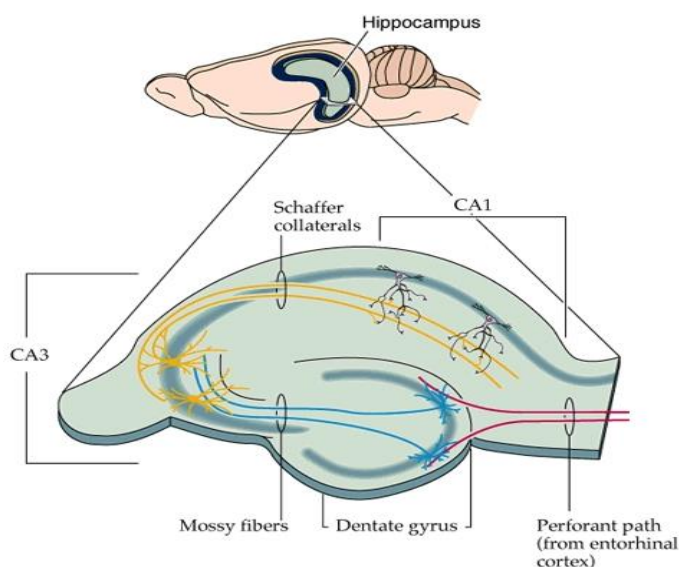
Figure 1.1: Pathways through the rodent hippocampus. Input enters via the entorhinal cortex and synapses on the granule cells of the dentate gyrus (DG). DG axons project to the CA3 region via mossy fibers. CA3 pyramidal neurons project to the CA1 region. Output is primarily through the CA1 pyramidal neurons back to the entorhinal cortex. (Figure courtesy of neurosciencenews.com)

    The hippocampus is perhaps the most intensely studied brain region; as such, network connections and various cell types have been characterized in some detail. Input entering the hippocampus flows unidirectionally via three well-defined pathways (Andersen et al., 1973). First, the entorhinal cortex contains axons that project onto the granule cells of the dentate gyrus; this is known as the perforant path. Second, neurons of the dentate gyrus project their axons (known as mossy fibers and thus the mossy fiber pathway) onto the pyramidal neurons of the CA3 region. Third, the CA3 region pyramidal neurons contain branching axons that travel out of the hippocampus through the fornix, as well as axons that synapse on CA1 pyramidal neurons within the CA1 region. Hippocampal output consists primarily of CA1 axons projecting back into the entorhinal cortex. The CA1 region receives mostly excitatory glutamatergic input from

the CA3 region; this input is extensively regulated by a network of GABAergic

interneurons. These interneurons serve to govern firing rate and ensure it occurs in

synchrony. There are at least 16 types of distinct interneurons in the hippocampus;

twelve synapse onto dendrites of pyramidal cells and four synapse onto other parts of

pyramidal neurons or onto other interneurons (Somogyi and Klausberger 2005;

Klausberger and Somogyi 2008; Klausberger 2009). Nearly all (92%) GABAergic

interneurons in the CA1 region synapse on pyramidal neuron dendrites (Megias et al.,

2001); however, little research has been conducted on the synapses on the cell bodies and

axons of these pyramidal neurons. The hippocampus, particularly the superior region

(mostly CA1 some CA3), contains a relatively high population of GABAergic

interneurons. While my hippocampal cell cultures contain a heterogeneous mixture of

pyramidal neurons and several type of interneurons, these cultures exclude the dentate

gyrus. They contain neurons only from the CA1 and CA3 regions, to decrease the

heterogeneity of the population (see methods). Furthermore, while hippocampal
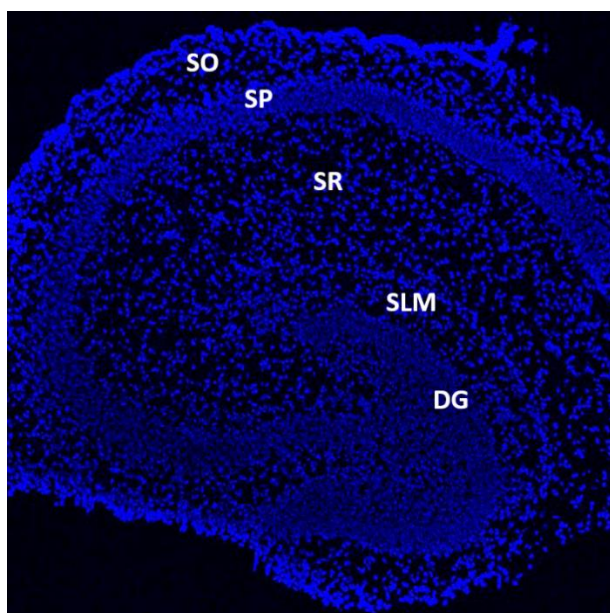
Figure 1.2: Cross sectional slice of a P7 rat hippocampus. Hippocamus was frozen, sliced into 20 μM sections, and stained with DAPI to visualize nuclei. The stratum oriens (SO) is most superficial, with the densely packed stratum pyramidale (SP) sitting below. The stratum radiatum (SR) contains interneurons that project to CA. The stratum moleculare/lacunosum (SLM) sits on top of the dentate gyrus (DG), which is densely packed with excitatory dentate granule cells. Scale bar = 100 μM.

interneurons are divided based primarily on antibody staining and morphology, the physiological role for many of these interneurons remains elusive. Data presented here present an opportunity to begin to define the physiological relevance of some of these interneuron types, especially during development when maturation of circuitry is occurring.

GABA$_B$ receptors

The GABA$_B$ receptors that we have demonstrated to enhance calcium current are are G protein coupled receptors that are members of the class C7 transmembrane-spanning G protein coupled receptor family. The class C family also includes metabotropic glutamate receptors, and its members share amino acid sequence identity of approximately 30% (Katritch et al., 2013). Importantly, several important sites such as the ligand binding domain, have much higher sequence identities, which allows for the development of several structural homology models. (Katritch et al., 2013). Thus, much of what is known about the various activation states and molecular interactions of the GABA$_B$ receptor is based on models of the metabotropic glutamate receptor. However, investigators have recently solved the extracellular domain of the receptor, both unbound (Geng et al., 2012), and when it is bound to a ligand (Geng et al., 2013). Cystallography data, homology modeling, and cloning work done in the early 1990's have provided a foundation of knowledge about GABA$_B$ receptor structure. It is composed of two distinct gene products which encode the GABA$_{B1}$ and GABA$_{B2}$ subunits, respectively. Physiological characterization showed that a functional receptor requires dimerization of GABA$_{B1}$ and GABA$_{B2}$ subunits (Kaupmann et al., 1998; Jones et al., 1998; Kuner et al.,

1999); the GABA$_{B1}$ subunit contains a motif that causes retention at the endoplasmic

reticulum (Margeta-Mitrovic et al., 2000). When GABA$_{B1}$ and GABA$_{B2}$ dimerize via a

coiled coil interaction on their C termini, the retention signal is hidden, and the receptor

will be trafficked to the membrane (Calver et al., 2001; Margeta-Mitrovic et al., 2001).
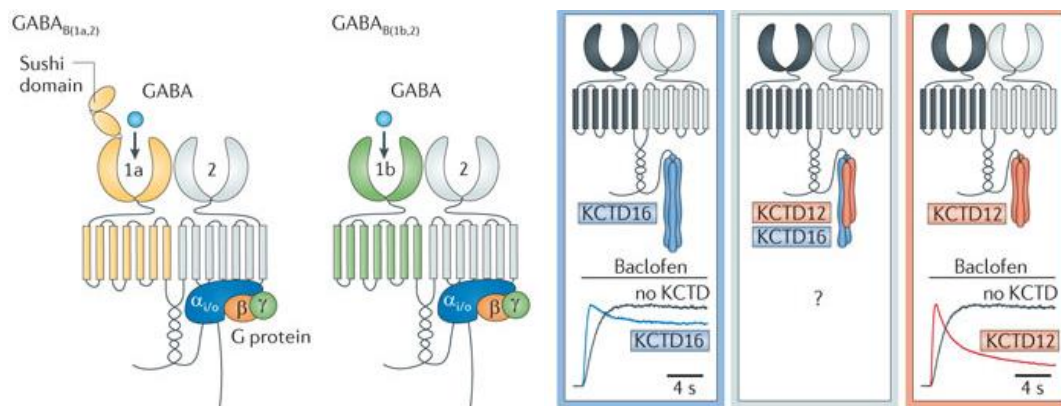
Figure 1.3: Schematic structure of GABA$_B$ receptors. (a) The ligand binds to the GABA$_{B1}$ subunit, and the G protein couples to the GABA$_{B2}$ subunit. GABA$_{B1a}$ is shown with sushi repeats. (b) Effects of GABA$_B$ receptor activation on inwardly rectifying potassium currents shown in the presence and absence of auxiliary subunits. KCTD, potassium channel tetramerization domain. Adapted by permission from Macmillan Publishers Ltd: [*Nature Reviews Neuroscience*] (**13**, 380-394), copyright (2012).

The simplest view of GABA$_B$ receptor signaling is that the B1 subunit binds the

ligand, whereas B2 couples to the G protein (Figure 1.3a). Homology models have

suggested the presence of a "venus flytrap" model, where the binding site is between two

lobes on the B1 N-terminus (Galvez et al., 1999). The first step in signal transduction is

the closure of the lobes around the ligand (Galvez et al., 2000). Interestingly, chimeric

models where the B2 N-terminus is replaced with the B1 N-terminus decreases ligand

affinity (Galvez et al., 2001; Geng et al., 2012). Therefore, while B1 is the site of

binding, there appears to be intramolecular communication and possible interaction of B2

to promote the most efficient ligand binding. Just as chimeric studies were used to show the importance of the B2 N-terminus in ligand binding, they were also used to describe in detail the components for G protein coupling. When B2 was swapped with any of the B1 intracellular loops, the result was formation of a nonfunctional receptor (Margeta-Mitrovic et al., 2001). Furthermore, specific point mutations within either intracellular loop 2 or 3 can also render the receptor nonfunctional (Havlickova et al., 2002; Duthey et al., 2002). The generation of $GABA_B$ subunit knockout mice has generally supported chimeric studies. $GABA_{B1}$ knockouts do not display electrophysiological or biochemical activity when a ligand is present (Prosser et al., 2001; Schuler et al., 2001; Queva et al., 2003). However, responses of $GABA_{B2}$ knockouts can be measured electrophysiologically in the hippocampus (Gassmann et al., 2004). This is suggestive that $GABA_{B1}$ subunits can function autonomously or, more likely, promiscuously with other receptors. Recent evidence has shown $GABA_{B2}$ functional interaction with M2 muscarinic receptors, expanding the possibilities beyond simple $GABA_{B1}/GABA_{B2}$ heteromers (Boyer et al., 2009).When GABA receptors were cloned, it was expected that there would be a host of splice variants and isoforms to correlate with the diverse signaling attributed to the receptor (Padgett and Slesinger 2010). Instead, only two splice variants of $GABA_{B1}$ were discovered, $GABA_{B1a}$ and $GABA_{B1b}$ (Kaupmann et al., 1997). $GABA_{B1a}$ and $GABA_{B1b}$ show no physiological or pharmacological distinction when expressed in heterologous expression systems (Brauner-Osborne and Krogsgaard-Larsen 1999; Ulrich et al., 2007). However, only $GABA_{B1a}$ contains 2 "sushi" domains, believed necessary for axonal targeting. This suggests B1a is primarily axonal, whereas B1b is dendritic. Knockout studies have verified these localizations (Vigot et al., 2006).

GABA$_B$ receptor signaling has traditionally been described by its coupling to a pertussis toxin-sensitive G$\alpha_{i/o}$ G protein (Pinard et al., 2010). Ligand binding causes the G protein (both Gα and G$\beta\gamma$) to release from the receptor in a GTP-dependent fashion. Downstream targets of the G protein itself often initiate a second messenger cascade which can have a wide range of effects on physiological functions (Figure 1.3). G
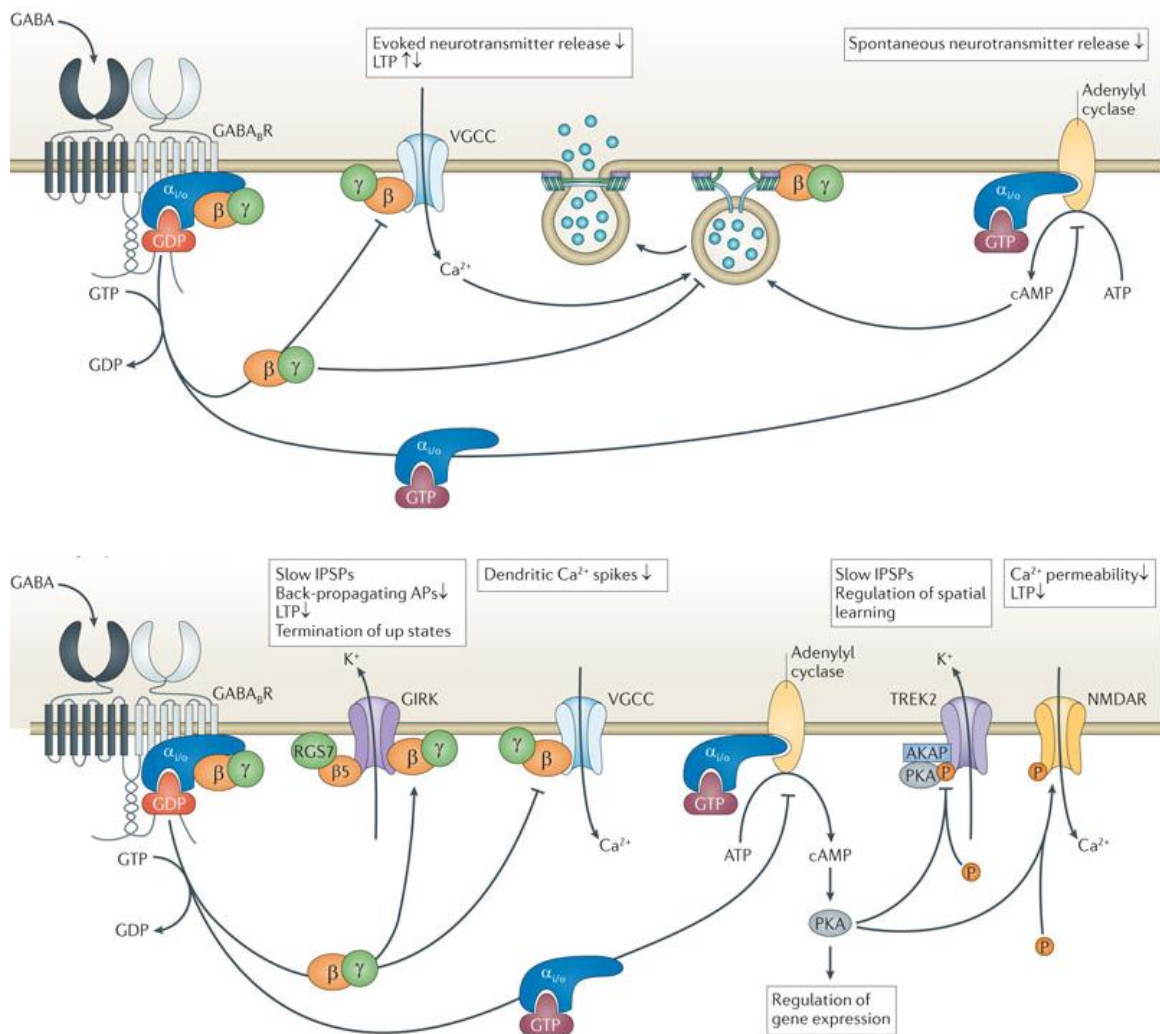
Figure 1.4: Downstream effectors of GABA$_B$ receptors. (a) Presynaptically, GABA$_B$ receptors decrease both evoked and spontaneous neurotransmitter release. (b) Postsynaptically, GABA$_B$ receptor activation results in increased outward potassium current, decreased activity of PKA, and reduced calcium currents. Reprinted by permission from Macmillan Publishers Ltd: [Nature Reviews Neuroscience] (**13**, 380-394), copyright (2012).

proteins also commonly target ion channels as a way of regulating excitability. The three most well understood targets of $G\alpha_{i/o}$ G proteins linked to $GABA_B$ receptors are voltage-gated calcium channels, inwardly rectifying potassium channels, and the enzyme adenylate cyclase (Gassmann and Bettler 2012).

Adenylyl cyclase is the enzyme that converts ATP into cyclic AMP (cAMP), one of the most ubiquitous second messengers in neurons. In this case it is the $G\alpha_{i/o}$ activated by $GABA_B$ receptors that inhibits activity of this enzyme (Nishikawa et al., 1997). By doing so, cAMP levels are reduced, thus resulting in reduction of downstream kinase activation, specifically protein kinase A (Figure 1.4b). Of particular interest is that under certain conditions, $GABA_B$ receptors can actually increase cAMP levels. While the $G\alpha_{i/o}$ is inactivated by regulator of G protein signaling (RGS) proteins, the $\beta\gamma$ subunits inhibit the GTPase activity of $G\alpha_s$ during β-adrenergic receptor stimulation. This leads to increased affinity of $G\alpha_s$ for adenylate cyclase. Thus, $GABA_B$ receptor activation can indirectly assist in the increase of adenylyl cyclase activity, resulting in increased protein kinase A activity (PKA, Robichon et al., 2004). This is important to work presented here, which also examines the ability of $GABA_B$ receptors to produce a bidirectional response via a different mechanism affecting voltage-gated calcium channel (VGCC) function.

G-protein inwardly rectifying potassium channels (GIRK channels) open to produce a slow inhibitory postsynaptic potential (Figure 1.4b). This occurs because positive potassium ions flow out of the cell, reducing its excitability. These GIRK channels hyperpolarize the membrane potential, and are the primary effectors of $GABA_B$ receptors postsynaptically (Misgeld et al., 1995). In contrast to the inhibitory effects in P/Q- and N- channels, the currents across GIRK channels are enhanced by the $\beta\gamma$ subunit

directly (Reuveny et al., 1994; Wickman et al., 1994). GIRK channels are homo- or

heterotetramers; it is thought that the subunit composition of the GIRK channel accounts

for its differing interactions with the $G\beta\gamma$, and thus accounts for the large differences in

GIRK channel kinetics in response to $GABA_B$ receptor activation (Cruz et al., 2004;

Padgett and Slesinger 2010). This hypothesis appears to be partially correct, although the

recently discovered $GABA_B$ auxiliary subunits also appear to play an important role in

influencing GIRK channel kinetics (Gassmann and Bettler 2012).

For many years there have been discrepancies about the differing kinetics seen

when $GABA_B$ receptors regulate GIRK channels in native neurons versus those in

expression systems. For example, activation kinetics were always much faster in native

neurons; this difference was thought to be due to the subunit composition of the GIRK

channel (Gassmann and Bettler 2012). However, biochemical evidence has shown that

$GABA_B$ receptors can assemble with auxiliary potassium channel tetramerization domain

(KCTD) proteins (Schwenk et al., 2010). These four proteins form a homotetramer that

can bind to the $GABA_{B2}$ C-terminus (Figure 1.3b). Expression of these KTCD tetramers

with $GABA_B$ receptors in heterologous expression systems abolished the differences seen

in these model systems when KCTD proteins were not included (Schwenk et al., 2010).

Thus, it appears that the $GABA_B$ receptor auxiliary subunits may significantly change the

function of the receptor. As pointed out by the authors who made the discovery

originally, KCTD proteins could influence any part of the signaling complex, including

what the downstream effector or channel of the $GABA_B$ receptor may be (Schwenk et al.,

2010).

GABA$_B$ receptors have been shown to couple to all types of high voltage activated calcium channels (P-, Q-, N-, and L-), with the exception of the R channel (Mintz and Bean 1993; Guyon and Leresche 1995; Huston et al., 1995; Harayama et al., 1998; Li and Stern 2004; Vigot et al., 2006). Dogmatically, ligand binding to the GABA$_B$ receptor liberates the βγ subunit to directly bind to the presynaptic VGCCs. This slows the activation of the VGCC and decreases its activity 10-50% (Figure 1.4a, Huston et al., 1990; Menon-Johansson et al., 1993; Guyon and Leresche 1995). Less presynaptic calcium inhibits vesicular neurotransmitter release. To a lesser degree than presynaptic inhibition, GABA$_B$ receptor signaling is also involved postsynaptically. For example, in the supraoptic nucleus, release of βγ caused by GABA$_B$ receptor activation leads to a decrease in firing because of the reduction in calcium currents (10-25%, Harayama et al., 1998). Finally, activation of GABA$_B$ receptors has also been shown to increase L-type calcium current (Shen and Slaughter 1999; Carter and Mynlieff 2004; Bray and Mynlieff 2011; Park et al., 2010). While there are fewer descriptions of this phenomenon, it is not pertussis toxin sensitive (Bray and Mynlieff 2011), and is likely mediated by a Gα$_q$ G protein which initiates a signaling cascade. This document will spend much time describing what is known about the pathway, and thus it will not be detailed presently.

G Proteins

GABA$_B$ receptors are known as G protein coupled receptors (GPCRs) because they associate in signaling complexes with molecules known as a guanine nucleotide-binding proteins. Simply referred to as heteromeric G proteins, these complexes are composed of

an α subunit, as well as β and γ subunits, which closely associate with each other. Upon

ligand binding to the GPCR on the extracellular side of the membrane, the G protein

associated with the GPCR on the intracellular side of the membrane will become

activated (Figure 1.5).   The conformational change that takes place within the GPCR

allows the G protein to exchange bound GDP for GTP on its Gα subunit. This exchange

causes the Gα subunit to dissociate from the GPCR and the Gβγ subunit complex. Both

the Gα and Gβγ can serve to initiate signal transduction cascades. Termination of

signaling occurs when the intrinsic GTPase activity of the Gα hydrolyses GTP to GDP,

restoring the affinity of the Gα to Gβγ. Proteins known as GTPase activating proteins

(GAPs) increase the rate at which hydrolysis occurs; in certain cases, the molecule

targeted by the G protein may possess GAP activity and thus increase rate of deactivation

(G protein signaling reviewed in McCudden et al., 2005; Wettschureck and Offermanns

2005; Milligan and Kostenis 2006). Bacterial toxins have aided greatly in determining

the function and molecular mechanisms of various G protein families. Cholera toxin

(CTX) produces a constitutively active α subunit of $Gα_s$ (Moss and Vaughan 1979; Van

Dop et al., 1984); pertussis toxin (PTX) causes $Gα_{i/o}$ to remain permanently bound to

GDP (inactive) and uncouples the heterotrimeric complex of $Gα_{i/o}$ G proteins from their

GPCR (Katada and Ui 1982; Kurose et al., 1983).

G proteins are named based on the identity of their α subunit. They are grouped

into families, often exerting similar effects, and sharing significant sequence similarity.

There are currently four families of Gα proteins with a total of 14 members (Simon et al.,

1991). A broad description of the divisions and functions of various G proteins can be

found in table 1. Of particular interest to this project is the $Gα_q$ family. The $Gα_q$ family

comprises 4 members: $G\alpha_q$, $G\alpha_{11}$, $G\alpha_{14}$, and $G\alpha_{15/16}$ (Mizuno and Itoh 2009). $G\alpha_q$ is found in all tissue types, and its α subunit amino acid sequence is used for comparison of sequence identity with other members (reviewed in Mizuno and Itoh 2009). $G\alpha_{11}$ demonstrates 90% sequence similarity with $G\alpha_q$, and is also distributed across all tissue types. $G\alpha_{14}$ demonstrates 80% sequence similarity with $G\alpha_q$, and is most commonly found in non-neuronal tissues, such as the kidney, liver, and lung; finally, $G\alpha_{15/16}$ is also not distributed in nervous system, but rather in hematopoetic cells only. Its α subunit demonstrates 57% sequence similarity to that of $G\alpha_q$. Structurally, all four

G protein family	Members	Distribution	Pharmacological Inhibitor	Common physiological action
$G\alpha_s$	α_s, α_{olf}	Ubiquitous Olfactory Epithelium	Cholera Toxin	Activates adenylyl cyclase
$G\alpha_{i/o}$	α_{i1}, α_{i2}, α_{i3}, α_o, α_z, α_{t-r}, α_{t-c}, α_{gust}	Ubiquitous Neuronal Neuronl Retinal rods Retinal cones Taste buds	Pertussis Toxin	Inhibits adenylyl cyclase, activates GIRK channels inhibits N-type channels increases PDE 6 activity (for rods, cones, and taste buds)
$G\alpha_q$	α_q, α_{11} α_{14} $\alpha_{15/16}$	Ubiquitous Kidney, lung Hematopoetic cells	YM-254890 (all but $\alpha_{15/16}$)	Activate β isoforms of phospholipase C
$G\alpha_{12/13}$	α_{12}, α_{13}	Ubiquitous		Activate small G proteins including RhoA

Table 1: Families of G proteins. Members are divided based on their α subunit, and described by their pharmacology, most common tissue distribution, and general physiological role. Adapted from Wettschureck and Offermanns 2005.

isoforms are similar, composed of a helical domain with 5 α helices, a switch region

(with both α helices and β sheets), and a GTPase domain. The physiological role of the

Gα_q family is to activate β isoforms of phospholipase C (PLCβ), which in turn catalyzes a

reaction in which phosphatidylinositol bisphosphate (PIP$_2$) is cleaved into inositol

trisphosphate (IP$_3$) and diacylglycerol (DAG). The result of cleaving PIP$_2$ and generating

these second messengers is to release calcium from intracellular stores (via the IP$_3$

receptor) and activate protein kinase C (PKC), both of which participate in a range of

cellular processes (signaling pathway reviewed in Rhee 2001). All four isoforms of

PLCβ (β1-β4) are stimulated by the Gα_q family and their associated G$\beta\gamma$, although

different Gα_q isoforms preferably activate different PLCβ isoforms. For example, the

Gα_q isoform is a poor activator of PLCβ-2, but not the other three isoforms of PLCβ

(Hepler et al., 1994; Jiang et al., 1994); G$\alpha_{15/16}$ can activate only PLCβ 1-3 (Kozasa et al.,

1993). The mechanism by which the Gα_q family members activate PLCβ is unknown;

however, truncation experiments have shown that the PLCβ C-terminus is required for

Gα_q interaction (Park et al., 1993). On the Gα_q protein, the third helix and linker to the

fourth β sheet change conformation when PLCβ is activated (Venkatakrishnan and Exton

1996). Truncation mutations verified these as essential regions. In terms of termination,

it was shown, somewhat surprisingly, that the intrinsic GTPase activity of Gα_q was rather

low; however, in the presence of PLCβ-1, activity significantly increased. This result

indicated PLC β-1 acts as a GAP to stimulate hydrolysis of GTP bound to Gα_q (Chidiac

and Ross 1999). While the first bacterial toxins such as PTX or CTX had no measurable

action on the activity of Gα_q G proteins, recently two compounds have been isolated that
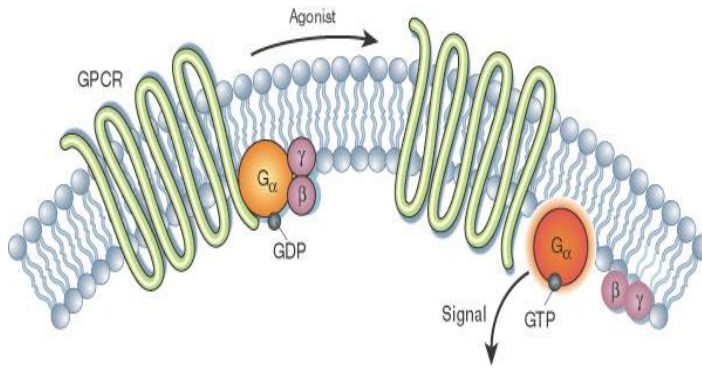
Figure 1.5: Schematic structure of G protein activation. Agonist binding to the receptor causes GDP to be exchanged for GTP, the complex to dissociate from the receptor, and the α and βγ subunits to initiate a signaling cascade. Reprinted by permission from Macmillan Publishers Ltd: [*Nature*] (**420**, 716-717), copyright (2002).

modulate $G\alpha_q$ signaling. The pathogenic bacterium *P. multocida* produces a protein known as PMT, which acts as a mitogen; pharmacologically, this compound appears to facilitate $G\alpha_q$ coupling to PLCβ-1 leading to the same response elicited by receptors coupled to $G\alpha_q$ family members (Wilson and Ho 2004). Importantly, PMT does NOT activate $G\alpha_{11}$ mediated pathways, because the $G\alpha_{11}$ isoform is missing a critical region in its helical domain where PMT appears to induce activation. A second modulator, YM-254890, has been isolated from *Chromobacterium* culture broth; it reduces the enhanced calcium signals induced by $G\alpha_q$, $G\alpha_{11}$, and $G\alpha_{14}$, but not $G\alpha_{15}$ (Takasaki et al., 2004). While the molecular mechanism is not yet known, YM-254890 is the most specific inhibitor of $G\alpha_q$ signaling currently available.

Voltage-gated Calcium Channels

Calcium entry into neurons is a tightly regulated process. Various intracellular storage sites, membrane transporters, and ion channels collectively determine the concentration of calcium within the cell. One well studied mechanism for calcium entry is the opening of voltage-gated calcium channels (VGCC) in response to depolarization. These channels are heteromers, composed of an α1 pore-forming subunit, as well as auxiliary

subunits which modify expression and kinetics of the channel. Two classes of VGCC

have been identified, based on whether they activate at low voltages (LVA, $V_a \sim$ -46 mV,

(Klockner et al., 1999) or high voltages (HVA, $V_a \sim$ +10 to -20 mV, Catterall et al.,

2005). VGCCs are subdivided based on sequence identity, pharmacology, and kinetics.

Collectively, there are a total of 10 α1 subunits classified into three families (reviewed in

Ertel et al., 2000, table 2). Within these families, there is greater than 70% sequence

identity, and less than 40% identity between families (Catterall 2011). LVA channels

(Ca_v 3.x) are known as T-type channels; they produce a transient current which helps

regulate excitability in neurons, aid in secretion in the kidney and liver, and regulate

smooth muscle contraction and proliferation (Cueni et al., 2009; Iftinca and Zamponi

2009). Ca_v 2.x channels are associated with neurotransmitter release in the central

nervous system and at the neuromuscular junction (Weiergraber et al., 2006; Snutch

2005; Nimmrich and Gross 2012). The Ca_v 1.x family contains isoforms 1.1 – 1.4. Ca_v

1.1 channels are found in the transverse tubules of skeletal muscle (Flucher and Franzini-

Armstrong 1996) where they are required for excitation contraction coupling (Rios et al.,

1992). Ca_v 1.4 channels are located in retinal photoreceptors and bipolar cells of the eye,

and are necessary for phototransduction (Baumann et al., 2004). Ca_v 1.2 channels are

found in cardiac and smooth muscle, and function in excitation-contraction coupling

(Striessnig 1999). Ca_v 1.3 channels are located on sensory cells, such as cochlear hair

cells, functioning to promote neurotransmitter release (Michna et al., 2003). Importantly,

Ca_v 1.2 and Ca_v 1.3 are also both found in neurons. In neurons, Ca_v 1.2 channels are

localized primarily postsynaptically on dendritic shafts and spines (Di Biase et al., 2011);

Ca$_v$ 1.3 channels are located preferentially on proximal dendrites and cell bodies (Hell et

al., 1993).

Channel Identification	Voltage Activation	α1 Subunit identification	Pharmacological antagonists	Common tissue distribution
L-type	HVA	Ca$_v$ 1.1 – 1.4	Dihydropyridines	All muscle types, neurons, retinal cells
P/Q-type	HVA	Ca$_v$ 2.1	ω-Agatoxin IVA	Neurons, heart, pancreas
N-type	HVA	Ca$_v$ 2.2	ω-Conotoxin GVIA	Neurons
R-type	HVA	Ca$_v$ 2.3	SNX-483	Neurons, heart, testes
T-type	LVA	Ca$_v$ 3.1 – 3.3	Ethosuximide	Brain, kidney, placenta

Table 2: Divisions of voltage-gated calcium channels based on pharmacology, kinetics, and sequence identity of the pore-forming α1 subunit. Adapted from Ertel et al., 2000.

The α1 subunit of Ca$_v$'s is a large protein (190-250 kDa) comprising four domains

(I-IV, Figure 1.6a). Each domain contains six membrane-spanning segments (S1-S6).

Within the transmembrane segments, S4 is the voltage sensor, and the loop between S5

and S6 serves as the selectivity filter and determines ionic conductance (Catterall 2011).

The intracellular loops serve as sites where protein-protein interactions occur. For

example, G proteins have been shown to regulate N-type channels between domains I and

II, the same loop where the auxiliary β subunit associates (De Waard et al., 1997; Herlitze

et al., 1997). Furthermore, the loop between domains II and III is the site of direct

interaction with SNARE proteins for Ca$_v$ 2.x channels (Sheng et al., 1994; Rettig et al.,

1996). The heavily spliced C-terminal end of neuronal calcium channels contains an IQ-

like motif that can interact with calcium binding proteins such as calmodulin (Lee et al.,

1999); perhaps most interestingly, L-type calcium channels (can regulate transcription when a spliced fragment binds to a nuclear protein (Gomez-Ospina et al., 2006). In addition to the central pore-forming α1 subunit, VGCC complexes associate with several auxiliary subunits (Figure 1.6b). The α2 and δ subunits are linked by disulfide bonds (Gurnett et al., 1996) and, along with the intracellular β subunit, help regulate trafficking, surface expression, α1 stability, and kinetics (Buraei and Yang 2013; Dolphin 2013). Some types of calcium channels also associate with transmembrane γ auxiliary proteins as well, and its effects are determined based on the isoform of beta subunit expressed (Yang et al., 2011).
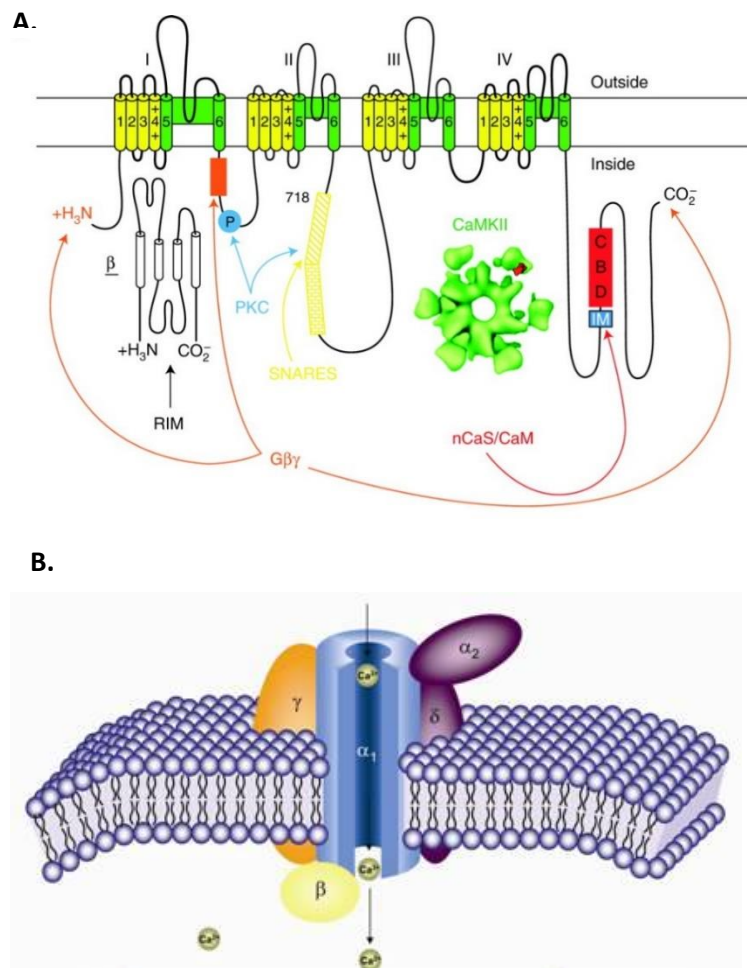
Figure 1.6: 2D and 3D structure of voltage-gated calcium channels. (A) Structure of the α1 subunit is comprised of four domains, each with 6 membrane-spanning helices. Interacting molecules, such as PKC, CaMKII, and the G protein βγ subunit modulate channel activity via association with the intracellular N- and C-termini, or intracellular loops. Figure adapted with permission from Cold Spring Harbor Laboratory Press. Catterall W.A., *Cold Spring Harb Perspect Biol* 2011;3:a003947. (B) Calcium channel complex with auxiliary subunits embedded in the membrane. These subunits influence trafficking, surface expression, and behavior of the channel itself. Figure courtesy of Dr. Tuck Wah Soong, Yong Loo Lin School of Medicine, National Singapore University.

The focus of much of this work involves the increased calcium flowing through neuronal L-type (Ca$_v$ 1.2 and 1.3) LTCCs. These LTCCs can be distinguished from other VGCCs by their sensitivity to dihydropyridines (Kanngiesser et al., 1988). However there is not a pharmacological means to separate the 4 isoforms of LTCCs; a series of knockout studies and experiments done in heterologous expression systems have attempted to describe the differences in function. Global knockout of Ca$_v$ 1.2 led to embryonic lethality because of its importance in the heart (Seisenberger et al., 2000). However, conditional knockouts of Ca$_v$ 1.2 in the cerebral cortex and hippocampus showed a loss of late phase long term potentiation and impairment of spatial memory formation (Moosmang et al., 2005; White et al., 2008). These data were associated with decreased cyclic AMP response element (CRE) dependent transcription in the CA1 region of the hippocampus, linking Ca$_v$ 1.2 with impairment in memory formation. The generation of Ca$_v$ 1.3 knockout animals has suggested a specific function for this LTCC subtype as well. Studies examining these animals revealed no obvious phenotypic defect or problems with motor function (Platzer et al., 2000). Instead, Ca$_v$ 1.3 mice are deaf, corresponding to a role for L-type current in cochlear hair cells (Platzer et al., 2000). In addition, conditional knockout of Ca$_v$ 1.3 also showed diminished slow afterhyperpolarization, an attribute often associated with increased learning and memory (Gamelli et al., 2011).

Several biophysical differences described between Ca$_v$ 1.2 and Ca$_v$ 1.3 are based primarily on work done in *Xenopus* oocytes. First, the activation threshold for Cav 1.3 is substantially more negative (around -55 mV) than for Ca$_v$ 1.2 (around -30 mV, Lipscombe et al., 2004). This means that Ca$_v$ 1.3 channels may activate at

depolarizations that are below threshold for action potential generation, which could indicate involvement in different signaling pathways. Second, dihydropyridines do not antagonize channels equally (Xu and Lipscombe 2001). For example, the sensitivity to LTCC antagonist nimodipine varies widely: IC_{50} for Ca_v 1.2 is 139 nM, whereas for Ca_v 1.3 it is 3 μM (Xu and Lipscombe 2001). Thus, early studies using a low micromolar concentration may still have some LTCC contribution to overall current. Finally, Ca_v 1.2 channels open significantly faster than do Ca_v 1.3 channels (Xu and Lipscombe 2001). Notably, these studies were done in heterologous expression systems, where auxiliary subunits and potentially other interacting proteins were missing. Whether these differences exist in native neurons is unknown.

Not only are there functional differences in the properties of Ca_v 1.2 and Ca_v 1.3, but there are differences in expression patterns as well. 80% of LTCCs in the brain are composed of the Ca_v 1.2 isoform compared to 20% Ca_v 1.3 (Hell et al., 1993). However, during hippocampal development, the composition is changing. During the early neonatal period, expression of Ca_v 1.2 was relatively high, but began to decrease by P12 (Kramer et al., 2012). This is in contrast to Ca_v 1.3, whose expression levels were low at P0 but increased steadily into adulthood (Kramer et al., 2012). Thus, any developmental phenomenon that correlates with a change in LTCC may involve the Ca_v 1.2 isoform, because of its relatively higher abundance during development.

Protein kinase C

Protein kinase Cs (PKCs) are a family of serine/threonine protein kinases that serve as secondary effectors in diverse pathways, from immune responses to regulation of

transcription. Currently, there are 15 known isozymes of PKC, with divisions based on

requirements for activation (table 3, reviewed in Zeng et al., 2012; Wu-Zhang and

Newton 2013). Conventional isozymes require both DAG and calcium to be activated,

whereas novel isozymes require DAG but not calcium. Atypical PKCs require neither

calcium nor DAG for activation. Many PKC isozymes may exist within a single cell,

though their method of activation and localization may be different (Roisin and Barbin

1997). Therefore, it is possible for many PKCs to regulate the activity of a single cell,

depending on the subcellular localization of PKC. Structurally, PKCs are generally

comprised of regulatory domains (C1 and C2) and a catalytic domain (C3 and C4),

connected by a linking domain (Figure 1.7, PKC structure reviewed in Steinberg 2008).

There is also a pseudosubstrate that binds the catalytic domain. The C1 domain contains

the binding site for DAG as well as phorbol esters, which are structural analogs of DAG

that mimic its activity. Work presented here focuses on the actions of specific

conventional and novel isozymes of PKC because the effect of $GABA_B$ receptor

activation on calcium current is mimicked by phorbol ester activation (Bray and Mynlieff

2011). The C2 domain binds phosphatidylserine (PS) and calcium in conventional

isozymes, but sequence alignment shows the calcium binding segment of the protein is

absent in novel and atypical PKCs; thus there is no calcium required for activation of

PKC Family	Isoforms	Requirements for activation	Phorbol ester sensitivity
Conventional	$\alpha, \beta_I, \beta_{II}, \gamma$	Calcium, DAG, phospholipids	Sensitive
Novel	$\delta_I, \delta_{II}, \delta_{III}, \epsilon, \eta, \theta$	DAG, phospholipids	Sensitive
Atypical	$\iota, \zeta, \lambda,$	Phospholipids	Insensitive

Table 3: 3 Families of PKC isozymes are divided based on their requirements for activation. Only the conventional and novel isoforms are sensitive to phorbol esters.

these isozymes. To become catalytically active, the C1 domain must bind DAG;

anchoring proteins help position PKCs near the membrane. A phospholipid, most

commonly PS, also embedded in the membrane, binds to the C2 domain, which causes a

conformational change in the PKC such that the pseudosubstrate is removed. For

conventional isozymes, binding of calcium to the C2 domain increases its affinity for PS.

With the pseudosubstrate removed, other proteins such as receptor for activated C kinase

(RACK) help position PKCs close to their substrates (Schechtman and Mochly-Rosen

2001). The active site of the catalytic domain is a bilobal structure, which forms a cleft.

It is within this cleft that both ATP and the substrate bind. Importantly, a hallmark of

PKC activation is the necessity for translocation to the plasma membrane.

All PKC isozymes are expressed in the mammalian central nervous system.

However, their expression levels vary widely during development (Roisin and Barbin

1997).   For example PKC γ is not expressed embryonically; only after P14 is any

expression detectable when it begins to rise rapidly. This is in contrast to an isoform

such as PKC ε, where expression is already high at the earliest time point examined, E17.

It continues to increase, though much more gradually than PKC γ. Expression also varies

depending on the tissue examined. In cardiac tissue, PKCα is expressed at a relatively
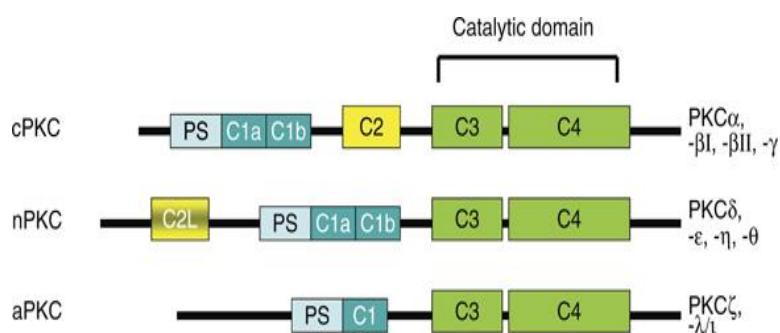
Figure 1.7: Domain classifications of the 3 PKC families. PS, phosphotidylserine binding domain; C1a, C1b, C2, calcium binding domains; C2L, calcium-like domain; C3 and C4, catalytic domain. Adapted by permission from Macmillan Publishers Ltd: [*Journal of Investigative Dematology*] (**129**, 2330-2332), copyright (2012).

high level in embryonic day 14 (E14) rats, with expression peaking in the neonate. As the animal ages, PKCα expression decreases threefold by adulthood (Rybin and Steinberg 1994). In hippocampal tissue, PKCα is low at E17 and steadily increases into adulthood. At P7, expression has reached approximately half its maximal expression and has increased almost fivefold from embryonic levels (Roisin and Barbin 1997). These expression data are pertinent for experiments attempting to determine the identity of a particular isozyme at a given age.

PKCs have been shown to phosphorylate L-type channels on both the I-II and II-III intracellular loops (Zamponi et al., 1997). How this phosphorylation modifies channel behavior and L-type current is still not clear, as both an increase and a decrease in L-type current have been reported. Differences in response vary with cell type as well as with the isozyme of PKC that is activated. For example, when α-adrenergic receptors were stimulated in cardiac myocytes, L-type current was enhanced in a PKC dependent manner. Notably, this pathway also required the activity of calcium/calmodulin dependent kinase II (CaMKII, O-Uchi et al., 2008). In heterologous systems, PKC activation with phorbol esters reduced whole cell current of Ca_v 1.3 channels (Baroudi et al., 2006). Furthermore, single channel recording of Ca_v 1.3 channels showed PKC activation decreased mean open time, increased mean closed time, and thus led to a reduction in open probability (Chahine et al., 2008). In some cases, L-type current is not affected at all. In dorsal root ganglion neurons obtained from embryonic mice, PKC activation did not change L-type current while decreasing N-type current (Gross and MacDonald 1989). Most important to the work presented here, $GABA_B$ receptor mediated calcium enhancement through L-type channels in neonatal hippocampal

cultures requires PKC activity (Bray and Mynlieff 2011). When a host of inhibitors are used, enhancement is abolished. Conversely, when phorbol esters are used to mimic activation, the enhancing response is observed. Thus, it is difficult to make broad statements about the functions of PKCs and L-type calcium channels because any change in condition (source of cells, age of the animal, isozyme of PKC) seems to produce a unique response.

Calcium/Calmodulin-dependent Protein Kinase II

CaMKII is found throughout the brain, where it makes up 1-2% of total protein. Structurally, it has a unique arrangement; there are twelve functional domains attached to a gear-shaped core (Fink and Meyer 2002). The twelve subunits are grouped into what appears to be two stacked hexamers; each subunit contains a catalytic, autoregulatory, and association domain (Figure 1.8). There are two primary subunits in neurons, α- and βCaMKII. Isoforms have a high sequence identity, with the exception of a 30 amino acid insertion in the β isoform. As a serine/threonine kinase, the catalytic domain binds both ATP and substrate; however the autoregulatory domain contains a pseudosubstrate site that binds to the catalytic domain, preventing catalytic activity. Perhaps the most important residue of CaMKII is Thr 286 (or Thr 287 in βCaMKII). When this residue is phosphorylated, the pseudosubstrate can no longer associate with CaMKII and autoinhibition is removed, and thus the catalytic domain is active. In a stepwise process, CaMKII will autophosphorylate and become active, even if calcium and calmodulin are no longer present (for more detailed review on CaMKII activation, see Hudmon and Schulman 2002b; Hudmon and Schulman 2002a). Studies have shown that L-type

channels are substrates for CaMKII. Both the α1 subunit (Hudmon et al., 2005) and specific beta isoforms of Ca_v 1.2 (Abiria and Colbran 2010) are shown to be phosphorylated. In either case, the calcium currents are enhanced through calcium-dependent facilitation, with sites of phosphorylation on the Ca_v 1.2 α1 subunit having been identified (Blaich et al., 2010). Ca_v 1.3 channels are also phosphorylated by CaMKII, but in a more indirect manner. CaMKII enhancement of Ca_v 1.3 currents occurs only in the presence of the protein densin, which has a binding site on the C-terminal tail of Ca_v 1.3 (Jenkins et al., 2010). Neither CaMKII nor densin alone will produce this current enhancement, but together, the two augment L-type current during repetitive stimuli. Thus, both neuronal forms of L-type channels have CaM binding sites, both are substrates for CaMKII, and both demonstrate current enhancement when phosphorylated by CaMKII. Since PKC, a known component of the pathway by which $GABA_B$ receptors lead to L-type current enhancement, has also been shown to phosphorylate CaMKII, and since CaMKII can enhance L-type current, part of the work described herein was to examine the potential role CaMKII may play in the enhancement of L-type current by $GABA_B$ receptors.

The current research focuses on determining the G protein that mediates calcium current enhancement, the isozyme of PKC that is involved in the pathway, and whether or not CaMKII participates in L-type calcium current enhancement.
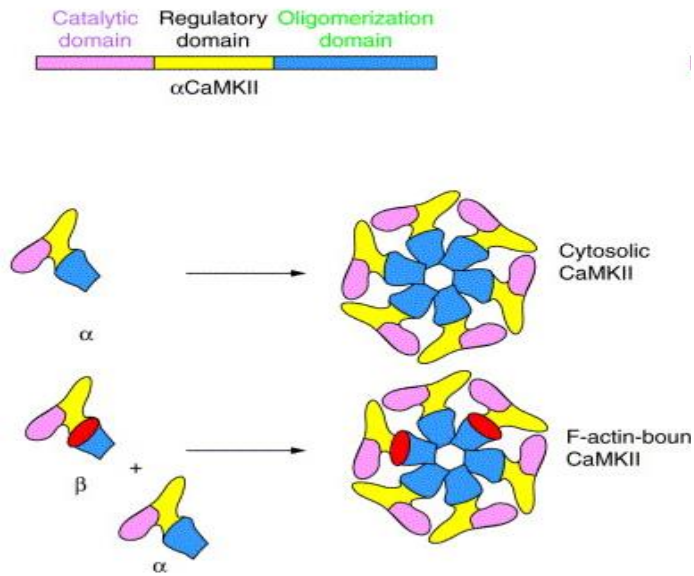
Figure 1.8: Domain organization and assembly of CaMKII. (a) A single subunit of CaMKII includes, a regulatory, catalytic, and oligomerization domain. (b) Twelve subunits assemble into a double hexemer. The highly homologous βCamKII subunit includes an F-actin localization insert for trafficking to the post-synaptic density. Adapted from *Current Opinion in Neurobiology*, 12(3). Fink, C.C. and Meyer T., Molecular mechanisms of CaMKII activation in neuronal plasticity, pp. 293-299, Copyright (2002), with permission from Elsevier.

CHAPTER 2

MATERIALS AND METHODS

Isolation of hippocampal neurons by cell culture

All animal protocols were approved by the Marquette University Institutional

Animal Care and Use Committee and followed guidelines provided by the United States

Public Health Service. Hippocampal neurons were isolated by a method that is specific

for postnatal rats and has been shown to keep neurons alive for up to three weeks in

culture (Mynlieff 1997). Sprague-Dawley rat pups aged 6-8 days postnatal were

anesthetized with CO_2 and immediately sacrificed by decapitation. The head was placed

in 70% ethanol for 3 minutes for sterilization, then rinsed in sterile rodent Ringer's

solution (146 mM NaCl, 5 mM KCl, 2 mM $CaCl_2$, 1 mM $MgCl_2$, 10 mM HEPES, 11 mM

D-glucose, pH 7.4 with NaOH). Dissections were performed within a NuAire table top

horizontal airflow workstation (Plymouth, MN) using sterile technique. The hippocampi

were excised from the brain and placed into cold (5˚C) sterile rodent Ringer's solution

with glucose bubbled with 100% oxygen. Hippocampi were sliced into sagittal sections

and transferred into PIPES-buffered saline (120 mM NaCl, 5 mM KCl, 1 mM $CaCl_2$, 1

mM $MgCl_2$, 25 mM D-glucose, 20 mM piperazine-N,N'-bis[2-ethanesulfonic acid], pH

7.0 with NaOH). The superior region of the hippocampi was isolated to reduce

heterogeneity of cultured neurons. The superior region was further cut into 1 mm^3

sections and placed in a sterile 3 mL glass vial. 1 mL of 0.5% trypsin and 0.01% DNase I

(Sigma-Aldrich, St. Loius, MO) in PIPES-buffered saline was added to the vial. Tissue

was incubated at room temperature for 30 minutes with 100% oxygen blown over the top

of the solution to allow the trypsin to permeate the tissue. A second incubation at 37˚C

for one hour followed, to maximize the proteolytic activity of the enzyme. The tissue

was rinsed with 1 mL trypsin inhibitor solution (1 mg/mL trypsin inhibitor, Type II-O:

chicken egg white (Sigma-Aldrich, St. Louis, MO) and 1 mg/mL bovine serum albumin)

in rodent Ringer's solution, then rinsed with Neurobasal-A growth media fortified with

B27 supplement (Life Sciences, Carlsbad, CA), 0.5 mM glutamine and 0.02 mg/mL

gentamicin. The tissue was placed in 1 mL fresh growth media and vigorously triturated

with a fire-polished Pasteur pipette. For electrophysiological experiments cells were

plated on 35 mm sterile culture dishes previously coated with poly-L-lysine (MW 38,500

– 60,000, Sigma –Aldrich, St. Louis, MO) dissolved in 0.15 M boric acid (pH 8.4 with

NaOH), as described in Mynlieff (1997). For calcium imaging experiments, cells were

plated on a glass 22x22 mm coverslip coated with poly-L-lysine. For confocal imaging

experiments, 75 µL of cell culture suspension was placed onto the poly-L-lysine-coated

glass center of a modified plastic cell culture dish (MatTek Corporation, Ashland MA).

Neurons settled at the bottom of the dish before adding $1 - 2$ mL of fresh media per dish.

Dishes were then placed in a 5% CO_2 water-jacketed sterile incubator maintained at 37˚C
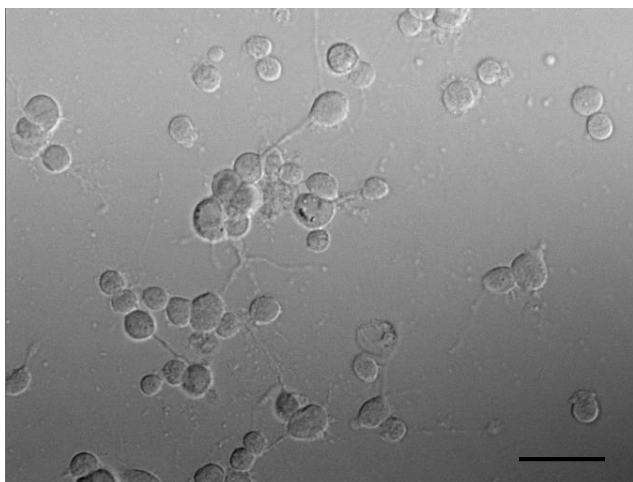
Figure 2.1: Appearance of neurons in culture after 24 hours. Cells appear spherical and many have begun to display characteristic branched morphology. Bright field image taken at 40x magnification. Scale bar = 20 µM.

for 24 –48 hours (Figure 2.1).

The use of cultured neurons within 20 – 24 hours for electrophysiological recording provides time for reinsertion of channels and receptors that may have been sheared off during enzymatic and mechanical digestion. Furthermore, process outgrowth is minimized, allowing for voltage control over the entire cell and preventing space clamp problems characteristic of electrophysiological recordings performed on neurons with long processes. Previous data from the laboratory showed that neurons in culture are still able to fire and display characteristic electrophysiological properties after enzymatic and mechanical digestion (Mynlieff 1997; Mynlieff 1999). Importantly, the U-tube delivery system of pharmacological compounds provides a means to apply compounds to a much smaller group of cells minimizing exposing the rest of the population of neurons to these compounds in the same culture dish.

One advantage to calcium imaging versus electrophysiology its high throughput. Electrophysiology samples only one cell at a time, whereas data acquisition via calcium imaging allows for measuring calcium influx in up to 50 cells per capture. A second advantage of calcium imaging is that cells with growing processes can easily be included in recordings. This is more difficult in electrophysiological experiments because of space clamp problems in cells with long axons or dendrites. Thus, while electrophysiology provides a much more accurate temporal resolution, calcium imaging offers some distinct advantages when used to measure calcium influx.

Culturing neurons for confocal microscopy allows the experimenter to treat with various compounds, then fix the cells in order to understand changes that those compounds may have caused. For example, activation of $GABA_B$ receptors is thought to

mobilize PKC and cause its translocation from the cytosol to the membrane of the neuron. By adding $GABA_B$ agonist baclofen to the culture and fixing it immediately, the movement of PKC can be assayed via immunostaining. This type of direct application and image analysis is more difficult in a slice, where pharmacological treatment will likely not reach all neurons in the slice. Furthermore, the detail of changes occurring within a single cell in isolation is easier to resolve than examining the changes of a single cell within a densely populated hippocampal slice.

The use of hippocampal cell cultures isolated from postnatal rats provides a useful system to study a $GABA_B$ receptor-mediated response. While embryonic cultures contain a large percentage of excitatory pyramidal neurons, postnatal cultures contain a greater percentage of GABAergic interneurons. Indeed, cultures from a 7 day postnatal rat showed $41.8 \pm 5.0\%$ of the neurons were immunoreactive for anti-GABA antibodies, suggesting these cells were inhibitory interneurons (Mynlieff 1997). A complication of working with primary hippocampal cultures is that there is no way to select for cell type specificity. For example, there are at least 16 types of inhibitory interneurons based on electrophysiological and immunocytochemichal profiles, as well as a large percentage of pyramidal neurons; in either calcium imaging or electrophysiology, it cannot be determined what type which type neuron is being examined without post-recording immunolabeling or single cell PCR.

Protein preparation and Western blotting

To prepare protein samples for Western blot analysis, whole hippocampal tissue samples were isolated from P6-P8 rats by sacrificing the rat and excision of the

hippocampus as described above, followed by homogenization of the tissue in ice-cold sucrose buffer (250 mM sucrose, 10 mM Tris, 10 mM HEPES, 1 mM EDTA, pH 7.2) with fresh protease inhibitors (1 ug/mL leupeptin, 0.5 mg/mL pepstatin, 0.5 mg/mL Pefabloc, Sigma-Aldrich, St. Louis MO). To isolate membrane-bound proteins, homogenized tissue was centrifuged at 3,622 x g for 10 minutes at 4˚C, followed by centrifugation of the supernatant at 39,104 x g for 30 minutes. The pellet from this centrifugation step was resuspended in sucrose buffer with protease inhibitors and stored at -80˚C until samples were analyzed via Western blot. In order to prepare cell culture samples for Western blot analysis, hippocampal cultures were obtained from 8 rats, yielding 24 dishes. Each dish was rinsed twice in ice cold phosphate buffered saline (PBS, 134.4 mM NaCl, 4.36 mMKCl, 10.56 mM Na_2HPO_4, 1.66 mM $Na_2H_2PO_4$, pH 7.4 with HCl). 1 mL of sucrose buffer with protease inhibitors was added to each of the 24 dishes, neurons were scraped from the dishes, and the suspension was centrifuged at 30,427 x g for 10 minutes. The pellet was resuspended in sucrose buffer with protease inhibitors and spun at 3,622 x g for 10 minutes. The supernatant was spun a final time at 48,497 x g for 30 minutes. The resulting pellet was resuspended in 30 μL sucrose buffer with protease inhibitors and stored at -80˚C until samples were analyzed by Western blot. To increase protein yield in the preparations, in certain experiments the cytosolic and membrane fractions were separated using ultracentrifugation based on a protocol from Wang et al., (2003). Cells were washed in Wang's buffer (20 mM Tris, 2.5 mM EGTA, 1 mM EDTA, 100 mM NaF, pH 7.5 with HCl). Protease inhibitors listed above were added, plus 2 mM dithiolreitol after 2 rinses in Wang's buffer. The neurons were scraped and spun at 30,427 x g for 8 minutes. The pellet was resuspended in Wang's buffer and

spun at 4,492 x g for 10 minutes. The supernatant was collected and spun at 100,000 x g for 45 minutes. After this spin, the supernatant was collected and retained as the cytosolic fraction. The pellet was resuspended once more in Wang's buffer plus 0.1% Triton-X 100. The suspension was spun at 30,427 x g for 15 minutes, and the supernatant was retained as the membrane fraction. All spins were done at 4˚C. Protein concentrations were measured with a biophotometer (Eppendorf North America, Hauppauge NY).

NuPage lithium dodecyl sulfate sample buffer (Life Sciences, Grand Island, NY) and reducing agent (500 mM dithiothreitol in PBS) were added to protein preparations and heated to 70˚C for 10 minutes. Preparations were run on a 12% Bis-Tris Novex Minigel® (Life Sciences, Grand Island, NY). Proteins were transferred onto a polyvinylidene difluoride membrane with a pore size of 0.45 µM. Membranes were washed for 5 minutes with PBS, then blocked for 1 hour with PBS plus 0.05% Tween, 5% nonfat dry milk, and 0.1% bovine serum albumin at room temperature. The membranes were decorated with primary antibodies added to the PBS blocking solution by rocking them overnight at 4˚C using antibodies listed in Table 4. Membranes were then brought to room temperature, rinsed in PBS with 0.05% Tween, and probed with either goat anti-rabbit or goat anti-mouse horseradish peroxidase conjugated secondary antibody (table 4) for 90 minutes at room temperature. The secondary antibodies were rinsed from the membrane with PBS and 0.05% Tween, protein bands were visualized on classic blue autoradiography film (Molecular Technologies, St. Louis, MO.) after a 5 minute exposure to SuperSignal West Dura Extended Duration chemiluminescent substrate (Pierce, Rockford IL).

Primary Antibody	Source	Host Species	Dilution	Application
$G\alpha_q$ alpha subunit	Genetex	Rabbit	1:500; 1:1000	Western blot; immunostaining
$G\alpha_{11}$ alpha subunit	Genetex	Rabbit	1:1000	Western blot
α/β tubulin	Cell Signaling Technologies	Rabbit	1:2000	Western blot
$GABA_B$ receptor B1 subunit	Neuromab	Mouse	1:1000	Immunostaining
GAD-6	Hybridoma Bank	Mouse	1:2000	Immunostaining
Secondary Antibody	**Source**	**Species**	**Dilution**	**Application**
Dylight 488	Thermo-Pierce	Goat-Anti Rabbit	1:1000-1:2000	Immunostaining
Dylight 550	Thermo-Pierce	Goat-Anti Mouse	1:1000-1-2000	Immunostaining
HRP-conjugated	Thermo-Pierce	Goat-Anti-Rabbit	1:2000-1:2500	Western blot

Table 4: List of primary and secondary antibodies used in experiments.

To quantify protein visualized via Western blotting, the integrated optical density (IOD) of each band was measured using Labworks 4.6 software (UVP, Inc., Upland CA). To control for gel loading, each lane was loaded with the same amount of protein as determined by measurement on a biophotometer. This was further controlled for by dividing the IOD for each protein of interest by the IOD of a control antibody (α/β-tubulin, Table 4) in the same lane. At least two separate samples were analyzed for each experiment.
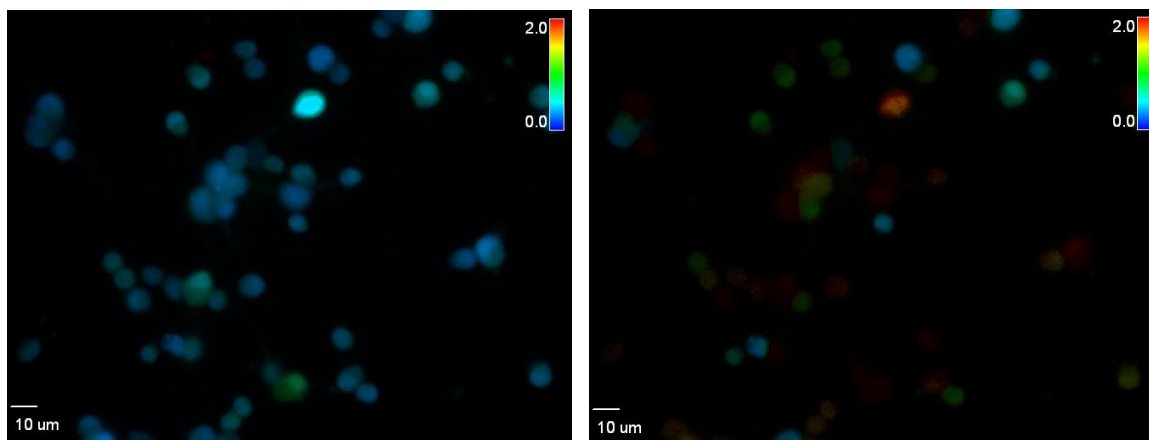
Figure 2.2: Image of cultured cells after 24 hours loaded with ratiometric Fura-2 AM dye. (Left) field of cells under nonstimulating conditions. (Right) same field of cells stimulated with 50 mM KCl show characteristic change in fluorescence.

Calcium Imaging

Cultured neurons on glass coverslips were incubated in 5 μM Fura-2 acetoxymethyl ester (Fura-2 AM, Life Technologies, Carlsbad CA) in calcium imaging Ringer's solution (CIR, 154 mM NaCl, 5.6 mM KCl, 2 mM $CaCl_2$, 1 mM $MgCl_2$, 10 mM HEPES, 11 mM glucose, pH 7.4 with NaOH) for 1 hour at room temperature in the dark. Cells were rinsed and incubated for 30 min at room temperature in CIR without Fura-2 AM to allow for de-esterification. Depolarization was induced by perfusion with high potassium solution (100 mM NaCl, 50 mM KCl, 2 mM $CaCl_2$, 1 mM $MgCl_2$, 10 mM HEPES, 11 mM glucose, pH to 7.4 with NaOH) for 30 seconds to open voltage-gated calcium channels (Figure 2.2). Throughout experiments, CIR was continually perfused at a rate of 2 mL/minute. Application of high KCl and/or pharmacological agents were perfused at approximately 3 pSi, producing perfusion at a rate greater than 5 times that of CIR perfusion.Each experiment consisted of an initial perfusion of KCl alone, followed by coapplication of KCl and pharmacological agents (Table 5). A final KCl stimulation was performed after drug treatment. The initial and final KCl responses were averaged

and compared with the response of KCl plus pharmacological agents. These agents were

perfused onto the cells for 15 seconds before addition of high KCl solution. Cells were

excited at 340 and 380 nm, and emissions were measured at 510 nm using Slidebook 5.0

software (Intelligent Imaging Innovations, Denver CO). The ratio of the emissions

intensity when Fura-2 is excited at 340 and 380 nm is directly correlated to changes in

intracellular calcium (Grynkiewicz et al., 1985). Control experiments were performed in

which the cell was stimulated 3 consecutive times with KCl. The initial and final

responses were averaged together, and compared with the middle response. This allowed

for determination of inherent variability within the system. The standard deviation for

the middle response, compared to the average of the initial and final responses, was

$\pm 11.20\%$. In order for a cell to be classified as "increasing" or "decreasing" in response

to 10 µM baclofen treatments during depolarization, a neuron had to show a response of

$\pm 21.4\%$ that of KCl controls, which represented two standard deviations from control

values. Average data represent the mean $\pm$ SEM.

Confocal imaging

Whole hippocampi from P6-P8 rats were excised and fixed in 4%

paraformaldehyde for 30 minutes at 4˚C. Hippocampi were cryoprotected in PBS

solution containing 30% sucrose for 90 minutes at 4˚C. The tissue was embedded in

optimal cutting temperature mounting medium (OCT, Sakura Finetek, Torrance, CA) and

frozen on dry ice. 20 µM transverse sections were sliced on a cryostat and placed on

glass slides. Hippocampal sections were permeabilized in PBS with 0.5% Triton X-100

for 20 minutes, then blocked for nonspecific binding with 10% goat serum (Life

Sciences, Carlsbad, CA) in PBS with 0.05% Triton X-100 for 60 minutes. Primary

antibodies were made in PBS with 0.05% Triton X-100 and 0.1% goat serum and were

incubated with the sections for 2 hours at room temperature. A list of primary antibodies

used can be found in table 4. After incubation, sections were rinsed 3 times in PBS

before addition of Dylight 488- and 550-conjugated secondary antibodies (Thermo

Scientific, Rockford IL) for 1 hour. (See Table 4 for specific dilutions and sources.)

After another 3 rinses, mounting medium with 4,6 diamidino-2-phenylindole (DAPI,

Vector Laboratories, Burlingame, CA) was applied, slides were covered with a glass

coverslip and sealed.

For preparation of cultured cells for confocal analysis, a similar procedure was

followed except as noted here. Cells grown on tissue culture dishes modified with glass

bottoms were fixed with 4% paraformaldehyde after removal of neurobasal A growth

media. Fixed cells were rocked with primary antibodies overnight at 4˚C before

decoration with secondary antibodies (See Table 4).

Images were acquired on a Nikon Perfect Focus Ti-E confocal microscope and

were analyzed on NIS Elements imaging software (Nikon Instruments, Melville, NY).

To determine colocalization in slices, regions of interest (ROIs) were selected from areas

within the stratum oriens, pyramidal cell layer, stratum radiatum, and dentate granule cell

layer. Prior to quantification, background fluorescence was removed by measuring

brightness of each fluophore in preparations not treated with primary antibodies, then

subtracting that brightness value from that of experimental slides. The Pearson

correlation coefficient (PCC) was determined for each region to quantify the degree of

colocalization between $G\alpha_q$ and $GABA_B$ receptors in each region. A higher PCC is

suggestive that proteins of interest are located in close proximity. PCC values were averaged by region, then compared via one-way ANOVA. When acquiring images to average and compare, microscope settings (scan speed, pinhole size, laser intensity) were not changed to allow for comparison across different preparations.

Electrophysiology

Calcium currents were measured using whole cell patch clamp electrophysiology in voltage clamp mode. Currents were collected using a Dagan 3900A patch clamp amplifier (Dagan Corporation, Minneapolis, MN), Digidata 1322 data acquisition system, and pClamp 9.0/10.0 software (Molecular Devices, Sunnyvale, CA). Recording immediately after dissociation minimizes space clamp problems, but in order to let the neurons recover from digestion and allow for sufficient knockdown, experiments were performed 24-48 hours after dissection. A Flaming/Brown P-87 Micropipette Puller (Sutter Instrument Co, Novato, CA) was used to pull electrodes of 4-10 MΩ from borosilicate glass capillary tubes. Pipettes were filled with internal solution (140 mM Cs-aspartate, 5 mM $MgCl_2$, 10 mM Cs_2EGTA, 10 mM HEPES, 2 mM ATP-Na_2, 0.1 mM GTP, pH 7.4 with CsOH and osmolarity of $310 - 320$ mOsm); neurons were kept in extracellular solution (10 mM $CaCl_2$, 145 mM TEACl, 10 mM HEPES, 1 μM tetrodotoxin (Tocris Bioscience, Bristol, United Kingdom), pH 7.4 with CsOH and osmolarity $300 - 310$). Whole cell currents were electronically filtered at 1 kHz and digitized at 2 kHz. Linear components of leak current were subtracted post-hoc by the passive resistance protocol in the pClamp 9.0/10.0 software.

To study drug effects on maximally achieved calcium currents, neurons were depolarized for from -80 mV to +10 mV for 300 ms. Analysis was performed during the last 50 ms of this pulse (the sustained component of the calcium current) to maximize the contribution of L-type (long lasting) current to total current (Figure 2.3). However, it is likely that there is contribution from the other types of HVA currents (P/Q-type, N-type, R-type), despite work showing that these channels inactivate much faster ($\tau = 50 - 80$ ms versus $\tau > 500$ ms for L-type calcium current (Tsien et al., 1988). In certain experiments, to reveal primarily L-type current, P/Q-type and N-type current were blocked with application of 1 µM ω-conotoxin MVIIC ($IC_{50} = 40$ nM, (Gandia et al., 1997). To examine the current-voltage relationship with and without baclofen, neurons were held at -80 mV and depolarized by a series of 10 mV steps from -50 mV to +50 mV. For electrophysiological studies, various drugs were applied on the order of seconds via U-tube delivery system. The U-tube was constructed of PE-10 polyethylene tubing housed in glass tubing, which allows for both rapid application and washout of pharmacological agents in an acute area. Fast Green FCF
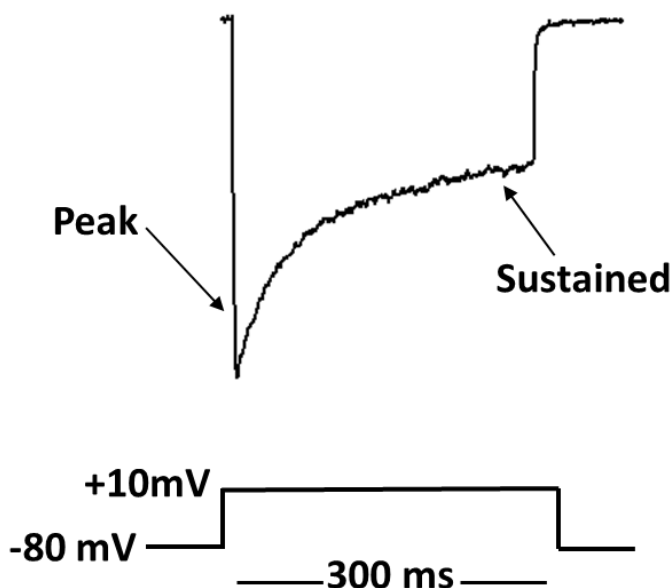
Figure 2.3: (Top) Typical calcium current trace elicited, containing both a peak and sustained component. (Bottom) Depolarizing pulse given for 300 ms from -80 to +10 mV.

(Sigma-Aldrich, St. Louis, MO) was added to the drug solution to visualize delivery. Table 5 contains concentrations of drugs used as well as their targets.

The core of research done in the Mynlieff laboratory is understanding how 10 µM baclofen, a $GABA_B$-specific agonist, enhances L-type calcium current. Since calcium currents often demonstrate either run-up or run-down in their current, multiple control depolarizations were given whenever possible. In order to characterize the response of neurons as either "increasing," "decreasing," or "no change" in their calcium currents, control pulses were given before application of baclofen, and again after washout. Control currents were plotted and a linear regression line was generated based on those controls, as well as a 95% confidence interval of this regression line. Neurons treated with baclofen were categorized based on where they fell with respect to the 95%
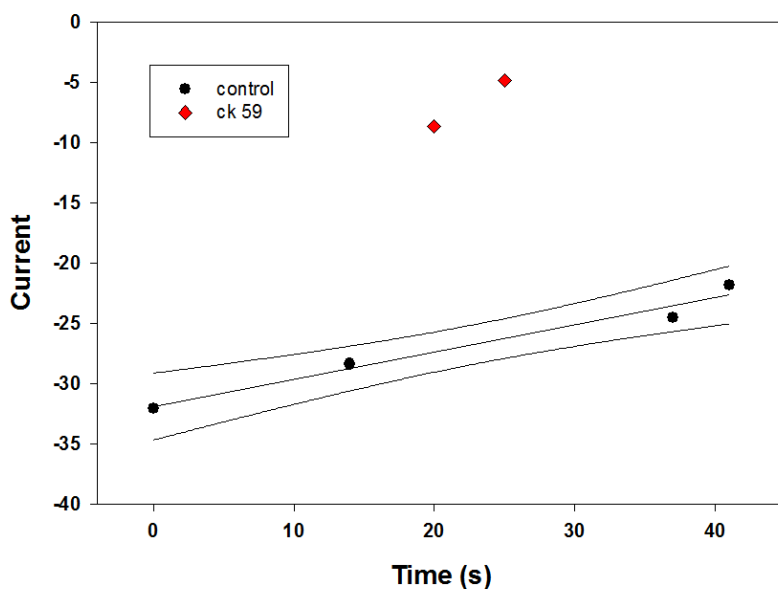
Figure 2.4: Representative linear regression trace with 95% confidence interval constructed. In this case, treatment with the drug (red diamonds) leads to currents that fall outside the confidence interval constructed from control pulses (black circles), suggesting a significant effect of the drug.

confidence interval. Furthermore, at any timepoint when pharmacological agents were applied, the linear regression equation allowed for calculation of an "expected" current

(that which would be expected if the agent were not present). This could then be compared with actual current when the agent was present (Figure 2.4)

Analysis of current-voltage (IV) data consisted of creating IV curves to describe L-type current at various voltages in either neurons treated with 10 μM baclofen or controls. Conductance values were calculated at each voltage step by dividing peak current elicited by the driving force. Driving force is the difference between the neuron's membrane potential and the reversal potential for an ion. It is defined by the equation $I_{ion} = g_{ion}(V_m - E_{ion})$, where $V_m - E_{ion}$ is the driving force. Conductance plots were generated to examine whether there was a shift in the activation voltage (voltage that causes channels to begin to open and current to be measured) or voltage that elicits half maximal current ($V_{1/2}$) in those neurons treated with baclofen.

Pharmacological Agent	Source	Concentration	Pharmacological Activity	IC_{50}/EC_{50}
RS-Baclofen	Sigma-Aldrich	10 μM	Activate $GABA_B$ receptors	2.8 μM
ω-Conotoxin MVIIC	Sigma-Aldrich	1 μM	Block N- and P/Q-type calcium channels	40 nM
Nimodipine	Sigma-Aldrich	20 μM	Block L-type calcium channels	140 nM – 2.7 μM
Nifedipine	Sigma-Aldrich	20 μM	Block L-type calcium channels	3 μM
CamKIIntide	EMD-Millipore	250 nM	Inhibit CaMKII signaling	50 nM
Ant-AIP-2	EMD-Millipore	50 nM	Inhibit CaMKII signaling	4 nM
CK59	EMD-Millipore	Various	Inhibit CaMKII signaling; block voltage-gated calcium channels	>10 μM for CaMKII; 52 μM for calcium channels

Table 5: Listing of pharmacological agents used in various studies

Protein knockdown with morpholinos

In order to selectively knock down proteins of interest, morpholinos (Gene-Tools LLC, Philomath, OR) were used to prevent translation of mRNA. Morpholinos (MO) are synthetic 25 amino acid-long oligos that are designed to bind near the start codon of specific mRNA. This binding prevents association of the translational machinery to the mRNA, thus yielding decreased protein. Morpholinos have several advantages over more traditional siRNA-mediated knockdown. First, because they are synthetic, MO are not subject to enzymatic degradation that often break down siRNA over time. Second, they achieve a highly specific knockdown, in contrast to siRNA mediated knockdown in which off target effects may occur. Finally, successful siRNA mediated knockdown in primary neuronal cultures has proven more difficult than in other cell types. Thus, the use of MO to achieve protein knockdown represents a viable and innovative alternative to more commonly used knockdown methods.
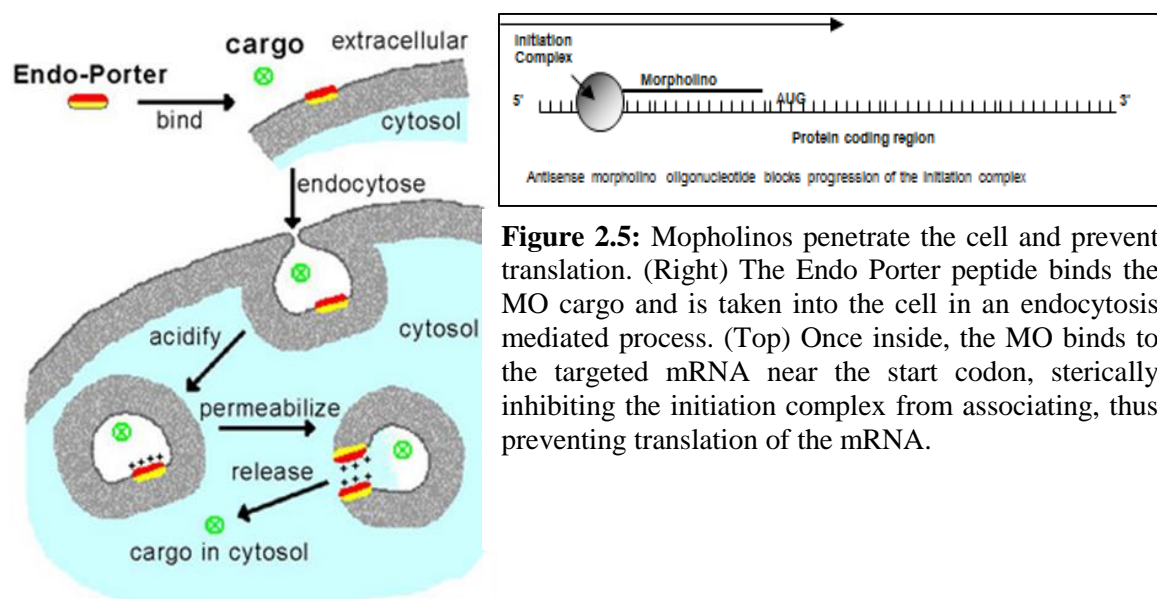
Figure 2.5: Mopholinos penetrate the cell and prevent translation. (Right) The Endo Porter peptide binds the MO cargo and is taken into the cell in an endocytosis mediated process. (Top) Once inside, the MO binds to the targeted mRNA near the start codon, sterically inhibiting the initiation complex from associating, thus preventing translation of the mRNA.

Morpholinos were introduced to cell cultures immediately after plating.   In order for the cell to take up the MO, the MO were cotransfected with EndoPorter, a proprietary peptide that brings "cargo" into the neurons via an endocytosis-mediated process. Control experiments were done with a variety of EndoPorter concentrations (2-10 µM) to ensure there were no cytotoxic effects. Delivery of MO was assessed using MO with a carboxyfluorescein tag fused to its 3' end, then examined with fluorescent microscopy. The sequence of the morpholino designed to knock down $G\alpha_q$ was 5' ACGCCATGATGGACTCCAGAGTCAT3'; it was delivered at a concentration of 2 µM together with 4 µM EndoPorter. Because G-proteins are known to have a relatively long half-life (Derrien et al., 1996), Western blot experiments were done to assay knockdown at both 24 and 48 hours post transfection. Control experiments were done on cell cultures treated with either a nonsense MO (5' AGCCAACGCCCCAATGATTCTGACT3') or cultures treated with EndoPorter only.

CHAPTER 3

<u>Demonstration of enhanced calcium entry upon GABA$_B$ receptor activation with</u>

<u>ratiometric calcium imaging and examination of IV relationship in cells that do not</u>

<u>demonstrate current enhancement</u>

INTRODUCTION

During early neonatal development, neuronal GABA receptors have been extensively studied. However, a large proportion of these studies involve the ionotropic GABA$_A$ receptor. GABA is considered the main inhibitory neurotransmitter in the mature mammalian nervous system; when GABA binds to its GABA$_A$ receptor, the receptor passes negatively charged chloride ions inward. This hyperpolarizes the neuron, and dampens excitability. However, in the developing nervous system, the chloride gradient is reversed, and GABA$_A$ receptor activation will allow for chloride efflux. Negative charge is lost from the cell, and this depolarization increases the cell's excitability (for review, see Ben-Ari 2002. Thus, there have been a multitude of studies examining this switch in chloride currents and changes in GABA$_A$ receptor function (Hutcheon et al., 2000; Banks et al., 2002; Bray and Mynlieff 2009; Holter et al., 2010; Kilb 2012).

The development of the metabotropic GABA$_B$ receptor is less well-defined. GABA$_B$-mediated potassium currents can be consistently recorded after the first postnatal week (Gaiarsa et al., 1995), and protein expression reaches adult levels after the second postnatal week (Lopez-Bendito et al., 2004). It has been suggested that GABA$_B$

receptors do not undergo a major functional alteration during development (Kilb 2012).

However work in the Mynlieff laboratory shows a potentially unique function of these

receptors during the early neonatal period. Activated GABA$_B$ receptors mediate both an

increase and decrease in calcium current; furthermore, the increase in calcium current

was through L-type calcium channels, while the decrease was through N-type calcium

channels. This inhibition has been previously described as occurring through N-type

channels; the mechanism of inhibition has also been detailed. (Guyon and Leresche 1995;

Harayama et al., 1998; Sun and Chiu 1999; Colecraft et al., 2000). Conversely, when

Carter and Mynlieff (2004) described the enhancement of L-type current in neonatal

hippocampal cultures, there was only one report of GABA$_B$ receptors enhancing such

current in neurons, in the salamander retina (Shen and Slaughter 1999). Unlike the

inhibition of N-type channels, the mechanism of this enhancement had not been clearly

worked out. Subsequent research in the Mynlieff laboratory revealed this enhancement

to be a developmental phenomenon. The proportion of neurons that demonstrate an

increase in response to GABA$_B$ receptor activation increases until P7, then decreases at

P14 (Bray and Mynlieff 2009). Thus, data from the Mynlieff laboratory suggest there is

a specific function of GABA$_B$ receptors during development.

Understanding how neurons regulate calcium levels during development is

critically important, as calcium is a crucial intracellular messenger. Calcium influx can

regulate neuronal differentiation, excitability, synapse formation, and gene transcription

(for review see Lohmann 2009; Michaelsen and Lohmann 2010; Hagenston and Bading

2011). L-type current is thought to be more involved with these processes than with

neurotransmission. Therefore, deciphering the pathway by which GABA$_B$ receptor

activation leads to increased intracellular calcium concentrations during neonatal development may be critical in understanding how mature neuronal circuitry is established.

The focus of this study was to provide further detail of the interplay between $GABA_B$ receptors and L-type current. Previous studies in the Mynlieff laboratory used whole-cell patch clamp electrophysiology to demonstrate L-type current enhancement and N-type current attenuation. However, the throughput of electrophysiology is low, so I sought to elucidate details of the pathway using the higher throughput method of ratiometric calcium imaging. Before examining any component of the $GABA_B$ receptor-mediated response, it was necessary to demonstrate this phenomenon was not an artifact of electrophysiological recording. Once calcium imaging was established as a viable method, the source of the calcium increase was investigated. Calcium concentrations are kept at low levels inside the cell, relative to extracellular concentrations. Calcium concentrations within the endoplasmic reticulum are high as well. While it has been shown that calcium current increases upon $GABA_B$ receptor activation, the contribution of calcium released from intracellular stores (i.e. the endoplasmic reticulum) was not known. Furthermore, in studies by Carter and Mynlieff (2004) and Bray and Mynlieff (2009, 2011), enhancement of L-type current always required depolarization to activate L-type channels. However, a recent report showed activation of $GABA_B$ receptors alone was sufficient to increase intracellular calcium levels (Kuczewski et al., 2011). I attempted to reproduce this effect to gain insight into a possible molecular mechanism for this enhancement. Finally, since I also observed an attenuation of calcium entry in a subset of cells, I sought to characterize the kinetic changes occurring, similar to how

Carter and Mynlieff (2004) described the enhancing effect by examining the change in activation voltage and conductance shift.

RESULTS

Ratiometric calcium imaging detects changes in intracellular calcium upon GABA$_B$

receptor activation

Previous studies in the Mynlieff laboratory have shown that cells treated with 10 µM baclofen may show changes in calcium current when these cells are given a depolarizing pulse from -80 to +20 mV. Cells showed a distribution of responses, where approximately 35% of neurons examined display attenuation of current, 25% of neurons display enhancement of current, and 40% of neurons do not display a significant effect on current. In order to examine whether this phenomenon could be demonstrated using ratiometric calcium imaging, cells were loaded with a ratiometric dye (Fura-2 AM) for 1 hour (see methods). Instead of a depolarizing pulse, neurons were treated with a high (50 mM) potassium chloride (KCl) solution to induce depolarization. 10 µM baclofen, a GABA$_B$ receptor-specific agonist, was preapplied for 15 seconds before the high KCl solution, as well as during the stimulation. High KCl was perfused onto the cells first for thirty seconds. After washout, baclofen and high KCl were coapplied. Following a final washout KCl was applied once again. The two high KCl alone values were averaged and compared with the middle (treatment) value.

Similar to electrophysiological data, calcium imaging data showed 3 distinct responses to baclofen treatment. In initial studies, 25.7% of neurons showed increased calcium entry; the average increase was 25.0%, compared to baseline calcium entry when cells were depolarized with high KCl alone (not in the presence of baclofen). 48.0% of cells showed a decrease in calcium entry, with an average decrease of 23.6%. Finally, 26.3% of cells did not respond to baclofen treatment with either an increase or a decrease

in calcium entry. These early studies considered an increase or a decrease to be ± 5% of

control KCl values. However, it became clear that there was greater inherent variability

in response of control cells than the 5% cutoff being used. Thus, cells were stimulated

with high KCl three times. The middle stimulation was considered the "treatment" and

compared with the average of stimulations 1 and 3. These data showed that KCl alone

varied ± 10.7% from one KCl treatment to another (N = 127). Therefore, using a 5%

cutoff was not strict enough, and I could have been considering cells that varied based

only on KCl treatment. Experiments were repeated using a value of ± 21.4% (twice the

standard deviation of the control response) to be considered increasing or decreasing,

respectively. As expected, the more stringent criteria changed the distribution of

responses. 46 of 392 cells (11.73%) showed an increase in current entry, with an average

increase of 39.29 ± 2.54% (Figure 3.1a). 106 (27.04%) cells showed a decrease in

calcium entry, with an average decrease of 36.23 ± 0.96% (Figure 3.1b). Finally, 240

(61.22%) showed no change in calcium entry with the new, more stringent criteria

applied (Figure 3.1c). Though there were fewer cells that showed enhanced calcium

entry upon $GABA_B$ receptor activation than when examined with electrophysiology, there

was still a significant difference between controls and those treated with 10 µM baclofen.

These results validated the electrophysiological studies and suggested ratiometric calcium

imaging can be used as a tool to understand the activated $GABA_B$ receptor-mediated
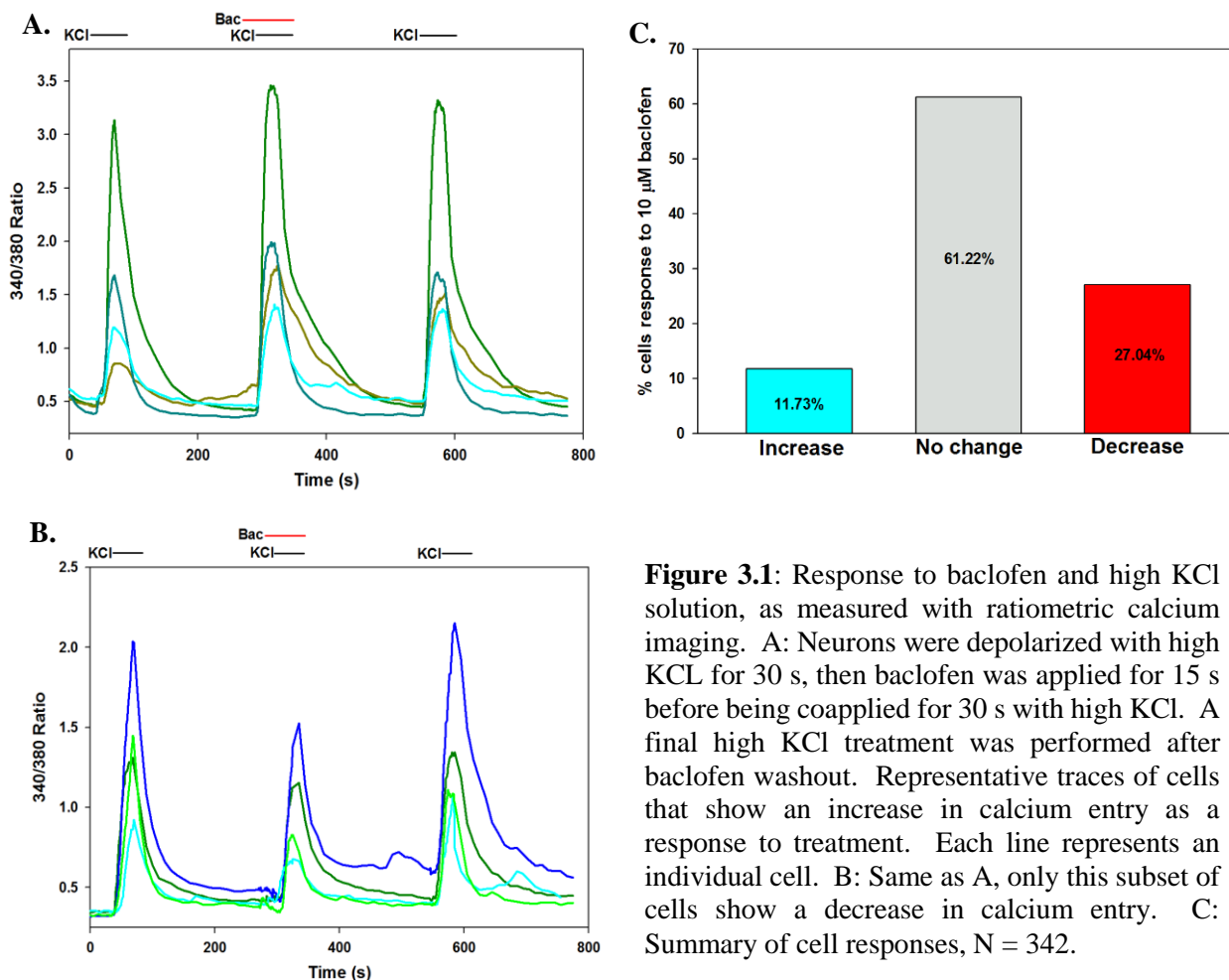
response.

Figure 3.1: Response to baclofen and high KCl solution, as measured with ratiometric calcium imaging. A: Neurons were depolarized with high KCL for 30 s, then baclofen was applied for 15 s before being coapplied for 30 s with high KCl. A final high KCl treatment was performed after baclofen washout. Representative traces of cells that show an increase in calcium entry as a response to treatment. Each line represents an individual cell. B: Same as A, only this subset of cells show a decrease in calcium entry. C: Summary of cell responses, N = 342.

Increasing intracellular calcium concentration is due to influx from the extracellular milieu

To determine the proportion of calcium that enters the cell through surface calcium channels versus that which is released from intracellular stores, calcium imaging was used, and the concentration of calcium in the perfusing solutions was adjusted. Typically, the high KCl solution contains 10 mM calcium; when the cell is depolarized, there is a gradient which causes the ions to flow inward from outside the cell. However, the hypothesis of GABA$_B$ receptor activation is that it activates a pathway by which PIP$_2$

is cleaved. One cleavage product, IP_3 can translocate to the endoplasmic reticulum (ER)

and activate IP_3 receptors on the ER membrane. These activated receptors are permeable

to calcium, and thus the calcium sequestered in intracellular stores may be released.

Therefore, high KCl solution was made with calcium absent. When cells were stimulated

for 30 seconds with 0 calcium-containing high KCl and baclofen, there was no detectable

change ($0.54 \pm 2.59\%$ increase) in intracellular calcium. However, when the same cells

were treated with 10 mM calcium-containing high KCl, the prototypical response ($114 \pm$

94.84% increase) was seen ($N = 88$, Figure 3.2 and Table 6). These data suggest that the

majority of calcium influx is through voltage-gated channels, rather than through release

from intracellular stores.
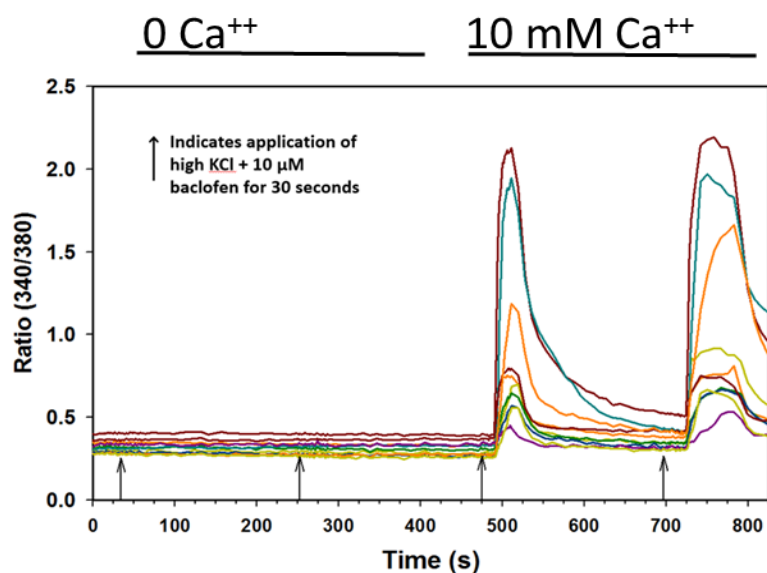
Figure 3.2: When high KCl is applied to open voltage-dependent channels but calcium is removed from the solution, no calcium entry is seen.   These data suggest that the source of calcium entry is from extracellular sources. The response is restored when calcium is added back to the depolarizing solution and the rinsing solution.

Treatment	Baseline 340/380 Ratio	Peak 340/380 Ratio	% change
50 mM KCl	0.42 ± 0.10	0.88 ± 0.35	114.74 ± 94.84
50 mM KCl with 0 mM Ca^{2+}, 10 µM Baclofen	0.44 ± 0.11	0.44 ± 0.10	0.54 ± 2.59

Table 6: Summary of cellular responses when depolarized with high KCl with or without calcium present in solutions. Data represent mean ± SEM.

Given that 10 µM baclofen did not cause an increase in intracellular calcium when no calcium was present in the extracellular solution and voltage-gated channels were open, it seemed unlikely that stimulation of $GABA_B$ receptors *without* depolarization would lead to change in intracellular calcium. However, it has been reported that increased concentrations (50 µM) of baclofen were sufficient to induce an increase in intracellular calcium in P0 hippocampal cultures (Kuczewski et al., 2011), thought to be caused by the pathway mentioned above. I used the same 50 µM concentration of baclofen and attempted to replicate these data; cells treated with KCl alone averaged a $144 \pm 90.16\%$ increase in intracellular calcium compared to baseline levels. The same cells averaged a $1.95 \pm 4.74\%$ change when 50 µM baclofen was applied (N = 68, Table 7). This result agrees with the data mentioned previously, that changes in intracellular calcium require opening of voltage-gated channels and extracellular calcium to be present. Furthermore, activation of $GABA_B$ receptors alone, even at high concentrations, cannot induce a change in intracellular calcium.

Treatment	Baseline 340/380 ratio	Peak 340/380 ratio	% change
50 mM KCl	0.31 ± 0.04	0.79 ± 0.37	144.32 ± 90.16
50 μM Baclofen	0.31 ± 0.05	0.32 ± 0.05	1.95 ± 4.74

Table 7: Summary of responses seen in cells depolarized with high KCl, or treated with $GABA_B$ agonist baclofen alone

Attenuation of calcium current does not shift activation voltage or conductance of calcium channels

While much of the focus of my work has been to detail mechanisms responsible for the enhancement of intracellular calcium upon $GABA_B$ receptor activation, there is a proportion of neurons that undergoes a reduction of intracellular calcium under the same conditions. The inhibitory response seen when baclofen is applied can be abolished by ω-conotoxin GVIA, suggesting it is specifically N-type channels that are inhibited (Carter and Mynlieff 2004). A more detailed kinetic analysis was performed on the neurons that demonstrated current enhancement, which showed that $GABA_B$ receptor-mediated increases in L-type current caused a decrease in the voltage at which the L-type channel begins to pass current, as well as a leftward shift in the conductance. This study did not examine similar parameters of N-type inhibition. When N-type channels were inhibited by G protein-coupled δ-opioid receptor activation or by neurotransmitters norepinephrine and somatostatin, inhibition was mediated through a slowing of activation kinetics; the peak component of the current developed significantly slower than controls (Golard and Siegelbaum 1993; Toselli et al., 1999). $GABA_B$-mediated N-type inhibition has been examined, and similar to N-type inhibition in other systems, voltage-dependent inhibition develops due to a slowed activation phase of the peak current (Tatebayashi and Ogata 1992). However, none of these studies examined whether the activation voltage of these

calcium channels were affected. Thus, the focus of this study was to examine whether N-type inhibition shifted activation voltage such that a stronger depolarization is required to pass current.

To determine whether activation voltage is shifted in cells that demonstrate attenuation of calcium current, neurons were held at -80 mV. Pulses 300 ms in duration were given from -50 mV to +50 mV in 10 mV steps. 10 µM baclofen was applied after control currents were elicited. After currents were measured in the presence of baclofen, the drug was washed out and another group of currents was collected. Since cell cultures contain a heterogeneous mix of neurons, each cell has a different array of voltage-gated calcium channel types. However, the maximal activation voltage of these currents was always between +10 mV and +20 mV. In order to determine a cell's response to baclofen treatment, peak current was measured at +20 mV in the presence and absence of baclofen, as well as after washout. A linear regression line of control values was constructed, to account for run up or run down commonly seen with calcium channel recordings. A 95% confidence interval was constructed, and the experimental value
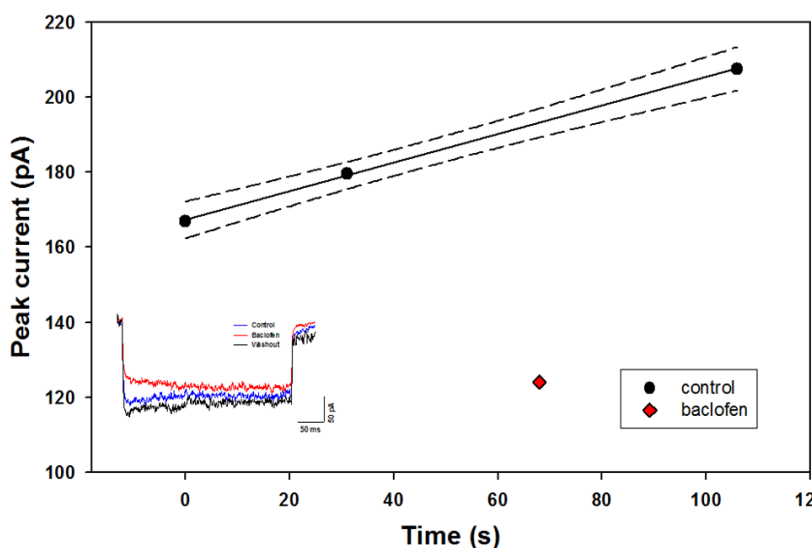
Figure 3.3: Linear regression line constructed from control 300 ms depolarizing pulses (black dots) surrounded by 95% confidence interval. Baclofen application (red diamond) is outside the confidence interval and is therefore considered as having a significant effect. Inset: raw trace containing values used to construct linear regression line. Blue line: control; red line: baclofen application; black line: washout.

plotted. If the experimental value was below the linear regression line and outside the confidence interval, it was considered to show attenuation of current (Figure 3.3).

Full current-voltage (IV) relationships of neurons that showed this reduction of current or those that showed no change (experimental fell within the 95% confidence interval) were constructed (Figure 3.4). The voltage at which channels begin to display current was derived from these measurements. Furthermore, conductance values were calculated by dividing peak current by the driving force. Conductance plots were constructed and the voltage was measured when the neuron reached half-maximal conductance ($V_{1/2}$). The $V_{1/2}$ for cells that do not show a difference in calcium current when GABA$_B$ receptors are activated is 8.3 ± 1.4 mV, compared to 8.2 ± 1.2 mV in controls (N = 15). The $V_{1/2}$ for cells that display attenuation of calcium current is 9.8 mV, compared to 8.5 mV in controls (N = 2, Figure 3.5). Baclofen application did not significantly shift a cell's activation voltage compared to its value before or after treatment. These data suggest N-type channel inhibition is not due to a change in activation voltage or whole cell conductance; more likely it is the slowed activation phase
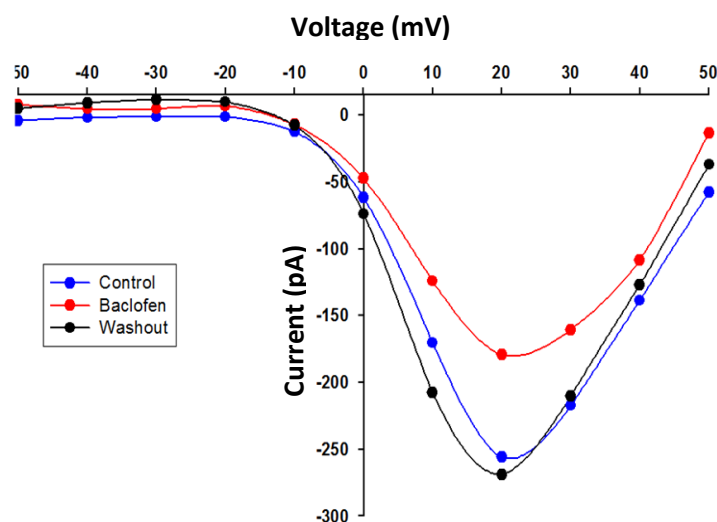
Figure 3.4: Current-voltage (IV) relationship in a neuron that demonstrates attenuation of current when treated with baclofen. The peak component of calcium current was measured during the 300 ms depolarizing pulse. The cell was held at -80 mV, and voltages were increased +10 mv from -50 to +50 mv. There is no shift in the IV curve when current is attenuated (red trace).

and voltage-dependent inhibition suggested by Tatebayashi and Ogata (1992).
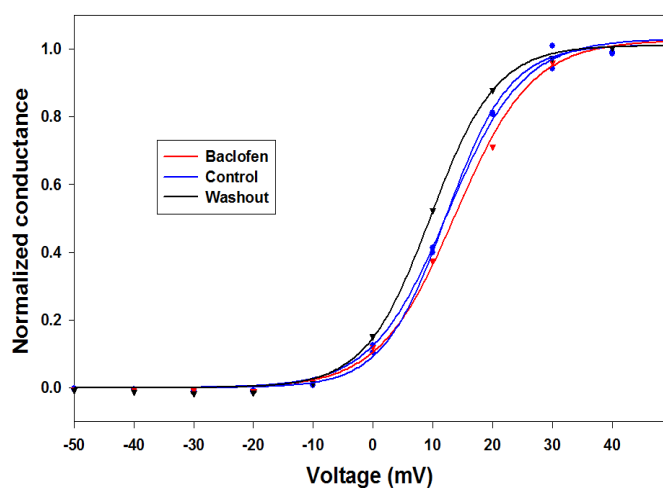
Figure 3.5: Activation curve of peak current in a neuron that demonstrates a decrease in response to baclofen application. Data were fit with a 3-parameter sigmoidal equation. Conductances were normalized at each test potential by dividing the conductance at each test potential by the maximal conductance obtained for that cell. Half-maximal activation voltage ($V_{1/2}$) was calculated for each individual cell.

DISCUSSION

GABA$_B$ receptor-mediated enhancement of L-type current was a phenomenon first described with the use of electrophysiology (Shen and Slaughter 1999). Since then, the Mynlieff laboratory has confirmed this finding in the developing mammalian system, also using electrophysiology (Carter and Mynlieff 2004; Bray and Mynlieff 2009; Bray and Mynlieff 2011). However, while electrophysiology can provide much faster temporal resolution, its throughput is limited. Thus I showed that calcium imaging can similarly be used to demonstrate this effect. It is important to note that calcium imaging does not measure calcium current directly; instead it measures a difference in fluorescent states of a specific fluorophore. The key to ratiometric imaging is that by using a dual wavelength fluorophore, not all cells are required to take up exactly the same concentration. For example, Fura-2 AM is excited at 340 nm when not bound to calcium; in its bound state, it is excited at 380 nm. Thus, the response of changing levels of fluorescence is simply a difference in ratio between free Fura-2 AM and Fura-2 AM bound to calcium in any given cell. As calcium enters, more calcium becomes bound by the Fura-2 AM, such that a change in fluorescence is actually a change in ratio 340 to 380 ratio; this serves as an indirect measure of calcium entry. Another concern regarding fluorescence measurements is that since the volumes within individual neurons in culture is unequal, one is only capturing data on a specific plane. If the plane is not the same, light intensity may vary from one compartment to the other. Using a dual length fluorophore like Fura-2 AM alleviates this issue. For example, a neuronal cell body may be more round, and its associated dendrite will be relatively flatter. Since the ratiometric

imaging is always comparing bound to free Fura-2 AM, any region of interest will always be compared to itself, dendrite to dentrite, or cell body to cell body.

It is also likely that calcium imaging does not have as much experimental bias as does electrophysiology. When performing calcium imaging, all cells are examined, regardless of size, morphology, etc. Only if they are unhealthy are they not included in data analysis. For example, a cell whose calcium levels do not return to baseline after high KCl is washed out will not be included in analysis, because it is likely not healthy enough to extrude calcium. Electrophysiological recording allows the experimenter to pick the cells from which he or she records. This artificial selection may not reflect the actual makeup of cells in culture. One concern of data presented here is that the proportion of cells that demonstrate enhancement of calcium entry is approximately half of that seen in electrophysiology. This is likely due to experimental bias. Because calcium imaging is likely a better representation of the all cell types in the culture, it is possible that enhancement measured here is more accurate than what is observed with other methods. Thus, while calcium imaging does not provide the fast temporal resolution of whole cell patch clamp recording, it has numerous advantages and can be used to show similar effects as electrophysiology.

Our laboratory and others that $GABA_B$ receptor activation can lead to increased levels of intracellular calcium (Shen and Slaughter 1999; Carter and Mynlieff 2004; Bray and Mynlieff 2009; Bray and Mynlieff 2011; Park et al., 2010; Kuczewski et al., 2011; Mitzuta et al., 2011; Im and Rhim 2012). However, despite this phenomenon being described several times, the mechanism responsible for enhanced calcium levels remain unknown. One hypothesis is that the behavior of the channel is modified, such that it

passes more current. An example of this possibility is that phosphorylation of the channel could lead to its being open for longer periods of time. A second hypothesis is that activation of $GABA_B$ receptors leads to activation of $PLC\beta$, generation of IP_3 after cleavage of PIP_2, and opening of calcium-permeable IP_3 receptors on the endoplasmic reticulum. If this hypothesis is correct, activation of $GABA_B$ receptors alone should induce increases in intracellular calcium levels. However, data presented here show applications of $GABA_B$ agonist baclofen resulted in no change in intracellular calcium levels when cells were not depolarized. When calcium channels were activated but no calcium was present extracellularly, baclofen still failed to cause an increase in intracellular calcium levels. These data are in agreement with previous data in the lab that enhanced calcium concentration is through L-type calcium channels. Kuczewski et al., (2011) was able to block baclofen mediated calcium enhancement by inhibiting L-type channels. This is particularly interesting because in this study, cells were never depolarized, suggesting some novel mechanism whereby L-type channels are activated by the $GABA_B$ response. Perhaps a more plausible scenario is that activation of $GABA_B$ receptors initiates a signal transduction cascade that leads to modulation of L-type channels, such that they can allow more calcium into the cell. This hypothesis is supported by data from Carter and Mynlieff (2004) which shows that L-channels activate at more hyperpolarized potentials in the presence of baclofen. It is possible that other kinetic changes underlie observed enhancement as well. Changes in open probability or mean open time of the channels due to a phosphorylation event could lead to increased concentrations of calcium; single channel recording would be required to examine this hypothesis.

In addition to observing enhancement of calcium entry when performing calcium imaging, a subset of cells also demonstrated reduced calcium entry. This finding was previously demonstrated in our laboratory, and characterized pharmacologically as inhibition of N-type calcium channels (Carter and Mynlieff 2004). I conducted studies that characterized the current-voltage relationship of neurons that demonstrate attenuation of N-type current, as well as those neurons whose current is not changed. The purpose was to examine whether these cells displayed a shift that may help explain how baclofen affects calcium channels. Not surprisingly, I found there is no change in activation voltage or $V_{1/2}$. The closely related P/Q-type channel is similarly inhibited by $GABA_B$ receptor activation, by the same mechanism as N-type channels. When the IV curve for P/Q-channel inhibition is shown, activation voltage does not change (Mintz and Bean 1993). Furthermore findings by (Carter 2002) showed only a slight leftward shift in the IV curve of cells that showed attenuation when exposed to baclofen; there was no significant difference in the activation voltage of these cells. My work essentially repeated these studies and led to the same conclusion. The most plausible hypothesis is that current develops more slowly due to the slowed activation phase of the N-type channel and characteristic voltage-dependent inhibition of these channels (Tatebayashi and Ogata 1992).

CHAPTER 4

The signaling pathway involved in GABA$_B$ receptor activation-mediated

increases in L-type calcium current

INTRODUCTION

GABA$_B$ receptor activation is most commonly linked to a response that decreases a neuron's excitability. Upon ligand binding, there are three well described inhibitory mechanisms. First is inhibition of voltage gated N- and P/Q-type calcium channels. Presynaptic inhibition leads to decreased release of neurotransmitter, while postsynaptic inhibition decreases dendritic calcium spikes. Second is activation of GIRK channels. When GIRK channels are active, potassium ions move out of the neuron, generating slow inhibitory postsynaptic potentials (IPSPs). Finally, GABA$_B$ activation decreases phosphorylation of target proteins due to reduced protein kinase A (PKA) activity. The G protein α subunit mediates the decrease in PKA activity through a signal transduction cascade; adenylate cyclase is inhibited from producing cyclic AMP (cAMP). Without cAMP, PKA remains catalytically inactive. It is the G protein βγ subunits which mediate the decrease in N- and P-Q current as well as GIRK current. Importantly, whether it is the α or βγ subunits which decrease excitability, GABA$_B$ receptors have always been linked with Gα$_{i/o}$ G proteins.

A less well described phenomenon is the enhancement of L-type calcium current upon GABA$_B$ receptor activation. This GABA$_B$ mediated increase in L-type current has been suggested to be a means by which GABA$_A$ receptors get inserted into membranes;

increased L-type current causes secretion of brain-derived neurotrophic factor (BDNF), which has been shown to modulate $GABA_A$ expression previously (Kuczewski et al., 2011). $GABA_B$ receptor-induced increases in L-type current also increase phosphorylation levels of extracellular signal-regulated protein kinase 1/2 ($ERK_{1/2}$, Im and Rhim 2012). $ERK_{1/2}$ is known to activate cAMP response element binding protein (CREB, Vanhoose et al., 2002; Tu et al., 2007) as well as be involved in synaptic plasticity (Giovannini 2006). However, while it has been shown that $GABA_B$ receptor activation can lead to $ERK_{1/2}$ activation, the targets of this activated $ERK_{1/2}$ remain unknown.

While there are few reports of $GABA_B$ receptor mediated increases in activity, there is even less known about the signaling cascade that promotes current enhancement. Initially, Shen and Slaughter (1999) described this enhancement as sensitive to protein kinase C (PKC) inhibition, and somewhat less sensitive to protein kinase A (PKA) inhibition. Furthermore, enhancement could be abolished by treatment with dihydropyridines, verifying L-current was being affected (Shen and Slaughter 1999; Carter and Mynlieff 2004). More recent work in our laboratory showed that, when treated with pertussis toxin to inhibit $G\alpha_{i/o}$ protein signaling, enhancement persisted (Bray and Mynlieff 2011). These data suggested that $GABA_B$ receptors couple to a G protein besides the canonical $G\alpha_{i/o}$ to produce enhancement.

A large portion of my work was to determine the signaling cascade that resulted when $GABA_B$ receptors were activated. Since $G\alpha_{i/o}$ G proteins were likely not involved, it was hypothesized that $GABA_B$ receptors may couple promiscuously to more than one G protein. The involvement of PKC suggested that $G\alpha_q$ was responsible for the observed

current enhancement, since $G\alpha_q$ activation has been demonstrated to activate

phospholipase C (PLC), which increases PKC activation. In order to test this hypothesis,

I employed a strategy of morpholino (MO)-induced knockdown. Furthermore, while

PKC has been demonstrated to be a requisite member of the signal transduction pathway,

the isoform had not been identified. When cells were treated with PKC activator phorbol

12-myristate 13-acetate (PMA), a phorbol ester, enhancement of calcium current could be

reproduced (Bray and Mynlieff 2011). Because only a subset of PKC isozymes are

sensitive to phorbol stimulation, and because the enhancing effect is maximally observed

at P7, it narrowed the possible candidates to three isozymes, α, β, and ε. Finally, it was

hypothesized that calcium/calmodulin-dependent kinase II (CaMKII) was involved in this

pathway, because a report from O-Uchi et al. (2008) showed that cardiac myocytes

demonstrate enhanced L-type current as a result of $G\alpha_q$ signaling, also mediated by PKC

and CaMKII.

RESULTS

Mopholino oligos effectively enter mammalian neurons grown in culture

In order to examine whether $GABA_B$ receptors exert their effects through

signaling the α subunit of the $G\alpha_q$ G protein complex, I employed the strategy of

knockdown via morpholino (MO) oligonucleotides. MO are synthetic oligos designed to

bind target mRNA and inhibit their translation. They are readily taken up by cells in

culture, and fused to a 3' carboxyfluorescein molecule to visualize delivery into the cell

(figure 4.1a and b).
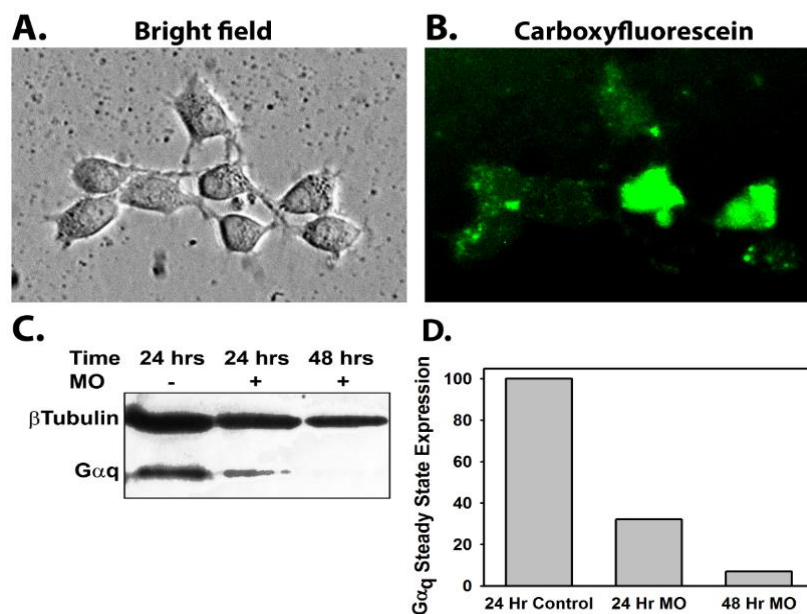
Figure 4.1: Introduction of morpholino (MO) oligos and their effect on cultured hippocampal neurons. A) Differential interference contrast image of a hippocampal culture from P4 rat pups treated with 10 μM control oligos and 2 μM Endo-Porter peptide, maintained in culture for 96 hours. B) Fluorescent image of cells pictured in A; MO were tagged with carboxyfluorescein for visualization and assessment of delivery. C) Western blot of proteins isolated from either control cultures (lane 1), cultures treated for 24 or 48 hours with 2 μM $G\alpha_q$ MO and 4 μM Endo-Porter (lanes 2 and 3, respectively). These cultures were obtained from P6-8 rats. The Western blot was decorated with $G\alpha_q$ antibodies and β-tubulin antibodies as a loading control D) Quantification of $G\alpha_q$ band density. Values were calculated by dividing integrated optical density (IOD) of the $G\alpha_q$ band by the IOD of the β-tubulin band to control for sample loading.

While this strategy is common in zebrafish, there are fewer reports of their successful use in mammalian neurons. Before proceeding with knockdown of $G\alpha_q$, it was necessary to verify that MO were able to be taken up by mammalian cells and were non-toxic. Cultures were treated with Endo-Porter, a proprietary molecule that causes endocytosis-mediated uptake of cargo (see Chapter 2 for figure), and a nonsense MO (one that did not bind to any known mRNA) and visualized after 24, 48, and 96 hours of incubation. Figure 4.1 shows cultures after 96 hour treatment. Cells appear healthy, displaying growing processes and maintaining their characteristic shape. When examined under fluorescence, every cell displays some level of fluorescence, suggesting universal uptake of the MO oligos. At concentrations $\geq 4\ \mu M$ oligos or $\geq 6\ \mu M$ Endo-Porter, treatment with MO began to negatively affect growth and viability of neuronal cultures (data not shown). Thus, $2\ \mu M$ MO and $4\ \mu M$ Endo-Porter were used.

Morpholino oligos effectively inhibit translation of $G\alpha_q$

To determine the effectiveness of MO-induced protein knockdown, neurons were treated with Endo-Porter alone, Endo-Porter and nonsense oligos, or Endo-Porter and MO against $G\alpha_q$ G protein. Western blotting was performed either 24 or 48 hours after treatment. Figure 4.1c shows that after 24 hours, significant knockdown was achieved. G proteins have relatively long half-lives, up to 30 hours (Derrien et al., 1996); thus MO were added to cell cultures for 48 hours to maximize knockdown. 48 hour treatment almost completely abolished the $G\alpha_q$ protein signal. Cultures treated with Endo-Porter alone or nonsense MO demonstrated comparable levels of $G\alpha_q$ protein expression as controls (data not shown). Thus, using the Endo-Porter delivery system, $G\alpha_q$ protein

expression in neuronal cultures was reduced without negatively impacting cell health or viability, determined both physiologically (by observing characteristic intracellular calcium increases upon depolarization) and morphologically. Due to the relatively long half-life of G proteins, all electrophysiological and calcium imaging experiments were performed following 48 hour incubation with $G\alpha_q$ to ensure the highest degree of protein knockdown possible.

$G\alpha_q$ is more highly expressed than $G\alpha_{11}$ in the neonatal hippocampus

$G\alpha_{11}$ shares 90% sequence similarity with $G\alpha_q$ and both proteins have a ubiquitous distribution pattern (Mizuno and Itoh 2009). Therefore, it was important to determine whether there could be nonspecificity in the MO knockdown of $G\alpha_q$ that may decrease expression of $G\alpha_{11}$ as well. Protein preparations from cultured cells were treated with either $G\alpha_q$ or nonsense MO and analyzed by Western blotting using $G\alpha_{11}$ antibodies. If the MO were specific to $G\alpha_q$, there would be no change in the expression of $G\alpha_{11}$. However, no signal was detected in these preparations, or in control preparations not treated with MO, nor those only treated with Endo-Porter (data not shown). This result was suggestive that either the basal level of $G\alpha_{11}$ was too low to detect with Western blotting in preparations of cultured neurons, or the $G\alpha_{11}$ antibody did not recognize its target. To determine whether the $G\alpha_{11}$ antibody could recognize $G\alpha_{11}$ G protein, protein samples were prepared from the superior region of the hippocampus so that the amount of protein loaded on a gel could be increased. Antibodies to $G\alpha_q$ and $G\alpha_{11}$ detected proteins of similar weights as expected. Figure 4.2 shows that the $G\alpha_{11}$ antibody does recognize its target, but only if 5-10 times the amount of protein was
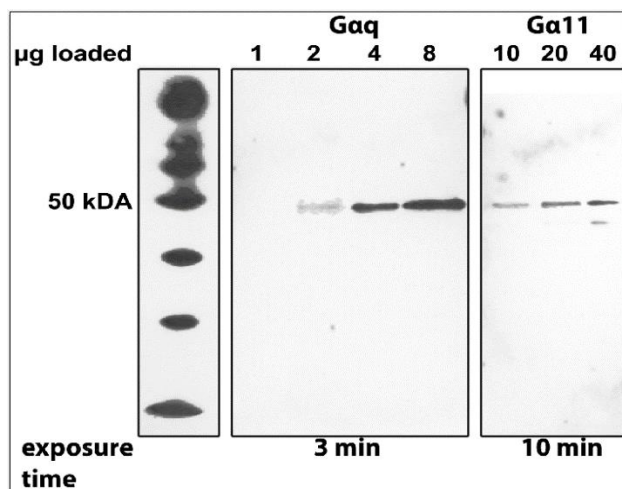
Figure 4.2: Expression levels of $G\alpha_q$ and $G\alpha_{11}$ in the superior region of the neonatal rat hippocampus. Western blot analyses were performed on samples using antibodies against $G\alpha_q$ or $G\alpha_{11}$. Lanes 1-4 (middle panel) were loaded with 10 times less protein than lanes 5-7. In order to visualize bands probed with $G\alpha_{11}$ antibody, exposure time was increased to 10 minutes (right panel), compared to 3 minute exposure used to visualize bands probed with $G\alpha_q$. The left panel shows markers used for molecular weight calculations.

loaded and the decorated membrane was exposed to film for a longer period of time.

When a lane loaded with 2 μg of protein was probed with $G\alpha_q$ antibody, the integrated

optical density (IOD) was 7.2. When a lane was loaded with 20 μg of protein and probed

with $G\alpha_{11}$ antibody, the IOD was 5.0, on the same film with the same exposure time.

These data suggest that $G\alpha_q$ expression is likely 10-fold or more higher than that of $G\alpha_{11}$.

With such a small basal level of $G\alpha_{11}$ expressed, it is not surprising that this protein was

undetectable in Western blots loaded with cultured cell preparations. Expression data

here supports a similar previous finding that $G\alpha_q$ is more highly expressed than $G\alpha_{11}$ in

hippocampal tissue.

Inhibiting $G\alpha_q$ expression abolishes baclofen-mediated voltage gated calcium current enhancement

Previous studies showed that the enhancing effect of $GABA_B$ receptor activation

on L-type current was not mediated by a $G\alpha_{i/o}$ G protein, because pertussis toxin (PTX)

treatment eliminated only attenuation of calcium current, while enhancement persisted in PTX-treated populations of neuronal cultures (Bray and Mynlieff 2011). Despite a lack of precedence for GABA$_B$ receptor coupling to Gα_q, downstream actions, including PKC activation, were consistent with the actions of a Gα_q G protein family member. Therefore, we chose to knock down Gα_q and assess whether application of the GABA$_B$ receptor agonist baclofen (10 µM) could still lead to L-type current enhancement. Hippocampal cultures treated with either nonsense or Gα_q MO were stimulated with a high KCl solution, followed by a high KCl solution containing 10 µM baclofen, and assessed with ratiometric calcium imaging. In nonsense MO-treated cells, 6 out of 64 cells (9.37%) demonstrated enhancement of calcium entry when baclofen was coapplied with high KCl (Figure 4.4b). This percentage is not statistically different than the percentage of cells showing enhancement treated with only 10 µM baclofen and no morpholinos. Conversely, none of the 207 cells treated with Gα_q morpholinos demonstrated enhancement of calcium entry when baclofen was coapplied with KCl (Figure 4.4d, Chi square, P < 0.001). Notably, 56 of the 207 cells (27.05%) still demonstrated inhibition of calcium entry, suggesting that G$\alpha_{i/o}$-mediated inhibition of channels was unaffected (data not shown). To verify the result that knockdown of Gα_q resulted in elimination of calcium current enhancement, whole-cell voltage clamp electrophysiology was used. In control cells treated with nonsense MO, 3 out of 25 cells demonstrated an enhancement of calcium current when baclofen was applied and cells were depolarized to +10 mV for 300 ms (Figure 4.4a). In contrast, 0 out of 16 cells treated with Gα_q MO for 48 hours demonstrated enhancement of calcium current under the same experimental conditions (Figure 4.4b). Though these electrophysiological

results failed to reach statistical significance, they follow the same pattern as the highly

significant calcium imaging data. Taken together, these sets of experiments demonstrate

that knockdown of $G\alpha_q$ G proteins abolished enhancement of calcium current or entry

upon $GABA_B$ receptor activation, linking a $G\alpha_q$ family member to this pathway and thus

the $GABA_B$ receptor itself.
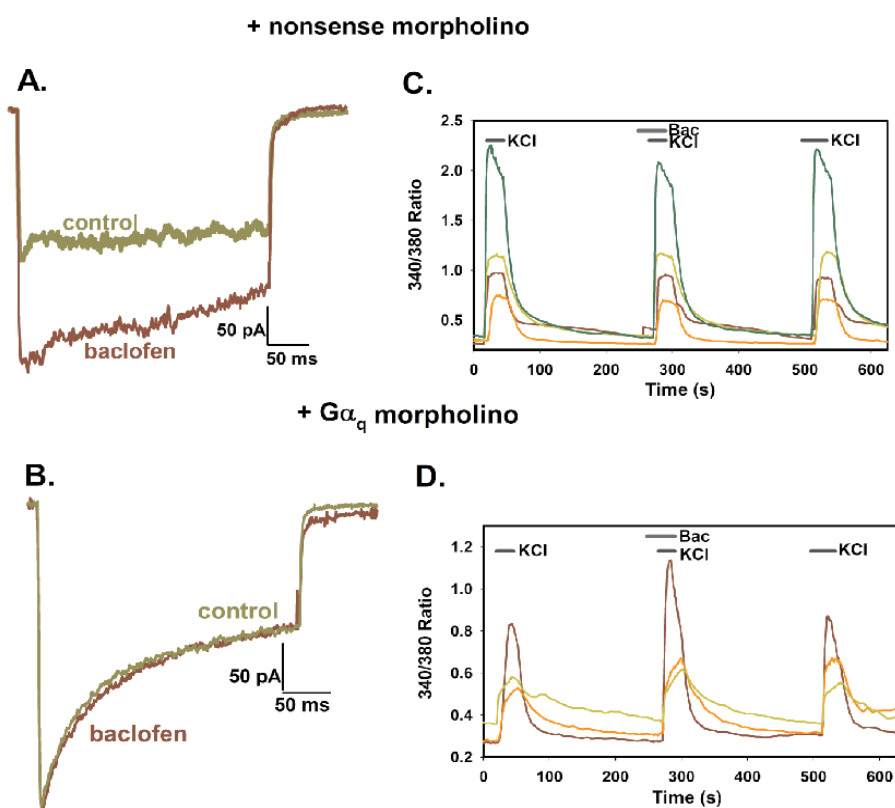
Figure 4.3: Effect of 48 hour treatment with $G\alpha_q$ MO on calcium entry in hippocampal neurons. Neurons were treated with either nonsense MO (A and C) or $G\alpha_q$ MO (B and D). Voltage gated calcium currents were elicited by a 300 ms depolarizing pulse to +10 mV from a holding potential of -80 mV in the absence (green trace) and presence of 10 µM baclofen (red trace; A and B). Increases in intracellular calcium were induced by high KCl solution-mediated depolarization were measured with ratiometric calcium imaging as the ration of the intensity when excited by 340 nm light over the intensity when excited by 380 nm light (C and D). Each colored line in C and D represents a single cell.

GABA$_B$ receptors colocalize with Gα_q G proteins

To further examine the possibility that GABA$_B$ receptors couple to G proteins, confocal imaging was used to determine whether these two proteins colocalize. Hippocampi were frozen and sliced into 20 µM sections, which were decorated with primary antibodies against GABA$_B$R1 and Gα_q. When sections were labeled with antibodies against GABA$_B$ receptors (red), nearly all areas were labeled, with the exception of the granule cells in the dentate gyrus. Labeling was most intense in the pyramidal cell layer and the region containing the mossy fibers; lighter labeling was also evident in the stratum oriens and stratum radiatum. At high magnification, there was a total absence of nuclear labeling with GABA$_B$ receptor antibodies, and a clear delineation between the nuclei and the cytoplasm. Antibodies against Gα_q labeled cells within both the pyramidal layer and the granule cell later. In addition, there appeared to be individual cell bodies labeled within the stratum oriens and stratum radiatum without any diffuse labeling throughout these layers, as seen with GABA$_B$ receptor antibodies. At low magnification, colocalization of the two fluorophores was most evident in the pyramidal cell layer and was absent from the dentate gyrus granule cell layer. Quantitative analysis done at high magnification in the superior region of the hippocampus supports qualitative evidence seen at low magnification. The average Pearson's Correlation Coefficient (PCC), used to determine colocalization, was 0.125 ± 0.03 (S.E.M.) in the stratum oriens. The PCC was 0.476 ± 0.03 in the pyramidal cell layer and 0.102 ± 0.01 in the stratum radiatum. The colocalization of GABA$_B$ receptors and Gα_q is highest in the pyramidal cell layer, as suggested by the PCC value; the PCC is significantly higher in the pyramidal cell layer than either the stratum radiatum or stratum oriens ($P < 0.001$). The

	Anti-GABABR1	Anti-Gαq	Merged	Merged + DAPI
10X	A	B	C	D
60X	E	F	G	H
	I	J		
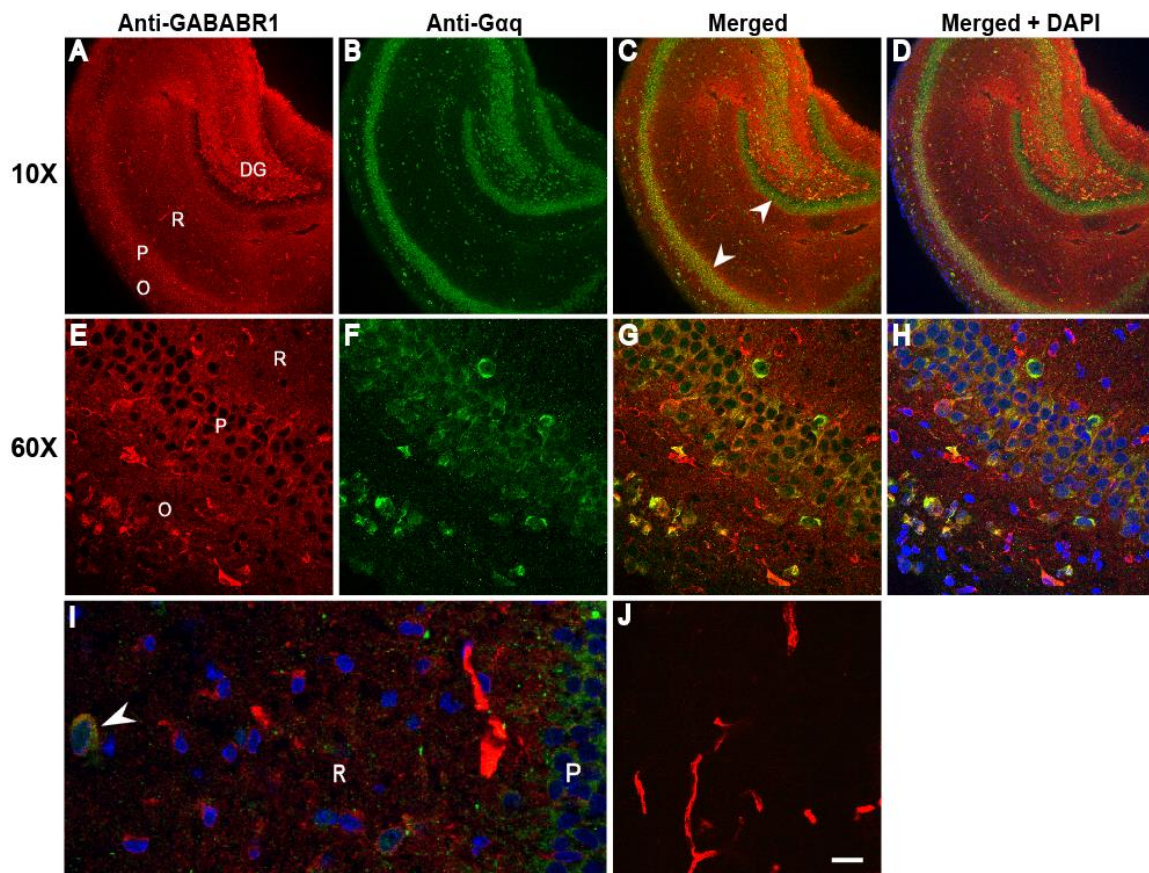
Figure 4.4: GABA_B receptors colocalize with Gα_q G proteins in rat hippocampus. Hippocampal sections were labeled with ployclonal rabbit anti-GNAQ and monoclonal mouse anti GABA_BR1 followed by Dylight® 488-conjugated goat-anti rabbit IgG (green) and Dylight® 550-conjugated goat-anti mouse IgG (red) for visualization. Nuclei were stained blue with DAPI. Colocalization of the red and green fluophores appears yellow in the merged images of (C, D, G, H, and I) White arrowheads in (C) indicate the colocalization seen in the pyramidal cell layer but not the dentate granule cell layer. Images in (A,B, E, and F) represent the proteins of interest in isolation with the images merged in column 3 and nuclear staining (blue) added in column 4. A-D: Low magnification image showing the whole section of hippocampus. E-H: High magnification image showing the pyramidal cell layer, the stratum oriens, and the stratum radiatum. I: A small number of cells in both the stratum oriens and the stratum radiatum appeared to show colocalization of GABA_B and Gα_q with a high PCC value. One of these cells in the radiatum is shown with a white arrowhead. J: Control sections were stained without primary antibodies to ensure specificity. Red blood vessels can be seen due to autofluorescence. Abbreviations: DG dentate gyrus, R stratum radiatum, P pyramidal cell later, O stratum oriens. Scale bar = 10 μM.

radiatum and oriens are not significantly different from each other (One way ANOVA

followed by Holm Sidak pairwise comparison). It should be noted that a small number of

neurons in the stratum radiatum and stratum oriens were labeled by antibodies against

$G\alpha_q$, and some of these neurons also appeared to be labeled with $GABA_B$ receptor antibodies. Indeed, these neurons had a relatively high (0.5 – 0.75) PCC value. The functional significance or physiological identity of these neurons is unknown.

CaMKII activity is not involved in $GABA_B$ receptor-mediated increases in intracellular calcium

PKC activity has been shown to be required in the signal transduction pathway beginning with $GABA_B$ receptor activation and ultimately resulting in increased calcium current (Bray and Mynlieff 2011). Recently, O-Uchi and colleagues described α_{1A}-adrenoreceptor coupling to $G\alpha_{q/11}$ to activate PKC, leading to an increase in L-type calcium current in cardiac myocytes (2008). Importantly, this study showed that CaMKII was a member of this pathway as well, because inhibition of CaMKII could abolish the enhancement of L-type current. PKC has been shown to phosphorylate CaMKII, and because L-type channels are known to be phosphorylated by CaMKII, the involvement of CaMKII in the activated $GABA_B$ receptor pathway was investigated. Cultured neurons were depolarized with a high KCl solution, followed by a high KCl solution containing both 10 µM baclofen and a cell-permeable CaMKII inhibitor Ant-AIP-II (50 nM, $IC_{50} = 4$ nM). Both baclofen and Ant-AIP-II were coapplied during a 15 second pretreatment period as well as during the high KCl application. This length of time has been demonstrated to be sufficient for inhibition of CaMKII (Aromolaran and Blatter 2005). 22 of 255 (8.63%) of cells continued to demonstrate increased calcium entry, despite the presence of the CaMKII inhibitor (Figure 4.5a). When the inhibitor/baclofen solution was washed off, the response returned to original levels. Because there have been reports

of nonspecific actions of CaMKII inhibitors on calcium channels (Gao et al., 2006; Karls and Mynlieff 2013), the result was confirmed using a second cell permeable inhibitor, CamKIINtide (IINtide, 250 nM, IC_{50} = 50 nM). A similar result was obtained where 47 of 432 (10.88%) neurons showed a reversible increase in calcium entry when baclofen was coapplied with IINtide (Figure 4.5b). These values are not significantly different from control cells treated with baclofen alone, where 46 of 392 (11.73%) of cells show increased calcium entry when treated with high KCl. (Figure 4.5c, Chi square).
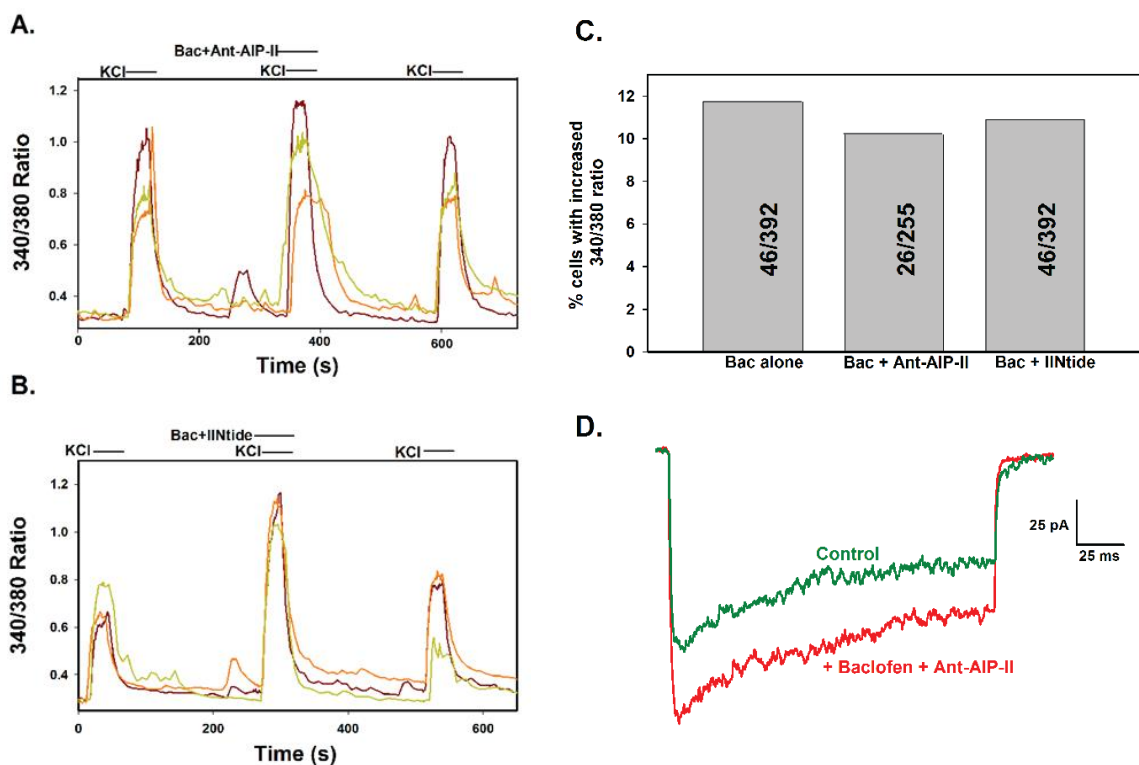
Figure 4.5: The increase in calcium entry due to $GABA_B$ receptor activation with baclofen is not affected by CaMKII inhibitors. Each colored line in A and B represents a single cell. A: Enhancement of the 340 to 380 ratio persists, despite the presence of CaMKII inhibitor Ant-AIP-II (50 nM). The enhancement is reversible, shown by the washout of baclofen and Ant-AIP-II. B: Enhancement of the 340 to 380 ratio persists, despite the presence of CaMKII inhibitor IINtide (250 nM). The enhancement is reversible, shown by the washout of baclofen and IINtide. C: Summary of the baclofen-mediated increase in the 340 to 380 ratio. There is no significant difference in number of cells demonstrating this increase in controls treated with only baclofen versus treatment with baclofen and Ant-AIP-II, or treatment with IINtide (Chi square). Total N inset in each bar. D: Electrophysiological recording elicited by a 300 ms test pulse from a holding potential of -80 mV to +10 mV shows persistent calcium current enhancement when baclofen and

In addition to calcium imaging, electrophysiological recordings were performed in the presence and absence of 50 nM Ant-AIP-II and 10 µM baclofen. Cells were depolarized to +10 mV from a holding potential of -80 mV to establish a baseline calcium current measurement. Addition of Ant-AIP-II with baclofen did not affect the enhancement of calcium current characteristically displayed in a subset of cells in response to baclofen alone. In these experiments, 4 of 23 (17.39%) of cells treated with Ant-AIP-II and baclofen displayed a significant increase in calcium current (Figure 4.5d). Thus, since neither inhibitor blocked enhancement of intracellular calcium in two different paradigms, it is likely that CaMKII is not involved in the GABA$_B$ receptor-mediated enhancement of L-type current.

PKCα translocates to the membrane upon GABA$_B$ receptor activation

A previous study demonstrated that activation of PKC by phorbol esters mimicked the effect of GABA$_B$ receptor stimulation on calcium currents in cultured hippocampal neurons (Bray and Mynlieff 2011). Therefore, only phorbol ester sensitive isozymes of PKC that are expressed in the early neonatal period were tested (Tanaka and Nishizuka 1994; Roisin and Barbin 1997). Recent experiments by Mynlieff analyzed immunohistochemical images with confocal microscopy to determine whether PKCα, PKCβ, or PKCε translocated from the cytosol to the plasma membrane after 10 minutes of baclofen treatment (Figure 4.6a and b). For each experiment, two different control conditions were run in parallel with the dishes treated with baclofen. Cells were either treated with no drugs (unstimulated) or with the phorbol ester, phorbol 12-myristate 13-
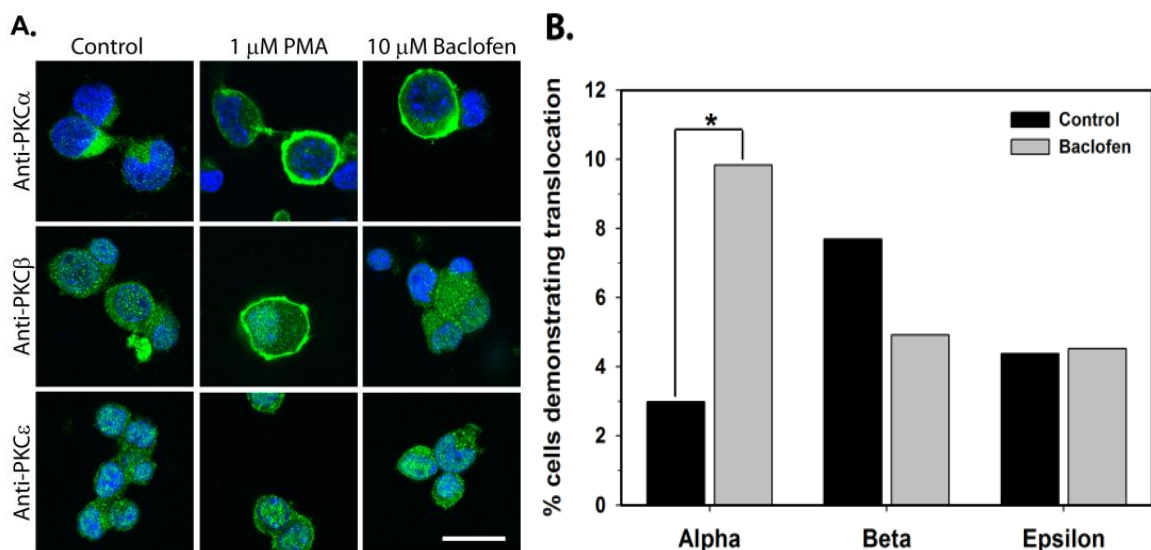
Figure 4.6: Activation of GABA$_B$ receptors causes translocation of PKCα in cultured hippocampal neurons. A) Prior to fixation for immunocytochemistry, cultured hippocampal neurons were treated with control media, the phorbol ester PMA (1 μM) in media, or baclofen (10μM) in media for 10 minutes. Cultured neurons were labeled with anti-PKCα, anti-PKCβ, or anti-PKCε antibodies followed by Dylight® 488 conjugated secondary antibodies for visualization (green). Nuclei are stained blue with DAPI B) The percent cells demonstrating translocation of PKCα, PKCβ, and PKCε in control cultures (black bars) was compared to the percent cells demonstrating translocation of PKCα, PKCβ, and PKCε following stimulation with the baclofen. N=568, 478, 104, 183, 183, and 177 for the PKCα control, PKCα with baclofen, PKCβ control, PKCβ with baclofen, PKCε control, and PKCε with baclofen. Scale bar: 20 μm. *P < *0.0001.*

acetate (PMA, 1 μM) to verify that the translocation to the membrane was visually

apparent in confocal images. Both treatment with PMA and baclofen caused

translocation of PKCα from the cytosol to the plasma membrane. A small percentage of

cells in each culture demonstrated spontaneous translocation of all 3 PKC isozymes

examined in unstimulated cultures (2.99-7.69% N = 104-568). Upon exposure to PMA

for 10 minutes, all 3 isozymes translocated to the plasma membrane in a subset of cells

(50.17% of 291 cells for PKCα, 20.34% of 188 cells for PKCβ, and 27.59% of 203 cells

for PKCε), confirming that the protocol was sufficient to demonstrate translocation

(Mynlieff, unpublished results). For PKCβ and PKCε, the percentage of cells

demonstrating translocation to the plasma membrane in the presence of 10 μM baclofen

was not significantly different than under nonstimulating conditions. However, the percentage of cells demonstrating translocation of PKCα with baclofen treatment (9.83%, $N = 478$) was significantly higher than the percentage of cells demonstrating spontaneous translocation under nonstimulating conditions (2.99%, $N = 568$; Fisher's exact test, *P < 0.0001*, Mynlieff, unpublished results). Therefore, since only PKCα was translocated to the membrane upon baclofen treatment and not PKCβ or PKCε, PKCα is most likely the isozyme activated in the signal transduction pathway.

DISCUSSION

Data presented here suggest that, in contrast to the commonly described coupling of GABA$_B$ receptors to G$\alpha_{i/o}$ G proteins, GABA$_B$ receptors can also couple to Gα_q G proteins. This polygamous coupling leads to the activation of PKCα and, independent of CaMKII, results in enhanced L-type calcium current in neonatal rat hippocampal cultures. The current hypothesis, shown in figure 4.7, is that once a ligand binds to the external face of the GABA$_B$ receptor, Gα_q is released from the intracellular side of the receptor. The α subunit activates the enzyme phospholipase Cβ, (PLCβ) which cleaves the membrane- bound phosphatidylinositol bisphosphate (PIP$_2$) into diacylglycerol (DAG) and inositol tris-phosphate (IP$_3$). The conventional isozyme PKCα, which requires both DAG and calcium for its activation, may directly phosphorylate the L-type channel such that it passes more current when open. However, this phosphorylation event may not be directly mediated by PKC; it is possible an unknown protein acts as an intermediary between PKCα and the L-type channel.

In order to test the involvement of Gα_q in the signal transduction pathway, I employed a knockdown strategy which inhibits translation of target mRNA via morpholino (MO) oligonucleotides. Traditionally, knockdown of protein expression involves the use of siRNA; however, MO offer a number of advantages. siRNA are sensitive to intracellular enzymes, can trigger innate immune response, and can cause changes in the methylation state of DNA (Bayne and Allshire 2005; Judge et al., 2005; Kawasaki et al., 2005; Marques and Williams 2005). None of these actions occur with MO, and they have been shown to be taken up in cultured cells, through endocytosis

stimulated by the Endo-Porter peptide (Hudziak et al., 1996). The lack of enzymatic

degradation makes MO particularly well suited for these studies because of the relatively

long half-life of G proteins. Despite these advantages, the use of MO in mammalian

systems is still relatively new compared to use in other model organisms, particularly

Danio rerio. Indeed, there is only one report of Endo-Porter mediated MO knockdown in

mammalian neurons (Chih et al., 2006). Thus, validation of protein knockdown

demonstrated here highlights the usefulness of this technique.
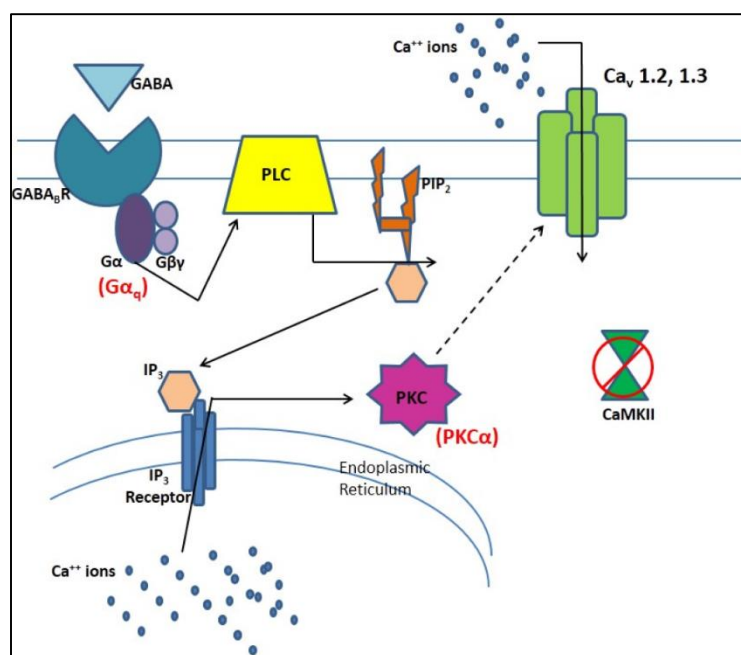
Figure 4.7: The current model for the pathway, which begins with GABA$_B$ receptor activation and results in enhanced L-type current. Ligand binding to the GABA$_B$ receptor leads to the activation of a Gα_q G protein, which putatively activates PLC. The activity of PLC hydrolyses PIP$_2$ into DAG and IP$_3$, which can activate PKC, specifically the α isozyme. PKCα bypasses CaMKII, leading to changes in the L-type calcium channel, such that L-type current is enhanced when the channel opens. Whether PKCα directly interacts with the channel is unknown. Abbreviations: PLC phospholipase C, PIP$_2$ phosphatidylinositol 4,5-bisphosphate, DAG diacylglycerol, IP$_3$ inositol trisphosphate, PKC protein kinase C.

Western blot analysis indicated that morpholinos were efficient in knocking down

Gα_q in primary hippocampal cultures, but given the high similarity in G protein mRNA

sequence to which MOs bind, it was necessary to verify specificity of this knockdown. The most likely candidate for nonspecific knockdown was $G\alpha_{11}$, due to its high sequence homology with $G\alpha_q$. The first 25 coding amino acids (the site of MO binding) are 92% identical. Despite MO being designed with 100% fidelity to the target, nonspecificity was a concern because of this sequence similarity. Furthermore, $G\alpha_{11}$ may compensate for missing $G\alpha_q$ in $G\alpha_q$-deficient mice, suggesting functional overlap as well (Korhonen et al., 2009). Data shown here suggests significantly higher expression of $G\alpha_q$ than $G\alpha_{11}$, consistent with other reports (Milligan 1993; Ihnatovych et al., 2002). However, caution must be used in interpreting these results. Because different antibodies were used to detect each protein, it is possible that the $G\alpha_{11}$ antibody is less effective and simply gives a weaker signal than the $G\alpha_q$ antibody, even if there is abundant protein. However, these Western blot data agree with other reports of greater $G\alpha_q$ expression. Furthermore, $G\alpha_q$ expression is highest during the first postnatal week (Ihnatovych et al., 2002); this temporal peak in expression corresponds to the time when the highest percentage of neurons demonstrate L-type calcium current enhancement with baclofen (Bray and Mynlieff 2009).

Experimental data from both electrophysiological and calcium imaging experiments support the hypothesis that $G\alpha_q$ is the G protein that couples to the $GABA_B$ receptor, ultimately leading to enhanced L-type current. In both paradigms, knockdown of $G\alpha_q$ eliminated the enhancing response. These data were supported by confocal imaging, which demonstrated the colocalization of $GABA_B$ receptors and $G\alpha_q$ G proteins. However, Mannoury la Cour et al. used an antibody/scintillation proximity assay to demonstrate a lack of coupling between $G\alpha_{q/11}$ and $GABA_B$ receptors (2008). One

potential problem with this study is that the reported EC_{50} value for baclofen was approximately 50 µM for $G\alpha_{i/o}$ coupling. This value is much higher than those used by others examining $G\alpha_{i/o}$ activation by $GABA_B$ receptors. Furthermore, the enhancing effect of baclofen on calcium current was seen at high nanomolar concentrations, while attenuation of calcium current requires micromolar concentrations (Shen and Slaughter 1999). Thus, it is possible that the assay used by Mannoury la Cour et al. (2008) is not sensitive enough to show $G\alpha_q/GABA_B$ coupling at low agonist concentrations.

The functional $GABA_B$ receptor is a heterodimer consisting of two subunits, $GABA_{B1a}$ and $GABA_{B1b}$, of which $GABA_{B1b}$ interacts with the G protein. The molecular interaction between the $GABA_B$ receptor and $G\alpha_{i/o}$ involves both the second and third intracellular loops of $GABA_{B1b}$ (Havlickova et al., 2002; Duthey et al., 2002). This interaction occurs with the extreme C-terminus of the G protein (Franek et al., 1999). The lack of sequence homology between $G\alpha_{i/o}$ and $G\alpha_q$ suggests that $G\alpha_q$ must couple to sites unique to those examined previously. Although this is the first example of $GABA_B$ receptors coupling to $G\alpha_q$, coupling of a receptor to multiple G proteins has been shown previously, including receptors that couple to both $G\alpha_q$ and $G\alpha_{i/o}$. Another possibility is that the $\beta\gamma$ subunit of the $G\alpha_{i/o}$ G protein may increase intracellular calcium by the same pathway as $G\alpha_q$. This has been shown to occur in airway smooth muscle (Mizuta et al., 2011). In this study, stimulation of $GABA_B$ receptors activated $G\alpha_i$ G protein and an increase in calcium entry was observed. When $\beta\gamma$ subunit signaling was pharmacologically blocked, no calcium entry was observed and IP_3 production was reduced. Furthermore, direct stimulation of $PLC\beta$ by $\beta\gamma$ has been reported in COS-1 cells (Camps et al., 1992), and this stimulation may occur synergistically with stimulation

by $G\alpha_q$ from a separately activated receptor (Smrcka and Sternweis 1993). However, if current enhancement was mediated by $G\alpha_{i/o}\beta\gamma$ subunits, it would be sensitive to pertussis toxin. When PTX was applied to cell cultures, baclofen-mediated current enhancement persisted. Furthermore, since $\beta\gamma$ signaling requires functional α subunit interaction for proper assembly (Smrcka 2008), knockout of $G\alpha_q$ would likely prevent $\beta\gamma$ from initiating cascades as well.

One question that remains unanswered is why only a subset of neurons show L-type enhancement when $GABA_B$ receptors are stimulated. The answer is likely that, with 16 different types of interneurons found in the hippocampus, perhaps only (a) certain type(s) exhibit this response. Immunohistochemical data have provided clues to a more specific, functional answer. Neurons (presumably interneurons) in both the stratum oriens and the stratum radiatum showed colocalization of $GABA_B$ receptors and $G\alpha_q$ G proteins. Studies are underway to determine which type(s) of interneuron(s) is responsible for the current enhancement observed. By examining colocalization of $G\alpha_q$ and interneuronal markers already known to colocalize with $GABA_B$ receptors, the specific cell type that demonstrates current enhancement can be identified. For example, cholecystokinin (CCK), somatostatin, calbindin, and neuropeptide Y all demonstrated colocalization with $GABA_B$ receptors. These markers help define cell type. The hypothesis is that at least one of these markers will colocalize with $G\alpha_q$, which would indicate the type of cell which exhibits L-type enhancement. Elucidating the cell type would provide a basis for determining the physiological relevance for $GABA_B$ mediated enhancement of L-type current.

CHAPTER 5

Calcium/calmodulin-dependent kinase II inhibitor CK59 demonstrates nonspecific,

reversible inhibition of voltage-gated calcium channels

INTRODUCTION

Calcium-calmodulin dependent kinase II (CaMKII) is a crucial signaling

molecule involved in many of the most fundamental behaviors of neurons, such as gene

expression and synaptic plasticity due to long term potentiation. It follows that the

distribution of this protein is widespread throughout the nervous system, and makes up

between 1-2% of total proteins in neurons. Given both its importance and its abundance,

CaMKII-mediated processes are currently under intense investigation. One of the most

common ways to study the role of CaMKII is via pharmacological inhibition. Changes in

the neuron may be revealed when a specific CaMKII inhibitor is applied, allowing the

investigator to attribute these changes to CaMKII activity. Unfortunately, a common

problem with kinase inhibitors, including CaMKII inhibitors, is their lack of specificity;

they may inhibit more targets than just CaMKII. Therefore, new, more specific inhibitors

are in high demand. This demand extends to a clinical setting, where more specific

CaMKII-related drugs would help avoid potentially harmful side effects.

Over 30 different isoforms (made up of various alternatively spliced α, β, γ, and δ

subunits) of CaMKII have been reported (for review see Fink and Meyer 2002; Wayman

et al., 2011). The primary neuronal subunits are α and β, which are highly homologous.

Subunits come together either as homo- or heterododecihedromers, with each subunit

containing a catalytic, regulatory, and oligomerization domain. The structure of CaMKII is analogous to a flower petal, where the oligomerization domain makes up the inner core, while that catalytic and regulatory domains form a stack of 2 hexomers (Gaertner et al., 2004; Rosenberg et al., 2006; see figure 1.8 from introduction). When calmodulin (CaM) binds to the regulatory domain, autoinhibition is disrupted, and the particular subunit interacting with CaM is free to autophosphorylate neighboring subunits, which causes their catalytic subunits to become active. CamKII inhibitors reduce the activity of the enzyme in different ways. For example, one of the most commonly used inhibitors, KN93, works to compete with CaM binding to the regulatory domain. This is in contrast to an inhibitor such as autocamtide 2-related inhibitory peptide (AIP), which specifically inhibits autophosphorylation (Ishida et al., 1995; Song et al., 2010). It follows that with different forms of inhibition, there are many different off target effects.

CaMKII phosphorylates a wide variety of proteins to modulate their activity, including voltage-gated calcium channels. Regulation of these channels, either positive or negative, occurs at sites on the channel within the intracellular loops or at the N and C termini. G protein βγ subunits (Li et al., 2004) as well as multiple kinases (Park et al., 2006; Wang et al., 2009) have been shown to interact with all types of voltage-gated calcium channels. Since changes in intracellular calcium concentration often work as a switch for many physiological processes, there is a great deal of interest surrounding how the behavior of these channels can be modified by various signaling molecules. The most direct approach is to expose cultured neurons to cell-permeable CaMKII inhibitors and observe what, if any, effect CaMKII inhibition has on L-type current enhancement. However, kinase inhibitors have been complicated by nonspecificity and off target

effects. For example, CaMKII inhibitor KN93 interacts with L-type calcium channels by reversibly inhibiting them (Gao et al., 2006). Previously regarded as one of the cleanest, most potent CaMKII inhibitors in existence, KN93 is not well suited to be used in my studies, which examine calcium channel activity. Recently a compound known as CK59 was synthesized, and has been shown to inhibit CaMKII activity (Konstantopoulos et al., 2007). While originally created to investigate the kinase responsible for insulin-mediated GLUT 4 glucose transporter translocation, CK59 also offered an attractive option to those studying CaMKII and calcium channels, due to its potency ($IC_{50} < 10$ μM) and cell permeability. I selected this inhibitor because of these factors, but it was immediately clear that similarly to KN93, CK59 displayed nonspecific inhibition in a reversible manner. Thus, I sought to better describe this nonspecific inhibition by examining which type of calcium channel (N-, P/Q- or L-type) was affected, as well as the potency of the inhibition.

RESULTS

CK59 inhibits depolarization-induced calcium entry

Ratiometric calcium imaging was used to explore the effects of CK59 and cell-permeable autocamtide-2 related inhibitory peptide (Ant-AIP-II). Ant-AIP-II is a compound that is an analogue of autocamtide-2 related inhibitory peptide (AIP) in which Ala^3 and Val^{10} are replaced with Lys and Phe respectively, giving the Ant-AIP-II 10 times greater potency than AIP (IC_{50} for Ant-AIP-II 4 nM, versus 40 nM for AIP). Furthermore, Ant-AIP-II contains the *Antennapedia* transport sequence fused to its amino terminus to enhance cell permeability. Ant-AIP-II has been demonstrated to successfully enter both glia and neurons (Watterson et al., 2001; Mauceri et al., 2004). Cells were depolarized with high KCl for 30 seconds, then KCl was washed away and cells allowed to return to baseline. Subsequently cells were pretreated with Ant-AIP-II for 15 seconds, followed by coapplication of Ant-AIP-II and high KCl for 30 seconds. This solution was washed away, and a final high KCl stimulation was performed. When 50 μM was CK59 applied ($IC_{50} = 10$ μM), the high KCl solution was not able to elicit as large an increase in intracellular calcium (Figure 5.1a). However, Ant-AIP-II treatment (50 nM) shows no significant effect of on calcium entry through voltage-gated channels using the same experimental protocol (Figure 5.1b). This CK59-mediated effect was reversible, as the response to the high KCl depolarization after washout was restored to baseline levels. On average, the increase in intracellular calcium was $44.83 \pm 1.88\%$ when compared to control levels of intracellular calcium (the increase seen when high KCl alone was perfused onto the cells (Figure 5.1c, N = 128; paired t-test, $P < 0.001$). There was no
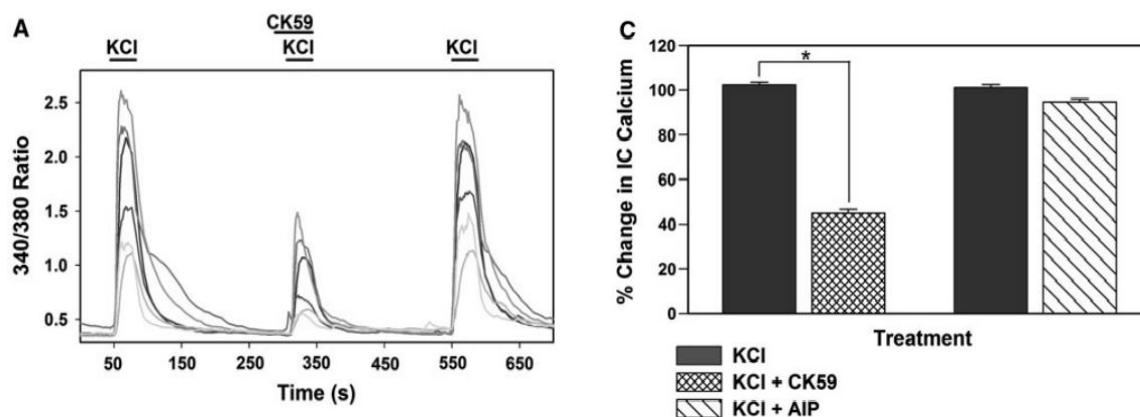
Figure 5.1: CaMKII inhibitor CK59 but not Ant-AIP-II significantly attenuates the amount of high KCl-induced increase in intracellular calcium when measured with ratiometric imaging. A: Example of 340/380 ratio obtained with high KCl solution alone or high KCl solution in the presence of 50 μM CK59. Each line shown represents an individual cell (N = 6). B: The same conditions as in A, but using 50 nM Ant-AIP-II (N = 6). C: Average change in intracellular calcium as determined by the 340/380 ratios with KCl alone (solid bars), KCl with CK59 (crossed hash bar, N = 128), or KCl with Ant-AIP-II (diagonal hashed bar, N = 255, *Paired t test, P < *0.001*)

significant reduction in calcium entry when neurons were exposed to Ant-AIP-II (94.68 ±

CaMKII 1.29) compared to control levels. (N = 255). Neither inhibitor had any effect on

the baseline levels of intracellular calcium. These data suggest that the novel

inhibitor CK59 shows off-target inhibition of voltage-gated calcium channels. However,

the data do not exclude the possibility that CK59 enhances the rate of calcium extrusion

in the presence of high intracellular calcium, thereby decreasing intracellular calcium

levels measured.

CK59 decreased calcium influx in a concentration dependent manner

In order to get a measurement of the potency of the CK59-mediated inhibition of voltage-gated calcium channels, a concentration-response curve was constructed. High KCl-induced increases in intracellular calcium were measured in the presence of 500 nM – 250 μM CK59. The solubility in DMSO limited the highest concentration of CK59. Control experiments done with DMSO diluted 1:250 in Ringer's solution with no CK59 did not affect high KCl-induced calcium influx at this concentration (data not shown). These concentration-response curve data were fit with a 3 parameter sigmoidal curve, which assumed that if the concentration was increased to high enough levels, all calcium entry would be blocked. The curve generated an IC_{50} of 52 μM (Figure 5.2). It is possible that this is an overestimate; if all calcium entry is not completely inhibited and instead CK59-mediated inhibition at a concentration of 250 μM is the actual maximum, then the IC_{50} would be closer to 22 μM.
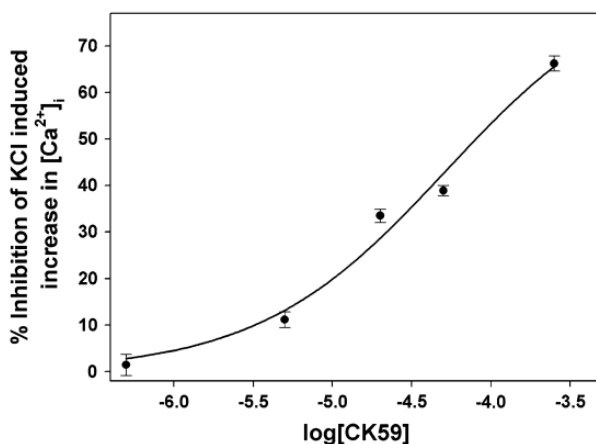
Figure 5.2: Various concentrations (0.5, 5, 20, 50, 250 μM; N = 122, 51, 166, 326, 122, respectively) of CK59 were applied to cells during high KCl-induced depolarization. The percent inhibition of high KCl-induced intracellular calcium by CK59 was calculated as $100\% - (100 \; x \frac{(Fura\ Ratio\ in\ CK59+KCl)}{(Fura\ Ratio\ in\ KCl)})$. Data were fit with a 3 parameter sigmoidal curve ($r^2 = 0.983$), to determine an IC_{50} value of CK59 in decreasing calcium influx, 52 μM.

The effects of CK59 on voltage-gated calcium current were measured directly using whole-cell patch clamp electrophysiology. Currents were elicited by a 300 ms depolarizing pulse to +10 mV from a holding potential of -80 mV. CK59 was applied via U-tube perfusion (Figure 5.3a). Calcium currents often show run-up or run-down of current, so control currents before and after CK59 treatment were used to construct a linear regression line surrounded by a 95% confidence interval (Figure 5.3b). If the inhibitor had no effect, the current elicited when CK59 was present would fall within the confidence interval. However, the total current was reduced with CK59 application, in agreement with calcium imaging data. In all 15 cells tested, CK59 significantly reduced the current an average of $32.05 \pm 1.86\%$ when compared to the linear regression line (Figure 5.3a). The difference in reduction of calcium entry observed when using ratiometric calcium imaging versus whole cell patch clamp electrophysiology likely stems from the length of time neurons were stimulated. In calcium imaging experiments, neurons were depolarized for 30 seconds so that the majority of calcium influx is through long lasting L-type channels, whereas electrophysiological experiments depolarize neurons for a relatively short 300 ms.

CK59 decreases calcium entry through more than one voltage-gated calcium channel

Since it had previously been reported that the CaMKII inhibitor KN93 reduced L-type calcium current, I assessed whether specifically L-type calcium channels were similarly inhibited by CK59 with whole cell recording. Calcium currents were measured during the final 50 ms of a 300 ms depolarizing pulse to +10 mV to minimize the

contribution of other current components while maximizing the long lasting (L-type) component of the current. Notably, N-, P/Q-, and R-type currents are still present during this period, as demonstrated in figure 5.3c, where current still remains after the L-type calcium channel antagonist nimodipine (20 μM) was used. Thus, the current remaining in the presence of nimodipine should primarily be comprised of N-, P/Q-, and R-types of calcium current. If CK59 only inhibited L-type channels, then the addition of CK59 in the presence of nimodipine should not further inhibit the total calcium current because the channels would already be blocked. Figure 5.3c illustrates the calcium current elicited in the presence and absence of CK59 (50 μM) in a cell pretreated with nimodipine (20μM). The current was reduced with CK59 in a reversible manner similarly to the non-nimodipine treated cells. CK59 caused a significant decrease in calcium current with an average reduction of $27.54 \pm 4.66\%$ (N = 7, Figure 5.3c). The reduction in voltage-gated calcium current elicited in the presence of the L-type calcium channel antagonist suggests that CK59 may inhibit N-, P/Q-, and/or R-type current(s).

Ratiometric calcium imaging experiments were done to confirm that CK59 can reduce calcium entry in the presence of an L-type calcium channel antagonist. Nimodipine (20 μM) was present in the bath for the entire time course of the experiment to block L-type calcium channels, and high KCl solution alone or high KCl solution with CK59 (50 μM) were applied acutely (Figure 5.4). Application of CK59 under these conditions reduced calcium entry to $43.73 \pm 1.38\%$ (N = 185) of the average calcium entry elicited by high KCl application alone. Given that both calcium current and entry decreased in the presence of the L-type calcium channel blocker nimodipine, it was hypothesized that CK59 exerts its effects by inhibiting another calcium channel type than
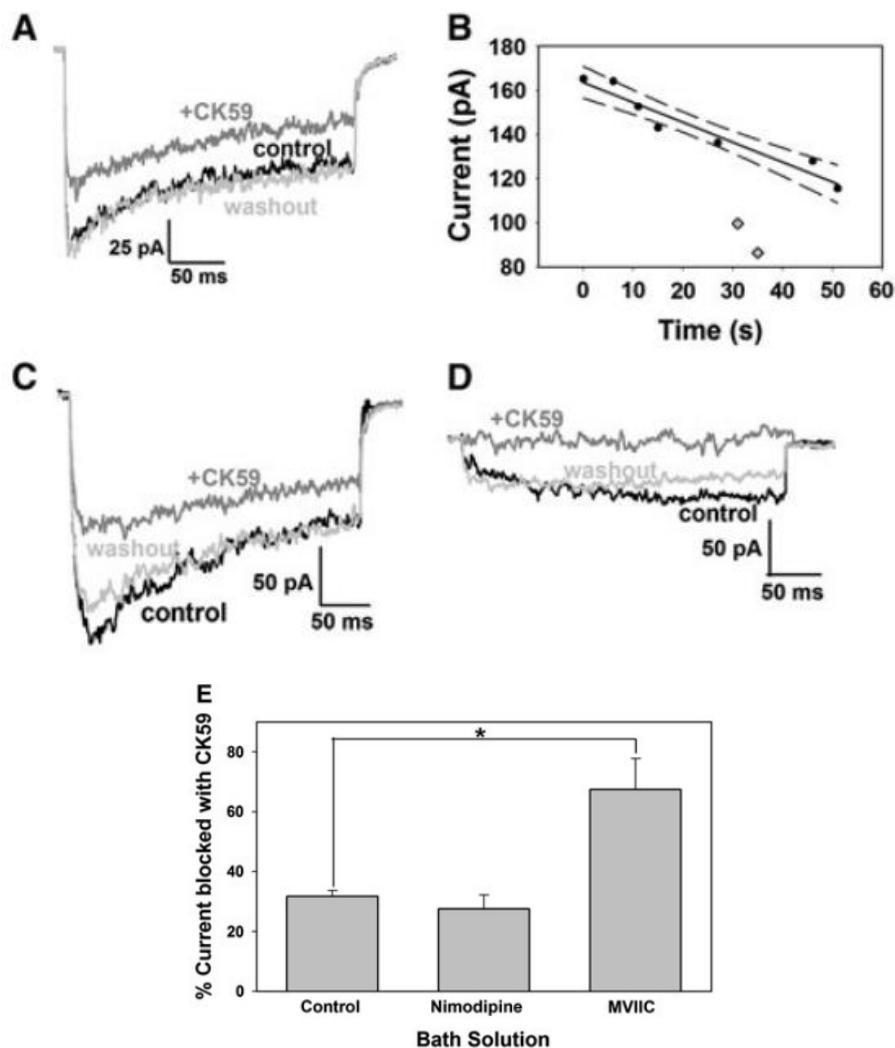
Figure 5.3: Calcium currents elicited by a 300 ms depolarizing pulse +10 mV from a holding potential of -80 mV demonstrate the nonspecific effects of CK59 (50 μM) on voltage-gated calcium channel types. A: CK59 application reduces whole cell calcium current in normal recording solution. Currents were recorded before (*black trace*), during (*grey trace*) or after (*light grey trace*) application of CK59. B: Control calcium currents were measured before and after application of CK59 (*filled circles*) and fit with a linear regression line surrounded by a 95% confidence interval (*dashed line*). Calcium currents elicited in the presence of CK59 (*grey diamonds*) fell outside the confidence interval for the control currents. The percentage of current blocked by CK59 was calculated by comparing the current in the presence of CK59 to the regression line for that specific timepoint. C: 20 μM nimodipine was bath applied and voltage-gated calcium currents were recorded before (*black trace*) during (*grey trace*) and after (*light grey trace*) application of CK59 (50 μM). D: 2 μM ω-conotoxin MVIIC was bath applied and voltage-gated calcium currents were recorded before *(black trace)* during (*grey trace*) and after (*light grey trace*) application of CK59 (50 μM). The traces illustrated in A, C, and D were recorded in different neurons. E: Average decrease in voltage-gated calcium currents seen with CK59 application (50 μM) in control bathing solution (N = 15), with 20 μM nimodipine (N = 7), and with 2 μM ω-conotoxin MVIIC (N = 5) in the bath. *Unpaired *t* test, P < 001.

L-type calcium channels, suggesting a different nonspecific effect from that of CaMKII

inhibitor KN93. However, the effect of CK59 on L-type calcium channels may have

been masked because nimodipine would already be blocking L-type channels in these

experiments. Therefore, experiments were performed to address the effect of CK59 more

specifically on L-type channels.

   To clarify if L-type calcium channels could also be blocked by CK59, ω-

conotoxin MVIIC (2 μM) was added to the bath during electrophysiological studies to

block N- and P/Q-type calcium channels. The current in figure 5.3d is drastically reduced

due to the presence of MVIIC. Comparing the raw current in 5.3c with the L-type

channel blocker nimodipine with the raw current in 5.3d with ω-conotoxin MVIIC

suggests that while L-type current is certainly present in these neurons, currents sensitive

to ω-conotoxin MVIIC (N- and P/Q-type) make up the bulk of the high voltage activated

whole-cell current in neonatal neurons of the superior hippocampus when a 300 ms

depolarizing pulse is applied. Addition of CK59 (50 μM) reduced the current even
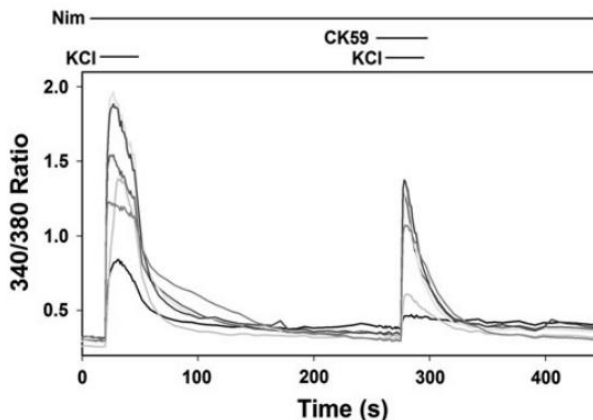
Figure 5.4: CaMKII inhibitor CK59 attenuates the high KCl-induced increase in intracellular
calcium in the presence of L-type calcium channel blocker nimodipine, when measured using
calcium imaging. Nimodipine (20 μM) was perfused during the entire measurement period.
The 340/380 ratio was measured in response to high KCl solution before and during CK59
application (50 μM), and representative cells are shown (N = 7 shown, total N = 185). Each
line represents an individual cell.

further, so that very little current remained when MVIIC and CK59 were simultaneously applied. Calcium currents in these studies were decreased an average of $67.47 \pm 10.38\%$ (N = 5; Figure 5.3d) which was a significantly larger decrease by CK59 than that seen when ω-conotoxin MVIIC was not present (unpaired t-test, $P < 0.001$, Figure 5.3e).

DISCUSSION

Data presented here show the off-target action of the CaMKII inhibitor CK59 on voltage-gated calcium channels. Both electrically stimulated currents in whole cell electrophysiological recording and high KCl-induced calcium influx were significantly reduced by CK59 in a dose-dependent manner. However, determining the exact calcium channel(s) targeted by CK59 is more difficult. Studies done in the presence of ω-conotoxin MVIIC strongly argue for L-type channel inhibition. As expected, when MVIIC was applied to the bath, the remaining current was reduced. When CK59 was applied while MVIIC was in the bath, there was near complete extinction of current in the majority of cells tested. However, in the presence of L-type channel blocker nimodipine, both calcium current and calcium entry were reduced when CK59 was applied. These data seem to contradict experiments performed in MVIIC. However, one possibility is that when nimodipine is present, L-type current is already being blocked. Therefore, any effect on L-type channels would be masked. The decrease in calcium levels in the presence of nimodipine after CK59 application does suggest inhibition of additional channels besides the L-type calcium channel. One possibility is that R-type calcium channels are inhibited by CK59. However, R-type current in the entorhinal cortex makes up only 11-13% of total calcium current (Castelli and Magistretti 2006). The small amount of current seen in the cells treated with MVIIC also suggests a large component of calcium influx is through N- and P/Q-type channels. Even if complete blockade of R-type current was assumed, this would likely not make up for the amount of inhibition seen in nimodipine-treated cells. There was a 27.54% reduction in whole cell calcium

current and 56.27% reduction in high KCl-mediated calcium entry when nimodipine was present. These data suggest that even if R-type channels are affected along with L-type channels, there must be another channel that is inhibited by CK59.

A second possibility that is that L-type channels were not completely blocked. This seems unlikely due to the high concentration of nimodipine used in these studies (IC_{50} = 139 nM for Ca_v 1.2 and 3 µM for Ca_v 1.3, respectively; Catterall 2005). It is more likely that at least one of the channels blocked by MVIIC is susceptible to inhibition by CK59. In either case, it seems that CK59 inhibits L-type channels as well as others. While the identity of the other channels that CK59 may inhibit in addition to L-type channels is not completely clear, it is evident that CK59 has off-target effects that inhibit the entry of calcium through voltage-gated calcium channels.

Figure 5.3d shows the effect of blocking N- and P/Q-type currents pharmacologically with MVIIC, then applying 50 µM CK59. The result of this experiment is that the remaining current not blocked by MVIIC is nearly completely blocked with CK59, and this current would likely be L-type current. Figure 5.3c shows the effect of blocking L-type current with nimodipine, then applying 50 µM CK59. While CK59 reduces current, there is a large component that still remains. There are two possibilities for this effect. First, it is possible that L-type channels have a lower IC_{50} for CK59 than the measured 52 µM for all calcium channels collectively. Thus, a complete block of L-type channels may occur at 50 µM. The same concentration may not completely block N- and P/Q-current. Alternatively, it is possible that there is a component of the current which CK59 does not inhibit whatsoever.   For example, if in

Figure 5.3c, L-current was blocked by nimodipine and only P/Q-current was blocked by

CK59, the remaining current could be N-type current, unaffected by either inhibitor.

CK59's IC_{50} for inhibition of CaMKII activity is <10 μM. Other nonspecific

CaMKII inhibitors that inhibit L-type calcium channels are more potent, both in their

primary and off-target effects. For example, the IC_{50} for KN93's effect on CaMKII is

0.37 μM (Sumi et al., 1991), whereas its IC_{50} for L-type channel inhibition is

approximately 1μM (Gao et al, 1996). The IC_{50} of the structurally related inhibitor KN62

is 0.9 μM for CaMKII activity; the IC_{50} for its off-target effects on calcium entry is

approximately 0.5 μM (Sihra and Pearson 1995). Given the relatively close IC_{50} values

for primary and off-target effects of these CaMKII inhibitors, caution must be exercised

when selecting a compound to pharmacologically inhibit CaMKII activity.

CHAPTER 6

GENERAL DISCUSSION

The central findings of work presented here detailed the signal transduction pathway of L-type calcium current enhancement upon $GABA_B$ receptor stimulation. It was demonstrated that $GABA_B$ receptors are capable of coupling to $G\alpha_q$ G proteins; this activation leads to increased $PKC\alpha$ activity. As reported previously in our laboratory and in others, this increased $PKC\alpha$ signal is necessary to increase L-type calcium channel activity. The entire cascade circumvents CaMKII. However, it is not clear whether $PKC\alpha$ phosphorylates L-type channels directly, or if there are more intermediaries in the process of calcium current enhancement.

Determination of the L-type channel isoform

The neuronal L-type calcium channel has two isoforms, Ca_v 1.2 and Ca_v 1.3. Because both channels are sensitive to dihydropyridines, there is no current way to separate their functions pharmacologically. Furthermore, while conditional knockout animals have been generated, there is the possibility that one isoform will be upregulated to compensate for the loss of the other isoform. Thus, it has been difficult to ascribe specific functions to a specific isoform. One question that remains in the signal transduction pathway described here is which calcium channel isoform mediates current enhancement. Expression data from the Mynlieff laboratory showed that expression of Ca_v 1.2 peaks within the first week of development, then decreases rapidly. These data have been confirmed by other investigators (Morton et al., 2013). Peak expression of Ca_v

1.2 coincides with the time point where the greatest number of cells show enhanced calcium entry after $GABA_B$ receptor activation, suggesting that Ca_v 1.2 is the channel responsible for mediating this enhancement. However, Ca_v 1.3 is expressed at P7 as well, albeit at lower levels. Furthermore, co-immuprecipitation and yeast two-hybrid assays show a physical interaction between the $GABA_B$ receptor and Ca_v 1.3 (Park and Rhim 2010). These data suggest Ca_v 1.3 may be responsible for current enhancement. A final possibility is that current enhancement occurs in both Ca_v 1.2 and Ca_v 1.3. Baclofen has been shown to enhance calcium levels through both Ca_v 1.2 and Ca_v 1.3 when measured in transfected HEK293 cells (Im and Rhim 2012). Thus, there is not a clear consensus on the calcium channel isoform that mediates L-type current enhancement in cultured hippocampal neurons.

Experiments using morpholino (MO) oligonucleotides to knock down either Ca_v 1.2 or Ca_v 1.3 will help identify the isoform mediated current enhancement. Knockdown of Ca_v 1.2 would allow the effects of Ca_v 1.3 exclusively to be observed. For example, if knockdown of Ca_v 1.2 abolishes L-type enhancement, then this is the channel targeted by $GABA_B$ receptor activation. If enhancement persists, then Ca_v 1.3 must be at least partially responsible for L-type enhancement. These studies should be feasible because use of MO in protein knockdown have been successful in our rat cultures. However, should MO knockdown prove unsuccessful, there is the possibility of determining which channel mediates L-type enhancement by examining the phosphorylation state of the channel. One drawback to this strategy is that it assumes enhancement is due to a phosphorylation event. A second drawback is this strategy would require purification of proteins that are not highly expressed (particularly Ca_v 1.3). However, identification of

the channel remains a crucial step in elucidating the physiological relevance of L-type enhancement.

The possibility of BDNF-mediated KCC2 expression

The influx of current through L-type calcium channels is critical throughout development and into adulthood. During embryogenesis, L-type current is required for neural crest cell migration and differentiation (Moran 1991). It is known that the hippocampus is a crucial site for long-term potentiation (LTP), which underlies synaptic plasticity. Pharmacological inhibition of L-type channels results in impaired induction of specific forms of LTP in young (P21 - P28) rats (Kapur et al., 1998). Particularly pertinent to studies in the Mynlieff laboratory is the relationship between the neurotransmitter GABA and L-type current as the hippocampal circuitry matures. During embryonic development, GABA acts as an excitatory neurotransmitter, but undergoes a switch to mediate inhibition (for review see Blaesse et al., 2009). Depending on experimental conditions (region of the hippocampus examined, cultured or slice preparation, recording parameters, etc.), the switch in the effect of GABA on hippocampal neurons ranges from P5 to P13 (Tyzio et al., 2007). This switch is based on chloride gradients established by chloride transporters, and the transporters themselves are regulated by calcium influx through L-type channels. Maturation of GABAergic circuitry is dependent on GABA itself (Ganguly et al., 2001). Activation of $GABA_A$ receptors is sufficient to open voltage-gated channels, and it is particularly the calcium flowing through L-type channels which regulate chloride transporter expression levels (Bray and Mynlieff 2009). Indeed, treating cultured cells with L-type channel

antagonists reduces expression of the chloride transporter K^+Cl^-co-transporter 2 (KCC2, Bray and Mynlieff 2009), the chloride transporter that is responsible for chloride efflux during adulthood.

Currently, the precise mechanism for how changes in L-type calcium current changes the expression of KCC2 is unknown. One hypothesis is that brain derived neurotrophic factor (BDNF) expression upregulates the levels of KCC2 in an L-type calcium-dependent manner. Several lines of evidence support this hypothesis. First, BDNF levels are higher in the first two weeks of postnatal development (Sathanoori et al., 2004), coinciding with the switch in GABAergic signaling from excitatory to inhibitory. Secondly, $GABA_A$-induced increases in intracellular calcium stimulate BDNF expression. The BDNF gene is complex; it encodes 4 exons that are noncoding on their own, as well as 4 promoters (Figure 6.1, Timmusk et al., 1993). Alternative splicing produces a single exon which encodes the BDNF protein. Within the four exons, transcripts that contain exon III are most sensitive to calcium-mediated induction. Within exon III, the transcription factor CREB is required to induce expression, but it is not sufficient. The promoter of exon III contains a binding site for 3 distinct transcription factors, including the most distal binding site, calcium response element (CaRE1, Tao et al., 2002). Induction of the BDNF gene can occur when CaRE1 is bound to the transcription factor CaRF. The activity of CaRF is dependent both on neuronal type and calcium concentration. CaRE1 does respond to depolarization when isolated from the BDNF promoter, but exhibits cooperativity with other CaREs. Currently, there are 3 known CaREs, and transcription factors are required at each CaRE in order to express exon III-containing BDNF. It is thought that different combinations of calcium-
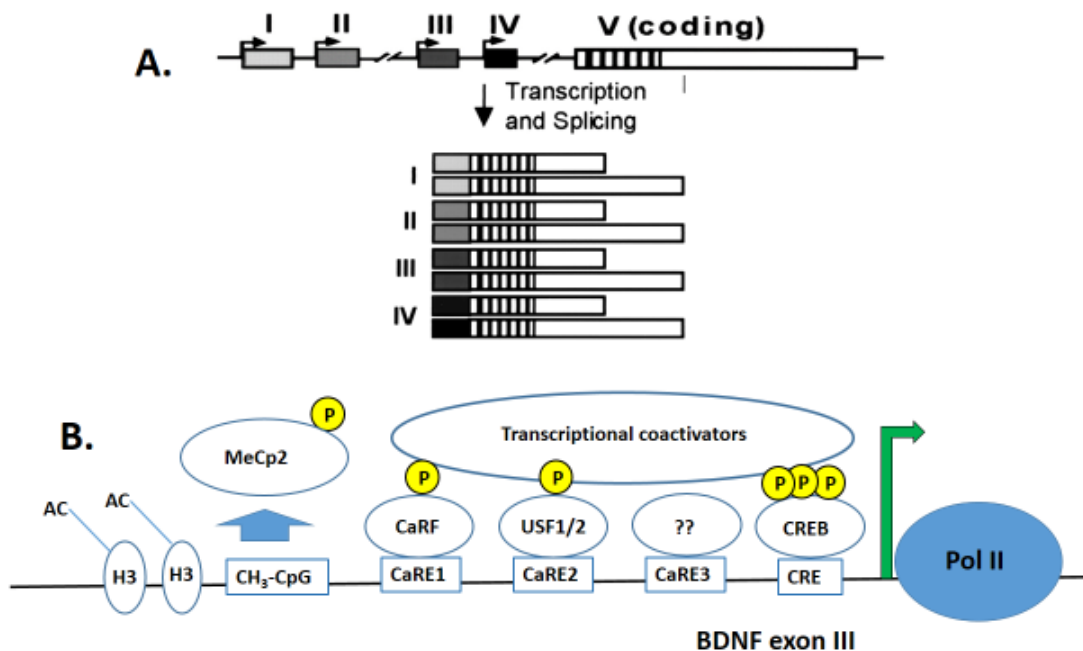
Figure 6.1: BDNF gene regions, and regulation of exon III. A: The BDNF gene can generate 8 distinct protein transcripts. There are 4 possible initial exons which can be alternatively spliced to form a single 3' exon. Each of the 4 splice variants may use one of two polyadenylation sites within the 3' untranslated region. B: The promoter III region on the BDNF gene is activated in response to calcium influx. At least 3 transcriptional activators, CaRF (calcium response factor), USF (upstream stimulatory factor) and CREB (calcium response element-binding protein) must be recruited to the promoter. In addition, MeCP2 (methyl CpG binding protein 2) must also be removed, which allows histone H3 to be acetylated (AC) and transcription of the BDNF gene to occur. Phosphorylation of MeCP2 and CaRF occurs through calcium/calmodulin-dependent kinases that are activated by calcium entering, in part, through L-type channels (Adapted with permission from West et al., 98(20): 11024-11031 (2001). Copyright (2001) National Academy of Sciences, U.S.A.

dependent transcription factors may be a mechanism for cell type specificity of gene induction due to depolarization.

Furthermore, the methylation state of BDNF is also influenced by intracellular calcium. Methylation of DNA commonly occurs where cytosine nucleotides reside next to guanine nucleotides (CpGs). Methlyated CpGs bind several proteins, including methyl-CpG binding protein 2 (MeCP2). MeCP2 binds to the promoter III region of BDNF DNA and functions to repress expression (Zhou et al., 2006). However, an

activity-dependent increase in calcium triggers phosphorylation of MeCP2 in a CaMKII-dependent mechanism (Chen et al., 2003). Phosphorylation of MeCP2 releases it from the promoter and allows promoter III-dependent BDNF transcription. Thus, increased intracellular calcium, potentially due to chloride efflux during development, can increase BDNF activity by two distinct mechanisms.

The mechanism by which BDNF increases KCC2 expression is also complex. Early growth response 4 (Egr4) is a transcription factor whose expression increases during and after neuronal activity. The KCC2 gene contains a binding site for Egr4 on its promoter (Uvarov et al., 2006). BDNF application activates TrkB receptors which lead to increased $ERK_{1/2}$ activity. $ERK_{1/2}$ in turn causes increased expression of Egr4, which is a requirement for transcription of KCC2 (Ludwig et al., 2011). Importantly, a direct pathway between L-type calcium current and increased KCC2 has not been demonstrated, nor has the $GABA_B$ mediated enhancement of L-type current been implicated in changing expression of KCC2. However, it has been shown that $GABA_B$ receptor activation increases L-type current, which results in increased levels of phosphorylated $ERK_{1/2}$ (Im and Rhim 2012). Furthermore, it has also been shown that activation of $GABA_B$ receptors increase secretion of BDNF (Kuczewski et al., 2011). Currently, there is not an established function for enhancement of L-type current in response to $GABA_B$ receptor activation. However, experiments examining whether this increased calcium changes KCC2 expression could provide a functional association that is currently lacking.

Besides causing increased synthesis of BDNF, L-type calcium current is also known to promote BDNF release. Spontaneous α-Amino-3-hydroxy-5-methyl-4-

isoxazolepropionic acid (AMPA) receptor activity in CA3 induces long term potentiation

of GABAergic synaptic transmission; this potentiation is dependent on BDNF release,

which in turn is dependent on L-type calcium current (Figure 6.2, Kuczewski et al.,

2008). Spontaneous post-synaptic currents generated by AMPA receptor activity activate

L-type channels. Activation leads to a BDNF release event, where BDNF diffuses to

neighboring TrkB receptors. When these TrkB receptors are activated, a $GABA_A$

receptor-mediated induction of long term potentiation is observed. Exactly how TrkB

receptor activation leads to an increase in postsynaptic calcium is unknown. However,

these data demonstrate that, in addition to regulating production of BDNF, L-type

calcium current may also be involved in activity-dependent release. Importantly, this

study showed that sustained glutamatergic activity is required for L-type channel

activation. Sustained glutamatergic receptor activation has been shown to downregulate

$GABA_B$ receptors through increased lysosomal degradation (Maier et al, 2010). One

hypothesis for this effect is that enhancement of L-current, perhaps through $GABA_B$

receptor activation, is necessary to get a spike in BDNF production and release when
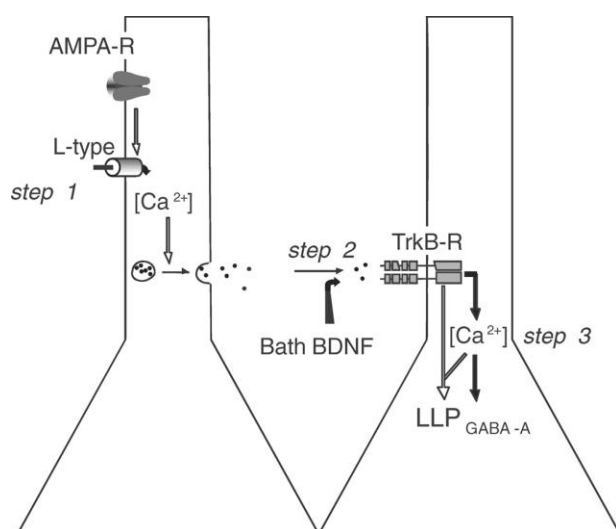
Figure 6.2: Influx of calcium current through L-type channels can induce BDNF release. The 3 step model proposes that spontaneous AMPA receptor current activates L-type channels (step 1). This increased intracellular concentration stimulates release of BDNF, which binds to pericellular TrkB receptors (step 2). Step 3 involves the activation of these receptors leading to long-term potentiation that is dependent on GABAergic signaling. Figure reproduced with permission from John Wiley & Sons Publishing, Inc. Kuczewski et al., 1;586 (Pt 21): 5119-5128, (2008).

KCC2 is expressed during development. Once GABAergic circuitry has matured, sustained glutamatergic activity supports basal BDNF levels and also downregulates $GABA_B$ receptor-mediated L-type enhancement.

Identification of the interneuron class that displays L-type enhancement

While the pathway between $GABA_B$ receptor activation and L-type current enhancement is now clearer, there is still a lack of understanding as to what cells are displaying this phenomenon. Within the CA1 region of the hippocampus, there are separate populations of excitatory pyramidal cells and inhibitory GABAergic interneurons. Generally, the pyramidal cells are considered a single population; because pyramidal cells make up a comparatively larger percentage of hippocampal cells than interneurons, it is unlikely that L-type enhancement is mediated through these cells. Conversely, there are at least 16 distinct classes of interneurons, with 12 classes that innervate particular regions of pyramidal cells and 4 classes that innervate other interneurons. Immunocytochemical markers, electrophysiological recording, and morphological differences define the different classes; this classification has started to uncover their specific functional significance. For example, one group of interneurons, known as basket cells, provide GABAergic synapses onto the soma and proximal dendrites of pyramidal cells (Somogyi and Klausberger 2005). Their output is localized to control both timing and frequency of action potential generation in pyramidal cells. Control of spike timing is required for rhythmical synchronization of pyramidal cell networks, so basket cell output is essential in the generation of oscillatory firing. However, although basket cells may be morphologically similar and have similar targets

on pyramidal cells, there are distinct populations of basket cells that form 3 of the 16 classes of interneurons.

One of the 16 classes of inhibitory interneurons are basket cells that express parvalbumin (PV) but not cholecystokinin. These PV+ basket cells show high frequency action potential firing (150 Hz) in short duration trains (Doischer et al., 2008). Their action potentials are locked in phase to fast oscillatory network firing, and thus provide stable and consistent inhibitory output onto their targets. These basket cells function differently than another class of interneurons, basket cells that express cholecystokinin (CCK). CCK+ cells fire at more moderate frequencies (50 Hz), and their action potentials are not timed to fast oscillations like PV+ basket cells (Lee et al., 2011). This less dependable firing leads to asynchronous release events seen only in CCK+ but not PV+ basket cells. Given the differences in firing frequency and precise timed firing, these separate populations of basket cells likely make distinct contributions to the complete neural network.

Finally, there is a third class of inhibitory interneuron that shows characteristics of a basket cell. It is CCK+, but also exhibits immunoreactivity for vesicular glutamate transporter 3 (VGLUT3, Somogyi et al., 2004). Because a cell that expresses a vesicular transporter is likely functionally distinct, it is put into a separate class. However, so little information is known about this cell type that it is possible that CCK+/VGLUT3+ cells are actually the same CCK+ cells, but may express VGLUT3 at a particular time point. Despite advances in methods combining imaging and physiology, how interneuronal classes are divided is still highly debated.

Which of the 16 inhibitory interneuron types may demonstrate L-type enhancement? One hint comes from a study that examined colocalization between $GABA_B$ receptors and neurochemical markers in the hippocampal CA1 region (Sloviter et al., 1999). PV+ interneurons do not demonstrate colocalization with $GABA_B$ receptors, which likely rules out any class that expresses parvalbumin, including PV+ basket cells. However, $GABA_B$ receptors do colocalize with interneurons expressing CCK, somatostatin, calbindin, and neuropeptide Y. Thus, future experiments in the lab will seek to colocalize one of these 4 interneuronal markers with $G\alpha_q$, since that is the G protein known to increase L-type current. One hypothesis is that increased intracellular calcium drives the maturation of one or more of these interneuronal types. Although there are 16 different interneuron classes, it is likely that not all classes mature during development in the same way (Levitt et al., 2004). One popular mechanism for maturation is activity-dependent regulation of gene expression. Influx of calcium, particularly though N-methyl-D-aspartate (NMDA) or L-type calcium channels triggers a signaling cascade that is necessary for differentiation, growth, and/or formation of synaptic connections (West et al., 2002). It has been shown that both neuronal calcium channel isoforms Ca_v 1.2 and Ca_v 1.3 colocalize with PV+ neurons. Furthermore, although these interneurons express both isoforms, levels of Ca_v 1.3 are more widely expressed (Jiang and Swann, 2005). This was a unique finding because it has been demonstrated previously that approximately 80% of total L-type channels are Ca_v 1.2 and only the remaining 20% are Ca_v 1.3 (Hell et al., 1993). This study suggested that influx of calcium through Ca_v 1.3 regulated development of these PV+ interneurons via an unknown mechanism. This is particularly interesting to our laboratory as we try to

identify the calcium channel isoform mediating current enhancement. The idea that a particular isoform of L-channels can regulate a particular class of interneurons is unique; it is also intriguing to consider whether L-type current enhancement is a requirement in neurons that depend on L-type current for maturation. It is unlikely that the cells examined by Jiang and Swann (2005) may be those that show enhanced colocalization with $G\alpha_q$ and undergo current enhancement, because $GABA_B$ receptors do not colocalize with PV+ interneurons.

L-type current controls gene expression

The timing of L-type current enhancement is of particular interest given that this type of current is known to regulate gene expression (Figure 6.3). The best-described mechanism for this regulation is through activation of transcription factors. For example, local entry of L-type current is known to activate calcineurin (Norris et al., 2002), a protein phosphatase that dephosphorylates the transcription factor NFATc within the cytoplasm. This dephosphorylation serves as a nuclear translocation signal, whereby NFATc will enter the nucleus and activate gene expression (Chung and Jan 2006). Other intermediaries, such as CaMK IV or Ras/mitogen-activated protein kinase (MAPK) pathways also serve to transmit local rises in L-type current to global changes in gene expression (Dolmetsch et al., 2001). Interestingly, these pathways involve the phosphorylation of transcription factor calcium/cAMP responsive element binding protein (CREB); activation of $GABA_B$ receptors has been shown to induce increases in

the ratio of phosphorylated CREB to nonphosphorylated CREB, and this increase can be

blocked by treatment with L-type calcium channel antagonist nifedipine (Kuczewski et

al., 2011).

More recently, a fragment of Ca$_v$ 1.2 (termed calcium channel associated

transcription factor, or CCAT) has been shown to be cleaved from the full-length protein

and act as a transcription factor (Gomez-Ospina et al., 2006). While the mechanism of

cleavage remains unclear, increasing L-type calcium current reduces the amount of

CCAT-mediated transcription that occurs. Furthermore, based on microarray data,

expression of a host of genes was shown to be both upregulated and downregulated based

on CCAT activity. One of the genes that showed the greatest increases in expression

upon CCAT recruitment to its promoter was connexin 31.1 (Cx31.1). Connexins are

proteins critical for the formation of direct electrical connections via gap junctions. The

synchronous firing pattern of interneurons is often dependent on gap junctions made up

of this connexin, and CCAT has been demonstrated to be prominently expressed in these
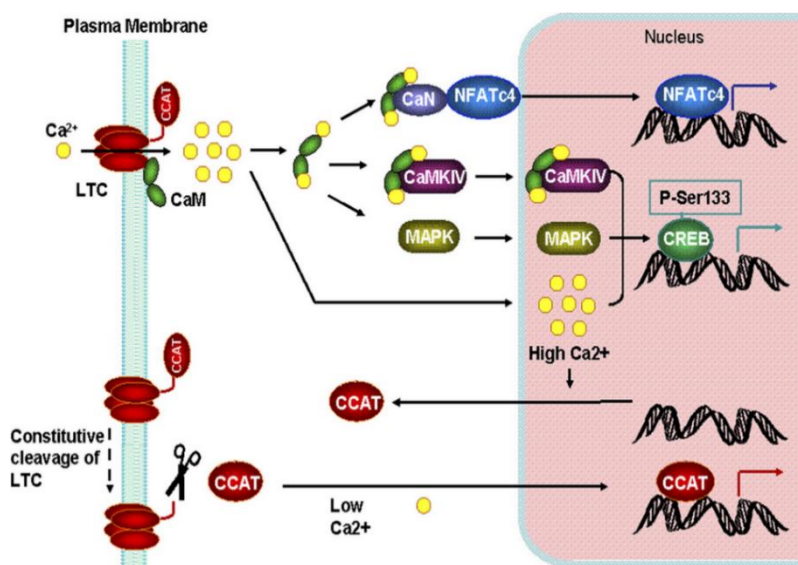
Figure 6.3: Regulation of gene expression by L-type channels. When L-type channels are open, local calcium signals are transduced by second messengers, activating gene expression. When calcium is low in the cell, the C-terminal of the L-type channel is cleaved, and translocates to the nucleus to act as a transcription factor Reprinted from *Nueron*, 52(6). Chung H.J and Jan L.Y., Channeling to the nucleus, pp 937-940, Copyright (2006), with permission from Elsevier.

cells (Connors and Long 2004). It is tempting to speculate that enhancement of L-type current may specifically play a role in CCAT-mediated expression of Cx31.1. One hypothesis is that as the inhibitory circuitry matures and direct electrical connections are made, the level of Cx31.1 needs to be downregulated. By P7, when enhancement of L-type current is greatest (Bray and Mynlieff 2011), Cx31.1 expression is inhibited, such that exact electrical coupling between classes of interneurons is precisely controlled. Would eliminating L-type current enhancement lead to aberrant electrical connections? Future experiments could be designed to look at CCAT levels or Cx31.1 expression in neurons that demonstrate L-type enhancement. If so, this would be evidence for the specific function of Ca_v isoform 1.2, as neither the Ca_v 1.3 isoform nor the N-type channel (Ca_v 2.1) C termini demonstrated any effect on transcription (Gomez-Ospina et al., 2006).

Isozyme-specific function of PKCα in L-type current enhancement

The regulation of calcium channels by PKC has been a matter of some controversy. The nonselective PKC activator PMA has been shown to enhance calcium current in Aplysia bag neurons (DeRiemer et al., 1985), neuroblastomas (Osugi et al., 1986), and frog sympathetic neurons (Yang and Tsien 1993). Paradoxically, inhibition of calcium current has been reported in chick dorsal root ganglion cells (Rane and Dunlap 1986) and PC-12 cells (a neuroendocrine tumor cell line, Di Virgilio et al., 1986). Even in the same cells, the effect of PKC stimulation can lead to opposite effects on calcium current (Tseng and Boyden 1991). Thus, to define the actions of PKC requires the identification of the isozyme of PKC that is active in a particular pathway. In cardiac Ca_v

1.2 channels, phosphorylation by PKCε on the N terminus is responsible for inhibition of L-type current (Yue et al., 2004). However, the serine at position 1928 on the Ca_v 1.2 C terminus has been demonstrated to be phosphorylated by multiple PKC isoforms in HEK293 cells, including PKCα (Yang et al., 2005). This phosphorylation led to an increase in L-type channel activity. Conversely, stimulation with PMA decreases the activity of Ca_v 1.3, mediated by PKCβII and PKCε (Baroudi et al., 2006). These results are not inconsistent with data presented here, since enhanced L-type current in cultured neurons is due to the actions of PKCα rather than PKCβ or PKCε. These studies also support the hypothesis that PKC is interacting with the L-type channel directly, rather than working through an intermediary. Furthermore, PKC is thought to associate with the plasma membrane via binding a receptor for activated C kinase (RACK) protein, which is generally in proximity to the target substrate (Kamp and Hell 2000). Studies designed to examine whether L-type channels colocalize or form complexes with RACKs would provide compelling evidence that PKCα does indeed directly phosphorylate L-channels. This isozyme-specific regulation is also suggestive that enhancement is occurring through Ca_v 1.2, and that inhibitory effects may reflect phosphorylation of Ca_v 1.3. It will be interesting to examine whether selective knockdown of Ca_v 1.3 leads to a greater proportion of neurons demonstrating current enhancement. It is possible that the temporal expression of Ca_v 1.2 and 1.3 plays a key role in governing PKC-dependent enhancement of L-type current.

Data presented here describe a signal transduction pathway initiated by $GABA_B$ receptor activation, resulting in enhanced L-type current in the developing mammalian

nervous system. Proposed experiments will help decipher what the physiological

relevance of this enhancement may be.

APPENDIX I

The expression of interneuronal marker GAD6 in cultured hippocampal neurons

In order to examine the effects of GABAergic stimulation on calcium currents, my studies have relied heavily on the use of P6-8 rat pups. Hippocampal cultures from these pups have demonstrated the greatest number of neurons that demonstrate L-type current enhancement, as opposed to either older or younger pups. Cells grown in culture are derived specifically from the superior region of the hippocampus, primarily CA1. Within this region, there are both inhibitory interneurons and excitatory pyramidal cells. Inhibitory interneurons, found primarily in the stratum oriens and stratum radiatium of the CA1 region, are more sparsely distributed relative to the excitatory neurons in the pyramidal layer. Because tissue from the superior region of the hippocampus was known to contain both excitatory and inhibitory neurons, a common question centers on the makeup of these neurons in culture. This question is particularly important to work presented here, because the $GABA_B$ mediated enhancement of L-type current is only observed in a minority of neurons. Since excitatory pyramidal cells compose a large percentage of total neurons in the hippocampus, it is not likely these are the neurons that demonstrate this effect. Instead, my work has focused on GABAergic interneurons that provide inhibitory input to the pyramidal cells. It follows that cell cultures which contain a relatively high population of interneurons would be best to study, because more cells would demonstrate the enhancement in which I am interested. However, in embryonic cultures from rats aged E17-20, there are reports of cultures enriched in pyramidal neurons (Banker and Cowan 1977). This is in contrast to reports that suggest significant

numbers of inhibitory neurons in embryonic cultures using anti-GABA antibodies

(Mattson and Kater 1989). Understanding the makeup of the cells in culture may offer

explanations as to why only a certain subset of neurons demonstrates $GABA_B$ receptor-

mediated enhancement of L-type current.

Studies performed in the laboratory have examined the percentage of cells in

culture that are immunoreactive for the GABA antibody, and thus assumed to be

GABAergic inhibitory interneurons (Figure A1.1). $37.5 \pm 2.3\%$ of neurons showed

GABA labeling after 24 hours in culture (Mynlieff 1997). This labeling was independent

of age; there was no significant difference in GABA labeling in neurons cultured from a

P7, P14, or P21 animal. When left in culture for longer periods, GABA labeling was

seen in more cells. Neurons cultured from a P21 animal and grown in vitro for 21 days

demonstrated that $74.2 \pm 2.7\%$ of cells were labeled with anti-GABA antibodies

(Mynlieff 1997). Furthermore, this report only gives the number of cultures examined

and not the total number of neurons labeled, so it is difficult to know how many cells

were examined.

Figure A1.1: Examples of GABA immunoreactive neurons in culture. A: Neurons from a P11 rat pup were dissociated and allowed to remain in culture 40 hours before fixation. Neurons were labeled with mouse anti-GABA primary antibodies, and biotinylated anti-mouse IgG were used as the secondary antibodies. Binding was visualized using a Vectastain Elite ABC Kit with a DIC microscope outfitted with Hoffman modulation optics. B: Cultured cell control with tissue taken from the same pup as in A. (From Mynlieff 1997)

I sought to verify these results using antibodies against glutamic acid decarboxylase (GAD). GAD catalyzes the conversion of glutamate to GABA and carbon dioxide. Thus, GAD is universally expressed in GABAergic cells. Neurons that express GABA must also express this enzyme. There are two genes which encode two isoforms of GAD, GAD 65 and GAD 67, respectively. The antibody against GAD that was used (GAD6) recognizes both isoforms. Using confocal microscopy, a total of 43 of 287 (14.98%) cells, isolated from 4 different animals, labeled for GAD. The total number of cells is a sum taken from 11 different images. As expected, labeling is largely absent in the nucleus. Furthermore, there are no gradations in labeling. It is clear which neurons express GAD (Figure A1.2), and are therefore assumed to be GABAergic interneurons. Notably, all neurons were isolated from P7 rat pups and kept in culture for 24 hours. The effect of age or time in culture was not examined.

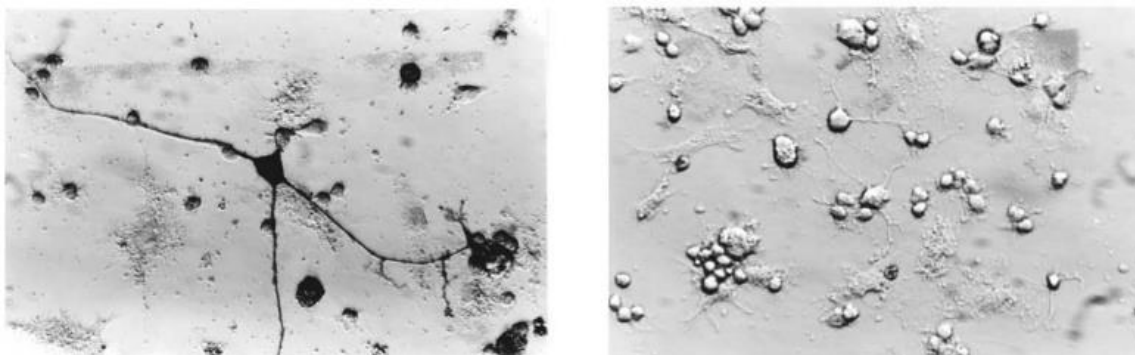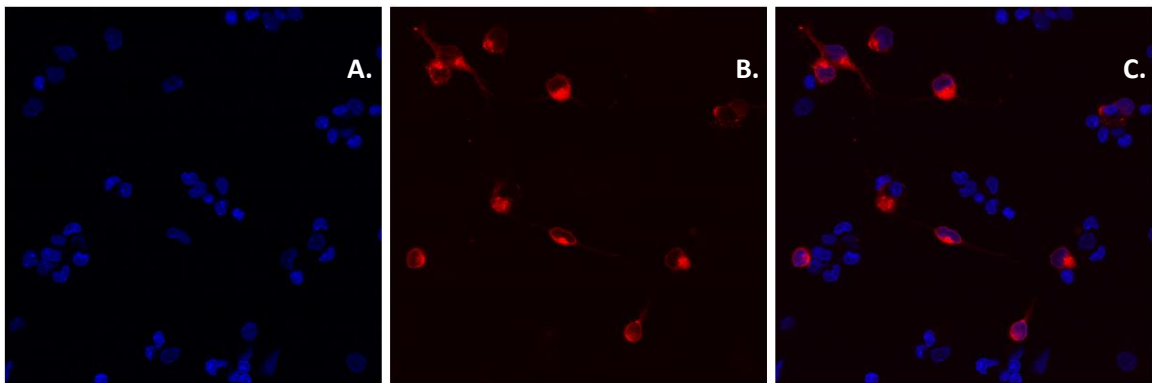**Figure A1.2:** Examples of GAD6 immunoreactive neurons in culture. Neurons from a P7 rat pup were dissociated and allowed to remain in culture overnight before fixation. Cells were decorated with anti-GAD6 primary antibodies and DyLight 550® secondary antibodies. A: DAPI was applied to visualize nuclei. B: GAD6 immunolabeling was not seen in the nuclei, but was around the periphery, often with a spot of particularly heavy labeling. GAD6 was also seen in the processes of several neurons. C: Overlay of panels A and B.

The immunohistochemistry performed here shows dramatically fewer neurons than data from (Mynlieff 1997). One possibility is that the antibody used by Mynlieff was not as specific as the GAD antibody. There are inherent difficulties in producing antibodies to GABA. Production of an antibody to a small molecule such as GABA requires it to be conjugated to a larger molecule; furthermore, the synthesis of GABA from glutamic acid involves removal of a carboxyl sidegroup. These problems could lead to production of an antibody that may recognize more than its desired target. Another possibility is that the resolution using confocal microscopy was better suited to discern which neurons were GABAergic. Interpreting the images seen with biotinylation, visualized under differential interference contract (DIC) microscopy may be unclear such that shadows or cells with a generally darker appearance may be considered positive. Confocal imaging with GAD6 antibodies provided clear images that were easily quantified.

Hippocampal cultures containing less than 15% inhibitory interneurons has important implications for how data are interpreted. The current hypothesis is that since not all neurons show $GABA_B$ receptor-mediated calcium current enhancement, there must be a subset of inhibitory interneurons that function differentially to account for this phenomenon. However, one possibility is that the calcium current enhancement is a much more generalized effect. Based on the percentage of neurons that demonstrate enhanced calcium entry when ratiometric calcium imaging is used, perhaps nearly all inhibitory interneurons exhibit this effect. Indeed, while work in the Mynlieff laboratory has shown calcium current enhancement to occur in only a subset of cells, other reports

do not observe the same effect. Thus, it is possible that current enhancement is always

observed when inhibitory interneurons are selected.

APPENDIX II

Inhibition of calcium channels by dihydropyridines as measured with ratiometric

calcium imaging

The focus of my work has been to understand the G protein coupled pathway through which L-type calcium current is enhanced. This current enhancement was shown to occur through L-type channels, because when L-channels were blocked with nimodipine, enhancement was eliminated. However, the currents recorded either with electrophysiology or the calcium entry recorded with calcium imaging, likely effects opening of all types (L-, N-, P/Q-, R-, and T) of calcium channels. Depending on the expression of each of these channels, whole cell calcium current may look very different from cell to cell. Furthermore, cultured cells from CA1 are not heterogeneous, so it is likely that there are many different cell types, and even within cell types, calcium current profiles will vary. It is important to this work to understand the relative contribution of L-type channels to whole cell calcium currents.

Particularly in calcium imaging, separation of current types with toxins is cost prohibitive because there is constant perfusion occurring. Instead through a combination of pharmacological methods and reliance on known channel kinetics, statements can be made about the type of channel through which calcium enters. For example, dihydopyridines nimodipine and nifedipine are selective blockers of L-type calcium channels. L-type current derives its name because it shows little voltage dependent inactivation (and thus is considered Long-lasting).   Understanding the total makeup and contribution of channels becomes important when trying to uncover roles for that

particular channel. Electrophysiological recordings done in the Mynlieff laboratory by a previous graduate student demonstrated that L-type calcium current made up less than 10% of total calcium current and was even lower in certain interneuronal classes (Figure A2.1). For example, only about 5% of total calcium current was inhibited by L-type channel antagonist nimodipine when applied to basket cells. However, this may be an underestimate, since in all cases except that of vertical cells, more than 50% of current is not blocked by N-, P/Q-, and L-channel antagonists. Initial studies measuring the contribution to L-type current using ratiometric calcium imaging suggested entry through L-channels was greater than that shown using electrophysiology; therefore I sought to clarify the percentage of calcium entry flowing through L-channels using calcium imaging and two different dihydropyridine inhibitors.
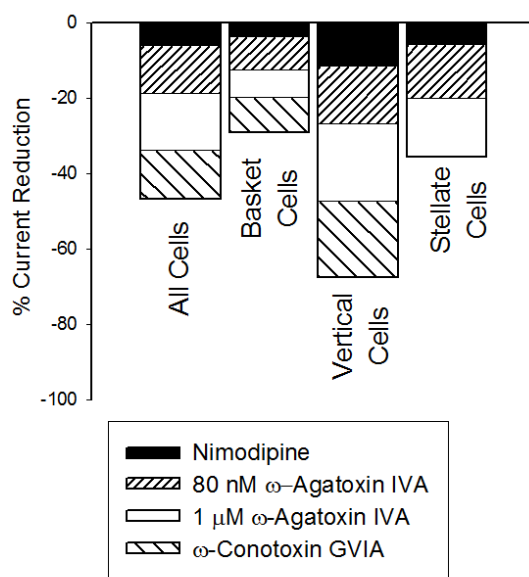
Figure A2.1: Components of whole-cell barium current in interneurons as measured by whole-cell patch clamp electrophysiology. Current-clamp measurements of action potentials were elicited by injecting a $0.1 - 0.2$ ms depolarizing current of $2 - 4$ nA, followed by a switch to voltage clamp mode for measurements of calcium currents. Barium currents were elicited from a holding potential of -80 mV by a 300 ms long depolarizing pulse to +10 mV. Action potential kinetics allowed interneurons to be categorized into classes. Calcium channel inhibitors were used to separate components of whole cell current. Nimodipine was applied at 5 μM, GVIA was applied at 3 μM. From (Carter 2002).

Several reports in the literature have attempted to describe the contribution of each type of calcium channel to total calcium current, and each has slightly different conditions.

For example, hippocampal cultures performed on newborn rats were grown in culture for 10-12 days. L-type current was found to be $22.7 \pm 5.2\%$ of total current (Isaeva et al., 1998). Another study used neurons derived from E18 hippocampi. This report described an age-dependent increase in L-type current, with the late component rising twofold from P7 to P21 (Blalock et al., 1999). This study achieved a 40% block with nimodipine when cells were kept in culture 21 days. A third study noted the difference in the component of L-type current based on how long cells are kept in culture (Chameau et al., 1999). E16-18 pups were grown in culture for 4 days. When treated with nifedipine, 40% of total current was blocked. This is in contrast to cells grown in culture for 16 days. In these neurons, only 7% of calcium was blocked with the dihydropyridine antagonist. In hippocampal slices of P15 – P29 rats, neurons of the entorhinal cortex showed the greatest sensitivity to dihydropyridines, where 52-55% of current was blocked when nifedipine was applied. Thus, it appears L-type as a proportion of total current is highly variable depending on recording and culturing conditions.

Thus, I sought to repeat these studies and examine levels of L-channel activity demonstrated in ratiometric calcium imaging, where the stimulation period is 3 orders of magnitude longer (300 ms stimulation for electrophysiological recordings compared to 30 s in calcium imaging). Two structurally similar dihydropyridines, nimodipine and nifedipine, were used to inhibit L-type channels. Neurons were first depolarized with a high KCl solution to obtain a control value. Once it was washed away and cells returned to baseline, the dihydopyridine was added for 15 seconds; KCl and the drug were coapplied for 30 seconds. The response with the drug and high KCl (treatment) was compared to the response with high KCl alone (control).

When nifedipine (20 μM) was applied, 33.91 ± 1.50% of the high KCl-induced response was blocked, suggesting this was the component of total calcium entry that entered via L-type channels (N = 278); when nimodipine (20 μM) was applied, 37.73 ± 1.39% of the response was blocked, (N = 381). These data are summarized in figure A2.2. Furthermore, of the 659 total cells tested, only 4 showed a blockage of greater than 90%. These data suggest that when measured via ratiometric calcium imaging, L-type current makes up a larger percentage of total calcium entry than what is observed with electrophysiology. This percentage falls within the reported values for the contribution of L-current in other systems.
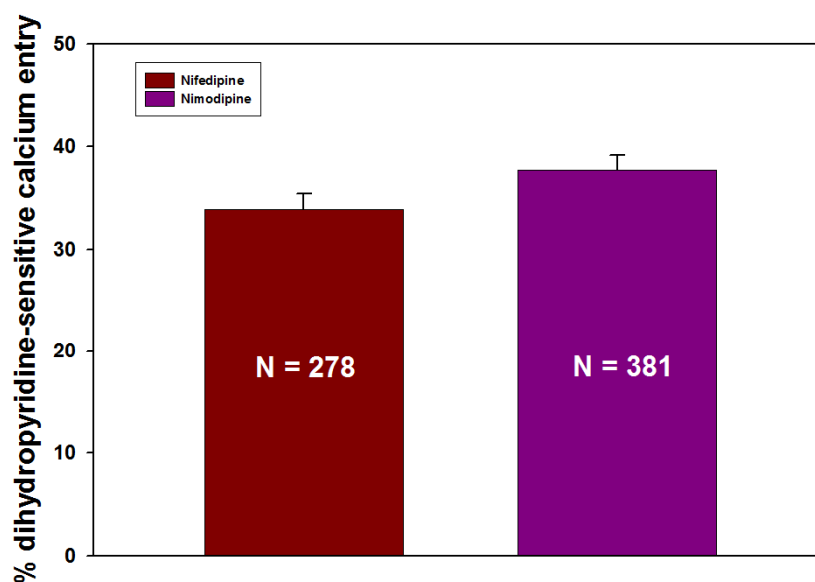
Figure A2.2: Dihydropyridine sensitivity of cultured hippocampal neurons as measured with ratiometric calcium imaging. High KCl was used to depolarize P7 cultured cells for 30 seconds. KCl was perfused off, and calcium levels returned to baseline before pretreatment with either nifedipine or nimodipine for 15 seconds. Either nimodipine or nifedipine (20 μM) plus high KCl were coapplied for 30 s. Each bar represents the percentage of L-type current blocked when compared with the normalized high KCl-alone response. Error bars represent SEM.

Understanding the relative contribution of L-type entry to total entry has important implications. Given the inherent variability of the system, questions may arise as to whether resolving small magnitude changes are accurate. For example, if one is measuring the ratio of calcium entry and records a baseline value of 0.30 and a peak value of 0.90, the influx through voltage-gated channels would be 0.6. Contribution of L-type channels would only account for approximately 30% of this change, or 0.18. Therefore, it is possible that only cells which respond more robustly to high KCl stimulation should be considered for analysis. This would be particularly true in studies measuring enhancement where knockdown of either neuronal Cav 1.X isoform is performed, and the contribution of only a single isoform is measured.

BIBLIOGRAPHY

Abiria S. A. and Colbran R. J. (2010) CaMKII associates with CaV1.2 L-type calcium channels via selected beta subunits to enhance regulatory phosphorylation. J. Neurochem. 112, 150-161.

Andersen P., Bland B. H. and Dudar J. D. (1973) Organization of the hippocampal output. Exp. Brain Res. 17, 152-168.

Aromolaran A.A. and Blatter L.A. (2005) Modulation of intracellular Ca2+ release and capacitative Ca2+ entry by CaMKII inhibitors in bovine vascular endothelial cells. Am J Physiol. Cell Physiol. 289:C1426-C1436.

Aronica E., Boer K., Redeker S., Spliet W. G., van Rijen P. C., Troost D. and Gorter J. A. (2007) Differential expression patterns of chloride transporters, Na+-K+-2Cl-- cotransporter and K+-Cl--cotransporter, in epilepsy-associated malformations of cortical development. Neuroscience 145, 185-196.

Banker G.A. and Cowan W.M. (1977) Rat hippocampal neurons in dispersed cell culture. Brain Res. 126, 397-42.

Banks M. I., Hardie J. B. and Pearce R. A. (2002) Development of GABA(A) receptor-mediated inhibitory postsynaptic currents in hippocampus. J. Neurophysiol. 88, 3097-3107.

Baroudi G., Qu Y., Ramadan O., Chahine M. and Boutjdir M. (2006) Protein kinase C activation inhibits Cav1.3 calcium channel at NH2-terminal serine 81 phosphorylation site. Am. J. Physiol. Heart Circ. Physiol. 291, H1614-H1622.

Baumann L., Gerstner A., Zong X., Biel M. and Wahl-Schott C. (2004) Functional characterization of the L-type Ca2+ channel Cav1.4alpha1 from mouse retina. Invest Ophthalmol. Vis. Sci. 45, 708-713.

Bayne E. H. and Allshire R. C. (2005) RNA-directed transcriptional gene silencing in mammals. Trends Genet. 21, 370-373.

Ben-Ari Y. (2002) Excitatory actions of gaba during development: the nature of the nurture. Nat. Rev. Neurosci. 3, 728-739.

Blaesse P., Airaksinen M.S., Rivera C. and Kaila K. (2009) Cation-chloride cotransporters and neuronal function. Neuron 61, 820-838.

Blaich A., Welling A., Fischer S., Wegener J. W., Kostner K., Hofmann F. and Moosmang S. (2010) Facilitation of murine cardiac L-type Ca(v)1.2 channel is modulated by calmodulin kinase II-dependent phosphorylation of S1512 and S1570. Proc. Natl. Acad. Sci. U. S. A 107, 10285-10289.

Blalock E.M., Porter N.M. and Landfield P.W. (1999) Decreased G-protein-mediated regulation and shift in calcium channel types with age in hippocampal cultures. J. Neurosci. 19, 8674-8684.

Bollag W. (2009) Protein kinase Cα puts the handcuffs on epidermal keratinocyte proliferation. J. Invest. Dermatol. 129, 2330-2332.

Boyer S. B., Clancy S. M., Terunuma M., Revilla-Sanchez R., Thomas S. M., Moss S. J. and Slesinger P. A. (2009) Direct interaction of GABAB receptors with M2 muscarinic receptors enhances muscarinic signaling. J. Neurosci. 29, 15796-15809.

Brauner-Osborne H. and Krogsgaard-Larsen P. (1999) Functional pharmacology of cloned heterodimeric GABAB receptors expressed in mammalian cells. Br. J. Pharmacol. 128, 1370-1374.

Bray J. G. and Mynlieff M. (2009) Influx of calcium through L-type calcium channels in early postnatal regulation of chloride transporters in the rat hippocampus. Dev. Neurobiol. 69, 885-896.

Bray J. G. and Mynlieff M. (2011) Involvement of protein kinase C and protein kinase A in the enhancement of L-type calcium current by GABAB receptor activation in neonatal hippocampus. Neuroscience 179, 62-72.

Buraei Z. and Yang J. (2013) Structure and function of the beta subunit of voltage-gated Ca(2)(+) channels. Biochim. Biophys. Acta 1828, 1530-1540.

Calver A. R., Robbins M. J., Cosio C., Rice S. Q., Babbs A. J., Hirst W. D., Boyfield I., Wood M. D., Russell R. B., Price G. W., Couve A., Moss S. J. and Pangalos M. N. (2001) The C-terminal domains of the GABA(b) receptor subunits mediate intracellular trafficking but are not required for receptor signaling. J. Neurosci. 21, 1203-1210.

Camps M., Carozzi A., Schnabel P., Scheer A., Parker P. J. and Gierschik P. (1992) Isozyme-selective stimulation of phospholipase C-beta 2 by G protein beta gamma-subunits. Nature 360, 684-686.

Carter T. J. and Mynlieff M. (2004) Gamma-aminobutyric acid type B receptors facilitate L-type and attenuate N-type Ca(2+) currents in isolated hippocampal neurons. J. Neurosci. Res. 76, 323-333.

Carter, T.J. (2002) Calcium channel modulation by GABA(B) receptor activation. (Doctoral Dissertation). Retrieved from Proquest Dissertations and Theses, Order No. 3078900.

Castelli L. and Magistretti J. (2006) High-voltage-activated Ca2+ currents show similar patterns of expression in stellate and pyramidal cells from rat entorhinal cortex layer II. Brain Res. 1090, 76-88.

Catterall W. A. (2011) Voltage-gated calcium channels. Cold Spring Harb. Perspect. Biol. 3, a003947.

Catterall W. A., Perez-Reyes E., Snutch T. P. and Striessnig J. (2005) International Union of Pharmacology. XLVIII. Nomenclature and structure-function relationships of voltage-gated calcium channels. Pharmacol. Rev. 57, 411-425.

Chahine M., Qu Y., Mancarella S. and Boutjdir M. (2008) Protein kinase C activation inhibits alpha1D L-type Ca channel: a single-channel analysis. Pflugers Arch. 455, 913-919.

Chameau P., Lucas P., Melliti K., Bournaud R. and Shimahara T. (1999) Development of multiple calcium channel types in cultured mouse hippocampal neurons. Neuroscience 90, 383-388.

Chen W.G., Chang Q., Lin Y., Meissner A., West A.E., Griffith E.C., Jaenisch R. and Greenberg M.E. (2003) Derepression of BDNF transcription involves calcium-dependent phosphorylation of MeCP2. Science 302, 885-889.

Chidiac P. and Ross E. M. (1999) Phospholipase C-beta1 directly accelerates GTP hydrolysis by Galphaq and acceleration is inhibited by Gbeta gamma subunits. J. Biol. Chem. 274, 19639-19643.

Chih B., Gollan L. and Scheiffele P. (2006) Alternative splicing controls selective trans-synaptic interactions of the neuroligin-neurexin complex. Neuron 51, 171-178.

Chung H.J. and Jan L.Y. (2006) Channeling to the nucleus. Neuron 52, 937-940.

Colecraft H. M., Patil P. G. and Yue D. T. (2000) Differential occurrence of reluctant openings in G-protein-inhibited N- and P/Q-type calcium channels. J. Gen. Physiol 115, 175-192.

Connors B.W. and Long M.A. (2004) Electrical synapses in the mammalian brain. Annu. Rev. Neurosci. 27, 393-418.

Cruz H. G., Ivanova T., Lunn M. L., Stoffel M., Slesinger P. A. and Luscher C. (2004) Bi-directional effects of GABA(B) receptor agonists on the mesolimbic dopamine system. Nat. Neurosci. 7, 153-159.

Cueni L., Canepari M., Adelman J. P. and Luthi A. (2009) Ca(2+) signaling by T-type Ca(2+) channels in neurons. Pflugers Arch. 457, 1161-1172.

De Waard M., Liu H., Walker D., Scott V. E., Gurnett C. A. and Campbell K. P. (1997) Direct binding of G-protein betagamma complex to voltage-dependent calcium channels. Nature 385, 446-450.

DeRiemer S.A., Strong J.A., Albert K.A., Greengard P. and Kaczmarek L.K. (1985) Enhancement of calcium current in Aplysia neurones by phorbol ester and protein kinase C. Nature 313, 313-316.

Derrien A., Langlois D. and Saez J. M. (1996) Expression and regulation of G alpha q and G alpha 11 mRNAs and proteins in bovine adrenal cells. Mol. Cell Endocrinol. 121, 65-74.

Di Biase V., Tuluc P., Campiglio M., Obermair G. J., Heine M. and Flucher B. E. (2011) Surface traffic of dendritic CaV1.2 calcium channels in hippocampal neurons. J. Neurosci. 31, 13682-13694.

Di Virgilio F., Pozzan T., Wollheim C.B., Vicentini L.M. and Meldolesi J. (1986) Tumor promoter phorbol myristate acetate inhibits Ca2+ influx through voltage-gated Ca2+ channels in two secretory cell lines, PC12 and RINm5F. J. Biol. Chem. 261, 32-35.

Doischer D., Hosp J.A., Yanagawa Y., Obata K., Jonas P., Vida I. and Bartos M. (2008) Postnatal differentiation of basket cells from slow to fast signaling devices. J. Neurosci. 28, 12956-12968.

Dolmetsch R.E., Pajvani U., Fife K., Spotts J.M. and Greenberg M.E. (2001) Signaling to the nucleus by an L-type calcium channel-calmodulin complex through the MAP kinase pathway. Science 294, 333-339.

Dolphin A. C. (2013) The alpha2delta subunits of voltage-gated calcium channels. Biochim. Biophys. Acta 1828, 1541-1549.

Duthey B., Caudron S., Perroy J., Bettler B., Fagni L., Pin J. P. and Prezeau L. (2002) A single subunit (GB2) is required for G-protein activation by the heterodimeric GABA(B) receptor. J. Biol. Chem. 277, 3236-3241.

Ertel E. A., Campbell K. P., Harpold M. M., Hofmann F., Mori Y., Perez-Reyes E., Schwartz A., Snutch T. P., Tanabe T., Birnbaumer L., Tsien R. W. and Catterall W. A. (2000) Nomenclature of voltage-gated calcium channels. Neuron 25, 533-535.

Fink C. C. and Meyer T. (2002) Molecular mechanisms of CaMKII activation in neuronal plasticity. Curr. Opin. Neurobiol. 12, 293-299.

Flucher B. E. and Franzini-Armstrong C. (1996) Formation of junctions involved in excitation-contraction coupling in skeletal and cardiac muscle. Proc. Natl. Acad. Sci. U. S. A 93, 8101-8106.

Franek M., Pagano A., Kaupmann K., Bettler B., Pin J. P. and Blahos J. (1999) The heteromeric GABA-B receptor recognizes G-protein alpha subunit C-termini. Neuropharmacology 38, 1657-1666.

Gaertner T.R., Kolodziej S.J., Wang D., Kobayashi R., Koomen J.M., Stoops J.K. and Waxham M.N. (2004) Comparative analyses of the three-dimensional structures and enzymatic properties of alpha, beta, gamma and delta isoforms of Ca2+-calmodulin-dependent protein kinase II. J. Biol. Chem. 279, 12484-12494.

Gaiarsa J. L., Tseeb V. and Ben-Ari Y. (1995) Postnatal development of pre- and postsynaptic GABAB-mediated inhibitions in the CA3 hippocampal region of the rat. J. Neurophysiol. 73, 246-255.

Galvez T., Duthey B., Kniazeff J., Blahos J., Rovelli G., Bettler B., Prezeau L. and Pin J. P. (2001) Allosteric interactions between GB1 and GB2 subunits are required for optimal GABA(B) receptor function. EMBO J. 20, 2152-2159.

Galvez T., Parmentier M. L., Joly C., Malitschek B., Kaupmann K., Kuhn R., Bittiger H., Froestl W., Bettler B. and Pin J. P. (1999) Mutagenesis and modeling of the GABAB receptor extracellular domain support a venus flytrap mechanism for ligand binding. J. Biol. Chem. 274, 13362-13369.

Galvez T., Prezeau L., Milioti G., Franek M., Joly C., Froestl W., Bettler B., Bertrand H. O., Blahos J. and Pin J. P. (2000) Mapping the agonist-binding site of GABAB type 1 subunit sheds light on the activation process of GABAB receptors. J. Biol. Chem. 275, 41166-41174.

Gamelli A. E., McKinney B. C., White J. A. and Murphy G. G. (2011) Deletion of the L-type calcium channel Ca(V) 1.3 but not Ca(V) 1.2 results in a diminished sAHP in mouse CA1 pyramidal neurons. Hippocampus 21, 133-141.

Gandia L., Lara B., Imperial J. S., Villarroya M., Albillos A., Maroto R., Garcia A. G. and Olivera B. M. (1997) Analogies and differences between omega-conotoxins MVIIC and MVIID: binding sites and functions in bovine chromaffin cells. Pflugers Arch. 435, 55-64.

Ganguly K., Schinder A.F., Wong S.T. and Poo M. (2001) GABA itself promotes the developmental switch of neuronal GABAergic responses from excitation to inhibition. Cell 105, 521-532.

Gao L., Blair L.A. and Marshall J. (2006) CaMKII-independent effects of KN93 and its inactive analog KN92: reversible inhibition of L-type calcium channels. Biochem. Biophys. Res. Commun. 345, 1606-1610.

Gassmann M. and Bettler B. (2012) Regulation of neuronal GABA(B) receptor functions by subunit composition. Nat. Rev. Neurosci. 13, 380-394.

Gassmann M., Shaban H., Vigot R., Sansig G., Haller C., Barbieri S., Humeau Y., Schuler V., Muller M., Kinzel B., Klebs K., Schmutz M., Froestl W., Heid J., Kelly P. H., Gentry C., Jaton A. L., van der Putten H., Mombereau C., Lecourtier L., Mosbacher J., Cryan J. F., Fritschy J. M., Luthi A., Kaupmann K. and Bettler B.

(2004) Redistribution of GABAB(1) protein and atypical GABAB responses in GABAB(2)-deficient mice. J. Neurosci. 24, 6086-6097.

Geng Y., Bush M., Mosyak L., Wang F. and Fan Q. R. (2013) Structural mechanism of ligand activation in human GABA(B) receptor. Nature 504, 254-259.

Geng Y., Xiong D., Mosyak L., Malito D. L., Kniazeff J., Chen Y., Burmakina S., Quick M., Bush M., Javitch J. A., Pin J. P. and Fan Q. R. (2012) Structure and functional interaction of the extracellular domain of human GABA(B) receptor GBR2. Nat. Neurosci. 15, 970-978.

Giovannini M. G. (2006) The role of the extracellular signal-regulated kinase pathway in memory encoding. Rev. Neurosci. 17, 619-634.

Golard A. and Siegelbaum S. A. (1993) Kinetic basis for the voltage-dependent inhibition of N-type calcium current by somatostatin and norepinephrine in chick sympathetic neurons. J. Neurosci. 13, 3884-3894.

Gomez-Ospina N., Tsuruta F., Barreto-Chang O., Hu L. and Dolmetsch R. (2006) The C terminus of the L-type voltage-gated calcium channel Ca(V)1.2 encodes a transcription factor. Cell 127, 591-606.

Gross R. A. and MacDonald R. L. (1989) Activators of protein kinase C selectively enhance inactivation of a calcium current component of cultured sensory neurons in a pertussis toxin-sensitive manner. J. Neurophysiol. 61, 1259-1269.

Grynkiewicz G., Poenie M. and Tsien R. Y. (1985) A new generation of Ca2+ indicators with greatly improved fluorescence properties. J. Biol. Chem. 260, 3440-3450.

Gurnett C. A., De W. M. and Campbell K. P. (1996) Dual function of the voltage-dependent Ca2+ channel alpha 2 delta subunit in current stimulation and subunit interaction. Neuron 16, 431-440.

Guyon A. and Leresche N. (1995) Modulation by different GABAB receptor types of voltage-activated calcium currents in rat thalamocortical neurones. J. Physiol 485 (Pt 1), 29-42.

Hagenston A. M. and Bading H. (2011) Calcium signaling in synapse-to-nucleus communication. Cold Spring Harb. Perspect. Biol. 3, a004564.

Harayama N., Shibuya I., Tanaka K., Kabashima N., Ueta Y. and Yamashita H. (1998) Inhibition of N- and P/Q-type calcium channels by postsynaptic GABAB receptor activation in rat supraoptic neurones. J. Physiol 509 (Pt 2), 371-383.

Havlickova M., Prezeau L., Duthey B., Bettler B., Pin J. P. and Blahos J. (2002) The intracellular loops of the GB2 subunit are crucial for G-protein coupling of the heteromeric gamma-aminobutyrate B receptor. Mol. Pharmacol. 62, 343-350.

Hell J. W., Westenbroek R. E., Warner C., Ahlijanian M. K., Prystay W., Gilbert M. M., Snutch T. P. and Catterall W. A. (1993) Identification and differential subcellular localization of the neuronal class C and class D L-type calcium channel alpha 1 subunits. J. Cell Biol. 123, 949-962.

Hepler J. R., Kozasa T. and Gilman A. G. (1994) Purification of recombinant Gq alpha, G11 alpha, and G16 alpha from Sf9 cells. Methods Enzymol. 237, 191-212.

Herlitze S., Hockerman G. H., Scheuer T. and Catterall W. A. (1997) Molecular determinants of inactivation and G protein modulation in the intracellular loop connecting domains I and II of the calcium channel alpha1A subunit. Proc. Natl. Acad. Sci. U. S. A 94, 1512-1516.

Hillman R., Sinani J. and Pendleton R. (2012) The role of the GABA(B) receptor and calcium channels in a Drosophila model of Parkinson's Disease. Neurosci. Lett. 516, 167-170.

Holter N. I., Zylla M. M., Zuber N., Bruehl C. and Draguhn A. (2010) Tonic GABAergic control of mouse dentate granule cells during postnatal development. Eur. J. Neurosci. 32, 1300-1309.

Hudmon A. and Schulman H. (2002a) Neuronal CA2+/calmodulin-dependent protein kinase II: the role of structure and autoregulation in cellular function. Annu. Rev. Biochem. 71, 473-510.

Hudmon A. and Schulman H. (2002b) Structure-function of the multifunctional Ca2+/calmodulin-dependent protein kinase II. Biochem. J. 364, 593-611.

Hudmon A., Schulman H., Kim J., Maltez J. M., Tsien R. W. and Pitt G. S. (2005) CaMKII tethers to L-type Ca2+ channels, establishing a local and dedicated integrator of Ca2+ signals for facilitation. J. Cell Biol. 171, 537-547.

Hudziak R.M., Barofsky E., Barofsky D.F., Weller D.L., Huang S.B. and Weller D.D. (1996) Resistance of morpholino phosphorodiamidate oligomers to enzymatic degradation. Antisense Nucleic Acid Drug Dev. 6, 267-272.

Huston E., Cullen G. P., Burley J. R. and Dolphin A. C. (1995) The involvement of multiple calcium channel sub-types in glutamate release from cerebellar granule cells and its modulation by GABAB receptor activation. Neuroscience 68, 465-478.

Huston E., Scott R. H. and Dolphin A. C. (1990) A comparison of the effect of calcium channel ligands and GABAB agonists and antagonists on transmitter release and somatic calcium channel currents in cultured neurons. Neuroscience 38, 721-729.

Hutcheon B., Morley P. and Poulter M. O. (2000) Developmental change in GABAA receptor desensitization kinetics and its role in synapse function in rat cortical neurons. J. Physiol 522 Pt 1, 3-17.

Iftinca M. C. and Zamponi G. W. (2009) Regulation of neuronal T-type calcium channels. Trends Pharmacol. Sci. 30, 32-40.

Ihnatovych I., Novotny J., Haugvicova R., Bourova L., Mares P. and Svoboda P. (2002) Opposing changes of trimeric G protein levels during ontogenetic development of rat brain. Brain Res. Dev. Brain Res. 133, 57-67.

Im B. H. and Rhim H. (2012) GABA(B) receptor-mediated ERK1/2 phosphorylation via a direct interaction with Ca(V)1.3 channels. Neurosci. Lett. 513, 89-94.

Ishida A., Kameshita I., Okuno S., Kitani T. and Fujisawa H. (1995) A novel highly specific and potent inhibitor of calmodulin-dependent protein kinase II. Biochem. Biophys. Res. Commun. 212, 806-812.

Jenkins M. A., Christel C. J., Jiao Y., Abiria S., Kim K. Y., Usachev Y. M., Obermair G. J., Colbran R. J. and Lee A. (2010) Ca2+-dependent facilitation of Cav1.3 Ca2+ channels by densin and Ca2+/calmodulin-dependent protein kinase II. J. Neurosci. 30, 5125-5135.

Jiang H., Wu D. and Simon M. I. (1994) Activation of phospholipase C beta 4 by heterotrimeric GTP-binding proteins. J. Biol. Chem. 269, 7593-7596.

Jiang M. and Swann J.W. (2005) A role for L-type calcium channels in the maturation of parvalbumin-containing hippocampal interneurons. Neuroscience 135, 839-850.

Jones K. A., Borowsky B., Tamm J. A., Craig D. A., Durkin M. M., Dai M., Yao W. J., Johnson M., Gunwaldsen C., Huang L. Y., Tang C., Shen Q., Salon J. A., Morse K., Laz T., Smith K. E., Nagarathnam D., Noble S. A., Branchek T. A. and Gerald C. (1998) GABA(B) receptors function as a heteromeric assembly of the subunits GABA(B)R1 and GABA(B)R2. Nature 396, 674-679.

Judge A. D., Sood V., Shaw J. R., Fang D., McClintock K. and MacLachlan I. (2005) Sequence-dependent stimulation of the mammalian innate immune response by synthetic siRNA. Nat. Biotechnol. 23, 457-462.

Kamp T.J. and Hell J.W. (2000) Regulation of cardiac L-type calcium channels by protein kinase A and protein kinase C. Circ. Res. 87, 1095-1102.

Kanngiesser U., Nalik P. and Pongs O. (1988) Purification and affinity labeling of dihydropyridine receptor from rabbit skeletal muscle membranes. Proc. Natl. Acad. Sci. U. S. A. 85, 2969-2973.

Kapur A., Yeckel M.F., Gray R. and Johnston D. (1998) L-Type calcium channels are required for one form of hippocampal mossy fiber LTP. J. Neurophysio.l 79, 2181-2190.

Karls A. S. and Mynlieff M. (2013) Nonspecific, reversible inhibition of voltage-gated calcium channels by CaMKII inhibitor CK59. Cell Mol. Neurobiol. 33, 723-729.

Katada T. and Ui M. (1982) Direct modification of the membrane adenylate cyclase system by islet-activating protein due to ADP-ribosylation of a membrane protein. Proc. Natl. Acad. Sci. U. S. A 79, 3129-3133.

Katritch V., Cherezov V. and Stevens R. C. (2013) Structure-function of the G protein-coupled receptor superfamily. Annu. Rev. Pharmacol. Toxicol. 53, 531-556.

Kaupmann K., Huggel K., Heid J., Flor P. J., Bischoff S., Mickel S. J., McMaster G., Angst C., Bittiger H., Froestl W. and Bettler B. (1997) Expression cloning of GABA(B) receptors uncovers similarity to metabotropic glutamate receptors. Nature 386, 239-246.

Kaupmann K., Malitschek B., Schuler V., Heid J., Froestl W., Beck P., Mosbacher J., Bischoff S., Kulik A., Shigemoto R., Karschin A. and Bettler B. (1998) GABA(B)-receptor subtypes assemble into functional heteromeric complexes. Nature 396, 683-687.

Kawasaki H., Taira K. and Morris K. V. (2005) siRNA induced transcriptional gene silencing in mammalian cells. Cell Cycle 4, 442-448.

Kilb W. (2012) Development of the GABAergic system from birth to adolescence. Neuroscientist. 18, 613-630.

Klausberger T. (2009) GABAergic interneurons targeting dendrites of pyramidal cells in the CA1 area of the hippocampus. Eur. J. Neurosci. 30, 947-957.

Klausberger T. and Somogyi P. (2008) Neuronal diversity and temporal dynamics: the unity of hippocampal circuit operations. Science 321, 53-57.

Klockner U., Lee J. H., Cribbs L. L., Daud A., Hescheler J., Pereverzev A., Perez-Reyes E. and Schneider T. (1999) Comparison of the Ca2 + currents induced by expression of three cloned alpha1 subunits, alpha1G, alpha1H and alpha1I, of low-voltage-activated T-type Ca2 + channels. Eur. J. Neurosci. 11, 4171-4178.

Konstantopoulos N., Marcuccio S., Kyi S., Stoichevska V., Castelli L.A., Ward C.W. and Macaulay S.L. (2007) A purine analog kinase inhibitor, calcium/calmodulin-dependent protein kinase II inhibitor 59, reveals a role for calcium/calmodulin-dependent protein kinase II in insulin-stimulated glucose transport. Endocrinology 148, 374-385.

Korff C. M. and Nordli D. R., Jr. (2006) Epilepsy syndromes in infancy. Pediatr. Neurol. 34, 253-263.

Korhonen H., Fisslthaler B., Moers A., Wirth A., Habermehl D., Wieland T., Schutz G., Wettschureck N., Fleming I. and Offermanns S. (2009) Anaphylactic shock depends on endothelial Gq/G11. J. Exp. Med. 206, 411-420.

Kozasa T., Hepler J. R., Smrcka A. V., Simon M. I., Rhee S. G., Sternweis P. C. and Gilman A. G. (1993) Purification and characterization of recombinant G16 alpha from Sf9 cells: activation of purified phospholipase C isozymes by G-protein alpha subunits. Proc. Natl. Acad. Sci. U. S. A 90, 9176-9180.

Kramer A. A., Ingraham N. E., Sharpe E. J. and Mynlieff M. (2012) Levels of Ca(V)1.2 L-Type Ca(2+) Channels Peak in the First Two Weeks in Rat Hippocampus Whereas Ca(V)1.3 Channels Steadily Increase through Development. J. Signal Transduct. 2012, 597214.

Kuczewski N., Langlois A., Fiorentino H., Bonnet S., Marissal T., Diabira D., Ferrand N., Porcher C. and Gaiarsa J.L. (2008) Spontaneous glutamatergic activity induces a BDNF-dependent potentiation of GABAergic synapses in the newborn rat hippocampus. J. Physiol. 586, 5119-5128.

Kuczewski N., Fuchs C., Ferrand N., Jovanovic J. N., Gaiarsa J. L. and Porcher C. (2011) Mechanism of GABAB receptor-induced BDNF secretion and promotion of GABAA receptor membrane expression. J. Neurochem. 118, 533-545.

Kuner R., Kohr G., Grunewald S., Eisenhardt G., Bach A. and Kornau H. C. (1999) Role of heteromer formation in GABAB receptor function. Science 283, 74-77.

Kurose H., Katada T., Amano T. and Ui M. (1983) Specific uncoupling by islet-activating protein, pertussis toxin, of negative signal transduction via alpha-adrenergic, cholinergic, and opiate receptors in neuroblastoma x glioma hybrid cells. J. Biol. Chem. 258, 4870-4875.

Lee A., Wong S. T., Gallagher D., Li B., Storm D. R., Scheuer T. and Catterall W. A. (1999) Ca2+/calmodulin binds to and modulates P/Q-type calcium channels. Nature 399, 155-159.

Lee S.Y., Foldy C., Szabadics J. and Soltesz I. (2011) Cell-type-specific CCK2 receptor signaling underlies the cholecystokinin-mediated selective excitation of hippocampal parvalbumin-positive fast-spiking basket cells. J. Neurosci. 31, 10993-11002.

Levitt P., Eagleson K.L. and Powell E.M. (2004) Regulation of neocortical interneuron development and the implications for neurodevelopmental disorders. Trends Neurosci. 27, 400-406.

Li B., Zhong H., Scheuer T. and Catterall W.A. (2004) Functional role of a C-terminal Gbetagamma-binding domain of Ca(v)2.2 channels. Mol. Pharmacol. 66, 761-769.

Li J., Ning Y., Hedley W., Saunders B., Chen Y., Tindill N., Hannay T. and Subramaniam S. (2002) The Molecule Pages database. Nature 420, 716-717.

Li Y. and Stern J. E. (2004) Activation of postsynaptic GABAB receptors modulate the firing activity of supraoptic oxytocin and vasopressin neurones: role of calcium channels. J. Neuroendocrinol. 16, 119-130.

Lipscombe D., Helton T. D. and Xu W. (2004) L-type calcium channels: the low down. J. Neurophysiol. 92, 2633-2641.

Lohmann C. (2009) Calcium signaling and the development of specific neuronal connections. Prog. Brain Res. 175, 443-452.

Lopez-Bendito G., Shigemoto R., Kulik A., Vida I., Fairen A. and Lujan R. (2004) Distribution of metabotropic GABA receptor subunits GABAB1a/b and GABAB2 in the rat hippocampus during prenatal and postnatal development. Hippocampus 14, 836-848.

Ludwig A., Uvarov P., Soni S., Thomas-Crusells J., Airaksinen M.S. and Rivera C. (2011) Early growth response 4 mediates BDNF induction of potassium chloride cotransporter 2 transcription. J. Neurosci. 31,644-649.

Maier P.J., Marin I., Grampp T., Sommer A. and Benke D. (2010) Sustained glutamate receptor activation down-regulates GABAB receptors by shifting the balance from recycling to lysosomal degradation. J. Biol. Chem. 285, 35606-35614.

Mannoury la Cour C., Herbelles C., Pasteau V., de N. G. and Millan M. J. (2008) Influence of positive allosteric modulators on GABA(B) receptor coupling in rat brain: a scintillation proximity assay characterisation of G protein subtypes. J. Neurochem. 105, 308-323.

Margeta-Mitrovic M., Jan Y. N. and Jan L. Y. (2000) A trafficking checkpoint controls GABA(B) receptor heterodimerization. Neuron 27, 97-106.

Margeta-Mitrovic M., Jan Y. N. and Jan L. Y. (2001) Function of GB1 and GB2 subunits in G protein coupling of GABA(B) receptors. Proc. Natl. Acad. Sci. U. S. A 98, 14649-14654.

Marques J. T. and Williams B. R. (2005) Activation of the mammalian immune system by siRNAs. Nat. Biotechnol. 23, 1399-1405.

Mattson M.P. and Kater S.B. (1989) Development and selective neurodegeneration in cell cultures from different hippocampal regions. Brain Res. 490, 110-125.

Mauceri D., Cattabeni F., Di L.M. and Gardoni F. (2004) Calcium/calmodulin-dependent protein kinase II phosphorylation drives synapse-associated protein 97 into spines. J. Biol. Chem. 279, 23813-23821.

McCudden C. R., Hains M. D., Kimple R. J., Siderovski D. P. and Willard F. S. (2005) G-protein signaling: back to the future. Cell Mol. Life Sci. 62, 551-577.

Megias M., Emri Z., Freund T. F. and Gulyas A. I. (2001) Total number and distribution of inhibitory and excitatory synapses on hippocampal CA1 pyramidal cells. Neuroscience 102, 527-540.

Menon-Johansson A. S., Berrow N. and Dolphin A. C. (1993) G(o) transduces GABAB-receptor modulation of N-type calcium channels in cultured dorsal root ganglion neurons. Pflugers Arch. 425, 335-343.

Michaelsen K. and Lohmann C. (2010) Calcium dynamics at developing synapses: mechanisms and functions. Eur. J. Neurosci. 32, 218-223.

Michna M., Knirsch M., Hoda J. C., Muenkner S., Langer P., Platzer J., Striessnig J. and Engel J. (2003) Cav1.3 (alpha1D) Ca2+ currents in neonatal outer hair cells of mice. J. Physiol. 553, 747-758.

Milligan G. (1993) Regional distribution and quantitative measurement of the phosphoinositidase C-linked guanine nucleotide binding proteins G11 alpha and Gq alpha in rat brain. J. Neurochem. 61, 845-851.

Milligan G. and Kostenis E. (2006) Heterotrimeric G-proteins: a short history. Br. J. Pharmacol. 147 Suppl 1, S46-S55.

Mintz I. M. and Bean B. P. (1993) GABAB receptor inhibition of P-type Ca2+ channels in central neurons. Neuron 10, 889-898.

Misgeld U., Bijak M. and Jarolimek W. (1995) A physiological role for GABAB receptors and the effects of baclofen in the mammalian central nervous system. Prog. Neurobiol. 46, 423-462.

Mizuno N. and Itoh H. (2009) Functions and regulatory mechanisms of Gq-signaling pathways. Neurosignals. 17, 42-54.

Mizuta K., Mizuta F., Xu D., Masaki E., Panettieri R. A., Jr. and Emala C. W. (2011) Gi-coupled gamma-aminobutyric acid-B receptors cross-regulate phospholipase C and calcium in airway smooth muscle. Am. J. Respir. Cell Mol. Biol. 45, 1232-1238.

Moosmang S., Haider N., Klugbauer N., Adelsberger H., Langwieser N., Muller J., Stiess M., Marais E., Schulla V., Lacinova L., Goebbels S., Nave K. A., Storm D. R., Hofmann F. and Kleppisch T. (2005) Role of hippocampal Cav1.2 Ca2+ channels in NMDA receptor-independent synaptic plasticity and spatial memory. J. Neurosci. 25, 9883-9892.

Moran D. (1991) Voltage-dependent -L-type Ca2+ channels participate in regulating neural crest migration and differentiation. Am. J. Anat. 192, 14-22.

Morton R.A., Norlin M.S., Vollmer C.C. and Valenzuela C.F. (2013) Characterization of L-type voltage-gated Ca(2+) channel expression and function in developing CA3 pyramidal neurons. Neuroscience 238, 59-70.

Moss J. and Vaughan M. (1979) Activation of adenylate cyclase by choleragen. Annu. Rev. Biochem. 48, 581-600.

Mynlieff M. (1997) Dissociation of postnatal hippocampal neurons for short term culture. J. Neurosci. Methods 73, 35-44.

Mynlieff M. (1999) Identification of different putative neuronal subtypes in cultures of the superior region of the hippocampus using electrophysiological parameters. Neuroscience 93, 479-486.

Nimmrich V. and Gross G. (2012) P/Q-type calcium channel modulators. Br. J. Pharmacol. 167, 741-759.

Nishikawa M., Hirouchi M. and Kuriyama K. (1997) Functional coupling of Gi subtype with GABAB receptor/adenylyl cyclase system: analysis using a reconstituted system with purified GTP-binding protein from bovine cerebral cortex. Neurochem. Int. 31, 21-25.

Norris C.M., Blalock E.M., Chen K.C., Porter N.M. and Landfield P.W. (2002) Calcineurin enhances L-type Ca(2+) channel activity in hippocampal neurons: increased effect with age in culture. Neuroscience 110, 213-225.

Osugi T., Imaizumi T., Mizushima A., Uchida S. and Yoshida H. (1986) 1-Oleoyl-2-acetyl-glycerol and phorbol diester stimulate Ca2+ influx through Ca2+ channels in neuroblastoma x glioma hybrid NG108-15 cells. Eur. J. Pharmacol. 126, 47-51.

O-Uchi J., Sasaki H., Morimoto S., Kusakari Y., Shinji H., Obata T., Hongo K., Komukai K. and Kurihara S. (2008) Interaction of alpha1-adrenoceptor subtypes with different G proteins induces opposite effects on cardiac L-type Ca2+ channel. Circ. Res. 102, 1378-1388.

Padgett C. L. and Slesinger P. A. (2010) GABAB receptor coupling to G-proteins and ion channels. Adv. Pharmacol. 58, 123-147.

Park D., Jhon D. Y., Lee C. W., Ryu S. H. and Rhee S. G. (1993) Removal of the carboxyl-terminal region of phospholipase C-beta 1 by calpain abolishes activation by G alpha q. J. Biol. Chem. 268, 3710-3714.

Park H. W., Jung H., Choi K. H., Baik J. H. and Rhim H. (2010) Direct interaction and functional coupling between voltage-gated CaV1.3 Ca2+ channel and GABAB receptor subunit 2. FEBS Lett. 584, 3317-3322.

Park J.Y., Kang H.W., Moon H.J., Huh S.U., Jeong S.W., Soldatov N.M. and Lee J.H. (2006) Activation of protein kinase C augments T-type Ca2+ channel activity without changing channel surface density. J. Physiol. 577, 513-523.

Perez-Garci E., Larkum M.E. and Nevian T. (2013) Inhibition of dendritic Ca2+ spikes by GABAB receptors in cortical pyramidal neurons is mediated by a direct Gi/o-beta-subunit interaction with Cav1 channels. J. Physiol. 591, 1599-1612.

Pinard A., Seddik R. and Bettler B. (2010) GABAB receptors: physiological functions and mechanisms of diversity. Adv. Pharmacol. 58, 231-255.

Platzer J., Engel J., Schrott-Fischer A., Stephan K., Bova S., Chen H., Zheng H. and Striessnig J. (2000) Congenital deafness and sinoatrial node dysfunction in mice lacking class D L-type Ca2+ channels. Cell 102, 89-97.

Pravettoni E., Bacci A., Coco S., Forbicini P., Matteoli M. and Verderio C. (2000) Different localizations and functions of L-type and N-type calcium channels during development of hippocampal neurons. Dev. Biol. 227, 581-594.

Prosser H. M., Gill C. H., Hirst W. D., Grau E., Robbins M., Calver A., Soffin E. M., Farmer C. E., Lanneau C., Gray J., Schenck E., Warmerdam B. S., Clapham C., Reavill C., Rogers D. C., Stean T., Upton N., Humphreys K., Randall A., Geppert M., Davies C. H. and Pangalos M. N. (2001) Epileptogenesis and enhanced prepulse inhibition in GABA(B1)-deficient mice. Mol. Cell Neurosci. 17, 1059-1070.

Queva C., Bremner-Danielsen M., Edlund A., Ekstrand A. J., Elg S., Erickson S., Johansson T., Lehmann A. and Mattsson J. P. (2003) Effects of GABA agonists on body temperature regulation in GABA(B(1))-/- mice. Br. J. Pharmacol. 140, 315-322.

Rane S.G. and Dunlap K. (1986) Kinase C activator 1,2-oleoylacetylglycerol attenuates voltage-dependent calcium current in sensory neurons. Proc. Natl. Acad. Sci. U. S. A. 83, 184-188.

Rettig J., Sheng Z. H., Kim D. K., Hodson C. D., Snutch T. P. and Catterall W. A. (1996) Isoform-specific interaction of the alpha1A subunits of brain Ca2+ channels with the presynaptic proteins syntaxin and SNAP-25. Proc. Natl. Acad. Sci. U. S. A 93, 7363-7368.

Reuveny E., Slesinger P. A., Inglese J., Morales J. M., Iniguez-Lluhi J. A., Lefkowitz R. J., Bourne H. R., Jan Y. N. and Jan L. Y. (1994) Activation of the cloned muscarinic potassium channel by G protein beta gamma subunits. Nature 370, 143-146.

Rhee S. G. (2001) Regulation of phosphoinositide-specific phospholipase C. Annu. Rev. Biochem. 70, 281-312.

Rios E., Pizarro G. and Stefani E. (1992) Charge movement and the nature of signal transduction in skeletal muscle excitation-contraction coupling. Annu. Rev. Physiol 54, 109-133.

Robichon A., Tinette S., Courtial C. and Pelletier F. (2004) Simultaneous stimulation of GABA and beta adrenergic receptors stabilizes isotypes of activated adenylyl cyclase heterocomplex. BMC. Cell Biol. 5, 25.

Roisin M. P. and Barbin G. (1997) Differential expression of PKC isoforms in hippocampal neuronal cultures: modifications after basic FGF treatment. Neurochem. Int. 30, 261-270.

Rosenberg O.S., Deindl S., Comolli L.R., Hoelz A., Downing K.H., Nairn A.C.and Kuriyan J. (2006) Oligomerization states of the association domain and the holoenyzme of Ca2+/CaM kinase II. FEBS J. 273, 682-694.

Rybin V. O. and Steinberg S. F. (1994) Protein kinase C isoform expression and regulation in the developing rat heart. Circ. Res. 74, 299-309.

Sathanoori M., Dias B.G., Nair A.R., Banerjee S.B., Tole S. and Vaidya V.A. (2004) Differential regulation of multiple brain-derived neurotrophic factor transcripts in the postnatal and adult rat hippocampus during development, and in response to kainate administration. Brain Res. Mol. Brain. Res. 130, 170-177.

Schechtman D. and Mochly-Rosen D. (2001) Adaptor proteins in protein kinase C-mediated signal transduction. Oncogene 20, 6339-6347.

Schuler V., Luscher C., Blanchet C., Klix N., Sansig G., Klebs K., Schmutz M., Heid J., Gentry C., Urban L., Fox A., Spooren W., Jaton A. L., Vigouret J., Pozza M., Kelly P. H., Mosbacher J., Froestl W., Kaslin E., Korn R., Bischoff S., Kaupmann K., van der Putten H. and Bettler B. (2001) Epilepsy, hyperalgesia, impaired memory, and loss of pre- and postsynaptic GABA(B) responses in mice lacking GABA(B(1)). Neuron 31, 47-58.

Schwenk J., Metz M., Zolles G., Turecek R., Fritzius T., Bildl W., Tarusawa E., Kulik A., Unger A., Ivankova K., Seddik R., Tiao J. Y., Rajalu M., Trojanova J., Rohde V., Gassmann M., Schulte U., Fakler B. and Bettler B. (2010) Native GABA(B) receptors are heteromultimers with a family of auxiliary subunits. Nature 465, 231-235.

Seisenberger C., Specht V., Welling A., Platzer J., Pfeifer A., Kuhbandner S., Striessnig J., Klugbauer N., Feil R. and Hofmann F. (2000) Functional embryonic cardiomyocytes after disruption of the L-type alpha1C (Cav1.2) calcium channel gene in the mouse. J. Biol. Chem. 275, 39193-39199.

Sengupta P. (2013) The Laboratory Rat: Relating Its Age With Human's. Int. J. Prev. Med. 4, 624-630.

Sharfman, H. (ed.) (2007) The dentate gyrus. A comprehensive guide to structure, function, and clinical implications. Oxford, UK: Elsevier.

Shen W. and Slaughter M. M. (1999) Metabotropic GABA receptors facilitate L-type and inhibit N-type calcium channels in single salamander retinal neurons. J. Physiol 516 (Pt 3), 711-718.

Sheng Z. H., Rettig J., Takahashi M. and Catterall W. A. (1994) Identification of a syntaxin-binding site on N-type calcium channels. Neuron 13, 1303-1313.

Sihra T.S. and Pearson H.A. (1995) Ca/calmodulin-dependent kinase II inhibitor KN62 attenuates glutamate release by inhibiting voltage-dependent Ca(2+)-channels. Neuropharmacology 34, 731-741.

Simon M. I., Strathmann M. P. and Gautam N. (1991) Diversity of G proteins in signal transduction. Science 252, 802-808.

Sloviter R.S., Ali-Akbarian L., Elliott R.C., Bowery B.J. and Bowery N.G. (1999) Localization of GABA(B) (R1) receptors in the rat hippocampus by immunocytochemistry and high resolution autoradiography, with specific reference to its localization in identified hippocampal interneuron subpopulations. Neuropharmacology 38, 1707-1721.

Smrcka A. V. (2008) G protein betagamma subunits: central mediators of G protein-coupled receptor signaling. Cell Mol. Life Sci. 65, 2191-2214.

Smrcka A. V. and Sternweis P. C. (1993) Regulation of purified subtypes of phosphatidylinositol-specific phospholipase C beta by G protein alpha and beta gamma subunits. J. Biol. Chem. 268, 9667-9674.

Snutch T. P. (2005) Targeting chronic and neuropathic pain: the N-type calcium channel comes of age. NeuroRx. 2, 662-670.

Somogyi J., Baude A., Omori Y., Shimizu H., El M.S., Fukaya M., Shigemoto R., Watanabe M. and Somogyi P. (2004) GABAergic basket cells expressing cholecystokinin contain vesicular glutamate transporter type 3 (VGLUT3) in their synaptic terminals in hippocampus and isocortex of the rat. Eur. J. Neurosci. 19, 552-569.

Somogyi P. and Klausberger T. (2005) Defined types of cortical interneurone structure space and spike timing in the hippocampus. J. Physiol. 562, 9-26.

Song Y.H., Cho H., Ryu S.Y., Yoon J.Y., Park S.H., Noh C.I., Lee S.H. and Ho W.K. (2010) L-type Ca(2+) channel facilitation mediated by H(2)O(2)-induced activation of CaMKII in rat ventricular myocytes. J. Mol. Cell Cardiol. 48, 773-780.

Steinberg S. F. (2008) Structural basis of protein kinase C isoform function. Physiol Rev. 88, 1341-1378.

Striessnig J. (1999) Pharmacology, structure and function of cardiac L-type Ca(2+) channels. Cell Physiol Biochem. 9, 242-269.

Sumi M., Kiuchi K., Ishikawa T., Ishii A., Hagiwara M., Nagatsu T. and Hidaka H. (1991) The newly synthesized selective Ca2+/calmodulin dependent protein kinase II inhibitor KN-93 reduces dopamine contents in PC12h cells. Biochem. Biophys. Res. Commun. 181, 968-975.

Sun B. B. and Chiu S. Y. (1999) N-type calcium channels and their regulation by GABAB receptors in axons of neonatal rat optic nerve. J. Neurosci. 19, 5185-5194.

Takahashi T., Kajikawa Y. and Tsujimoto T. (1998) G-Protein-coupled modulation of presynaptic calcium currents and transmitter release by a GABAB receptor. J. Neurosci. 18, 3138-3146.

Takasaki J., Saito T., Taniguchi M., Kawasaki T., Moritani Y., Hayashi K. and Kobori M. (2004) A novel Galphaq/11-selective inhibitor. J. Biol. Chem. 279, 47438-47445.

Tanaka C. and Nishizuka Y. (1994) The protein kinase C family for neuronal signaling. Annu. Rev. Neurosci. 17, 551-567.

Tao X., West A.E., Chen W.G., Corfas G. and Greenberg M.E. (2002) A calcium-responsive transcription factor, CaRF, that regulates neuronal activity-dependent expression of BDNF. Neuron 33, 383-395.

Tatebayashi H. and Ogata N. (1992) Kinetic analysis of the GABAB-mediated inhibition of the high-threshold Ca2+ current in cultured rat sensory neurones. J. Physiol 447, 391-407.

Timmusk T., Palm K., Metsis M., Reintam T., Paalme V., Saarma M. and Persson H. (1993) Multiple promoters direct tissue-specific expression of the rat BDNF gene. Neuron 10, 475-489.

Toselli M., Tosetti P. and Taglietti V. (1999) Kinetic study of N-type calcium current modulation by delta-opioid receptor activation in the mammalian cell line NG108-15. Biophys. J. 76, 2560-2574.

Tseng G.N. and Boyden P.A. (1991) Different effects of intracellular Ca and protein kinase C on cardiac T and L Ca currents. Am. J. Physiol. 261, H364-H379.

Tsien R. W., Lipscombe D., Madison D. V., Bley K. R. and Fox A. P. (1988) Multiple types of neuronal calcium channels and their selective modulation. Trends Neurosci. 11, 431-438.

Tu H., Rondard P., Xu C., Bertaso F., Cao F., Zhang X., Pin J. P. and Liu J. (2007) Dominant role of GABAB2 and Gbetagamma for GABAB receptor-mediated-ERK1/2/CREB pathway in cerebellar neurons. Cell Signal 19, 1996-2002.

Tyzio R., Holmes G.L., Ben-Ari Y. and Khazipov R. (2007) Timing of the developmental switch in GABA(A) mediated signaling from excitation to inhibition in CA3 rat

hippocampus using gramicidin perforated patch and extracellular recordings. Epilepsia 48 Suppl. 5:96-105.

Ulrich D., Besseyrias V. and Bettler B. (2007) Functional mapping of GABA(B)-receptor subtypes in the thalamus. J. Neurophysiol. 98, 3791-3795.

Uvarov P., Ludwig A., Markkanen M., Rivera C. and Airaksinen M.S. (2006) Upregulation of the neuron-specific K+/Cl- cotransporter expression by transcription factor early growth response 4. J. Neurosci. 26, 13463-13473.

Van Dop C., Yamanaka G., Steinberg F., Sekura R. D., Manclark C. R., Stryer L. and Bourne H. R. (1984) ADP-ribosylation of transducin by pertussis toxin blocks the light-stimulated hydrolysis of GTP and cGMP in retinal photoreceptors. J. Biol. Chem. 259, 23-26.

Vanhoose A. M., Emery M., Jimenez L. and Winder D. G. (2002) ERK activation by G-protein-coupled receptors in mouse brain is receptor identity-specific. J. Biol. Chem. 277, 9049-9053.

Venkatakrishnan G. and Exton J. H. (1996) Identification of determinants in the alpha-subunit of Gq required for phospholipase C activation. J. Biol. Chem. 271, 5066-5072.

Vigot R., Barbieri S., Brauner-Osborne H., Turecek R., Shigemoto R., Zhang Y. P., Lujan R., Jacobson L. H., Biermann B., Fritschy J. M., Vacher C. M., Muller M., Sansig G., Guetg N., Cryan J. F., Kaupmann K., Gassmann M., Oertner T. G. and Bettler B. (2006) Differential compartmentalization and distinct functions of GABAB receptor variants. Neuron 50, 589-601.

Wang L., Rolfe M. and Proud C.G. (2003) Ca(2+)-independent protein kinase C activity is required for alpha1-adrenergic-receptor-mediated regulation of ribosomal protein S6 kinases in adult cardiomyocytes. Biochem. J. 373, 603-611.

Wang W.Y., Hao L.Y., Minobe E., Saud Z.A., Han D.Y. and Kameyama M. (2009) CaMKII phosphorylates a threonine residue in the C-terminal tail of Cav1.2 Ca(2+) channel and modulates the interaction of the channel with calmodulin. J. Physiol. Sci. 59, 283-290.

Watterson D.M., Mirzoeva S., Guo L., Whyte A., Bourguignon J.J., Hibert M., Haiech J. and Van Eldik L.J. (2001) Ligand modulation of glial activation: cell permeable, small molecule inhibitors of serine-threonine protein kinases can block induction of interleukin 1 beta and nitric oxide synthase II. Neurochem. Int. 39, 459-468.

Wayman G.A., Tokumitsu H., Davare M.A. and Soderling T.R. (2011) Analysis of CaM-kinase signaling in cells. Cell Calcium 50, 1-8.

Weiergraber M., Kamp M. A., Radhakrishnan K., Hescheler J. and Schneider T. (2006) The Ca(v)2.3 voltage-gated calcium channel in epileptogenesis--shedding new light on an enigmatic channel. Neurosci. Biobehav. Rev. 30, 1122-1144.

West A.E., Chen W.G., Dalva M.B., Dolmetsch R.E., Kornhauser J.M., Shaywitz A.J., Takasu M.A., Tao X. and Greenberg M.E. (2001) Calcium regulation of neuronal gene expression. Proc. Natl. Acad. Sci. U. S. A. 98:11024-11031.

West A.E., Griffith E.C. and Greenberg M.E. (2002) Regulation of transcription factors by neuronal activity. Nat. Rev. Neurosci. 3, 921-931.

Wettschureck N. and Offermanns S. (2005) Mammalian G proteins and their cell type specific functions. Physiol Rev. 85, 1159-1204.

White J. A., McKinney B. C., John M. C., Powers P. A., Kamp T. J. and Murphy G. G. (2008) Conditional forebrain deletion of the L-type calcium channel Ca V 1.2 disrupts remote spatial memories in mice. Learn. Mem. 15, 1-5.

Wickman K. D., Iniguez-Lluhl J. A., Davenport P. A., Taussig R., Krapivinsky G. B., Linder M. E., Gilman A. G. and Clapham D. E. (1994) Recombinant G-protein beta gamma-subunits activate the muscarinic-gated atrial potassium channel. Nature 368, 255-257.

Wilson B. A. and Ho M. (2004) Pasteurella multocida toxin as a tool for studying Gq signal transduction. Rev. Physiol Biochem. Pharmacol. 152, 93-109.

Wu-Zhang A. X. and Newton A. C. (2013) Protein kinase C pharmacology: refining the toolbox. Biochem. J. 452, 195-209.

Xu W. and Lipscombe D. (2001) Neuronal Ca(V)1.3alpha(1) L-type channels activate at relatively hyperpolarized membrane potentials and are incompletely inhibited by dihydropyridines. J. Neurosci. 21, 5944-5951.

Yang J. and Tsien R.W. (1993) Enhancement of N- and L-type calcium channel currents by protein kinase C in frog sympathetic neurons. Neuron 10, 127-136.

Yang L., Liu G., Zakharov S.I., Morrow J.P., Rybin V.O., Steinberg S.F. and Marx S.O. (2005) Ser1928 is a common site for Cav1.2 phosphorylation by protein kinase C isoforms. J. Biol. Chem. 280, 207-214.

Yang L., Katchman A., Morrow J. P., Doshi D. and Marx S. O. (2011) Cardiac L-type calcium channel (Cav1.2) associates with gamma subunits. FASEB J. 25, 928-936.

Yue Y., Qu Y. and Boutjdir M. (2004) Beta- and alpha-adrenergic cross-signaling for L-type Ca current is impaired in transgenic mice with constitutive activation of epsilonPKC. Biochem. Biophys. Res. Commun. 314,749-754.

Zamponi G. W., Bourinet E., Nelson D., Nargeot J. and Snutch T. P. (1997) Crosstalk between G proteins and protein kinase C mediated by the calcium channel alpha1 subunit. Nature 385, 442-446.

Zeng L., Webster S. V. and Newton P. M. (2012) The biology of protein kinase C. Adv. Exp. Med. Biol. 740, 639-661.

Zhou Z., Hong E.J., Cohen S., Zhao W.N., Ho H.Y., Schmidt L., Chen W.G., Lin .Y, Savner E., Griffith E.C., Hu L., Steen J.A., Weitz C.J. and Greenberg M.E. (2006) Brain-specific phosphorylation of MeCP2 regulates activity-dependent Bdnf transcription, dendritic growth, and spine maturation. Neuron 52, 255-269.